NASA-CR-195525

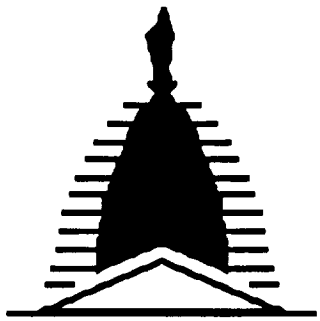

UNIVERSITY of
NOTRE DAME

NASA/USRA UNIVERSITY ADVANCED DESIGN PROGRAM 1992-1993

PROJECT CENTER MENTOR: NASA-AMES DRYDEN FLIGHT RESEARCH FACILITY

FINAL DESIGN PROPOSAL

The Airplane

A Simulated Commercial Air Transportation Study

April 1993

Department of Aerospace and Mechanical Engineering
University of Notre Dame
Notre Dame, IN 46556

(NASA-CR-195525) THE AIRPLANE: A SIMULATED COMMERCIAL AIR TRANSPORTATION STUDY Final Design Proposal (Notre Dame Univ.) 176 p

N94-24837

Unclas

G3/05 0204260

The AIRPLANE

By

The Airplane Guys Design Group

Marc D'Auteuil
Pete Geniesse
Michael Hunniford
Kathleen Lawler
Elena Quirk
Michael Tognarelli

April 8, 1993

Department of Aerospace and Mechanical Engineering
University of Notre Dame
Notre Dame, IN 46556

EXECUTIVE SUMMARY

The *Airplane* is a moderate - range, 70 passenger aircraft. It can carry more passengers in a shorter time and at a lower cost than the HB - 40 which currently dominates the Aeroworld market. It is designed to serve demands for flights up to 10,000 feet and it cruises at 31ft/s. The major drivers for the design of the *Airplane* are economic competitiveness, takeoff performance, and weight minimization.

The *Airplane* can be manufactured at a cost of $2,094 per aircraft. It flies at a cheaper cost per seat per thousand feet (CPSPK) of 0.81¢ at maximum range and capacity than the HB - 40 (0.9¢) at its maximum range and capacity. It is also a more economical carrier at its maximum range when filled to the passenger capacity of the HB - 40 (1.42¢). The CPSPK of the HB - 40 carrying 40 passengers 10,000 feet is, by comparison, 1.58¢. A further critical economic feature of the design of the *Airplane* is the direct operating cost. This cost is greatly driven by the cost of labor and materials for the manufacturing process. By building the *Airplane* for less money than the HB -40, the market may be overtaken since more seats may be filled and indeed, for the flight range targeted, will be filled due to high passenger demands. Fuel is conserved by transporting more passengers along a specific route in a particular time frame (i. e., smaller overall number of flights) and the added convenience of a quicker flight will attract more passengers. All of this translates into larger profit margins for airlines adding the *Airplane* to their fleets. In addition, the *Airplane* can take off at all but one of the airports which serve AeroWorld. This is an improvement on the competition, which serves all but two airports. Finally, the *Airplane* is weight efficient. This plays an important role in minimizing materials cost as well as decreasing the size of the lifting surfaces and propulsion system necessary for the *Airplane* to meet its range and performance objectives.

The *Airplane* is propelled by a single Astro 15 electric motor and a Zinger 12 - 8 propeller. This equipment is carried in the nose of the aircraft and eliminates the need for complex thrust balancing. The propulsion system is fueled by 12 1.2 V , 900 milliamp - hour batteries to accomodate the high current draw of the large propeller. The propulsion system choice is dictated by the runway lengths in Aeroworld which range between 20 and 40 feet and, hence, prescribe the necessary takeoff roll distance for the aircraft. The *Airplane*, with its 24 - foot roll distance, can serve all but one airport within AeroWorld, making its versatility across the market a strong selling point.

The wing section is a Spica airfoil which, because of its flat bottom, provides simplicity in manufacturing and thus helps to cut costs. The Spica has a relatively high stall angle of attack which allows the first - time pilot to adjust to the control sensitivity. The wing surface encompasses 9.5 ft^2 with an aspect ratio of 9.5. This is dictated by the necessary lift to meet the aforementioned takeoff criterion. The wing is rectangular , contains no sweep and is mounted at eight degrees of dihedral for roll stability. The wing is constructed of a single load bearing mainspar and shape - holding ribs coated with Monokote skin. These wing characteristics provide an overall simplicity in manufacturing and lend themselves to a lightweight structural makeup. The wing is given a slight incidence of three degrees to combine with the aircraft ground configuration to produce the necessary lift for the aircraft at takeoff.

The fuselage is 2.5" high by 7.5" wide with a rectangular cross - section. The fuselage houses the motor, flight deck and passenger compartments as well as the fuel and control actuating systems. The wing will be attached to the top of the fuselage as will the fuel and control actuator systems for easy disassembly and maintenance. Seats are arranged in the passenger compartment in 24 rows of three passengers on a single level. The layout calls for two seats to the right

and one to the left of a single aisle. Single level construction eliminates the complexity and added weight of having two floors on the aircraft. It is feared, however, that the very wide fuselage may create strong vortices which could have a very significant effect upon the directional stability and control. The fuselage is tapered at its aftmost section to alleviate this trailing vortex shedding. In addition, the twin vertical tail concept is employed to remove the directional control surfaces from the unsteady flows.

The aircraft center of gravity is located at 35 % mean aerodynamic chord when it is filled to capacity. The maximum forward center of gravity location is 28 % mean aerodynamic chord and occurs when the *Airplane* is filled with 20 - 25 passengers. These shifts fall within limits which call for the aircraft static margin to lie between 0.2 and 0.3. The static margin for the full aircraft is 0.225.

The aircraft is maneuvered about its pitch axis by means of an aft elevator on the flat plate horizontal tail. The twin vertical tail surfaces are also flat plates and each features a rudder for both directional and roll control. Along with wing dihedral, the rudders will be used to roll the aircraft. This option was chosen in lieu of ailerons in order to simplify wing construction, lighten the aircraft by the weight of a necessary servo, and reduce the associated cost. The control surfaces are designed to allow the pilot enough time to adjust for overshoot or undershoot from a distant, visual point of view of the aircraft dynamics.

The *Airplane* has a maximum range of 12,520 feet. Its maximum endurance is 8.7 minutes. Both of these quantities represent conditions for the aircraft without passengers. At maximum capacity, the range is 12,140 feet and endurance is 6.8 minutes. The *Airplane* will take off at a velocity of 23.0 ft/s which is safely higher than its stall speed of 19.3 ft/s. It has a maximum rate of climb of 12.4 ft/s and a minimum turn radius of 37.4 feet for a bank angle of 18

degrees. Its maximum lift - to - drag ratio is 11.3 and its cruise lift - to - drag ratio is 9.5.

There exist, of course, drawbacks or weaknesses in the design of the *Airplane* . These include a passenger imbalance in the fuselage seating area which must be compensated for by a leftward shift of the battery pack. In addition, the wide fuselage of the *Airplane* is expected to create destabilizing vortices which leaves the aircraft controllability in doubt despite an innovative tail design. The *Airplane* cannot cover as large a range as the HB - 40. Finally, its L/D at cruise is significantly smaller than its maximum L/D. This indicates an inefficiency which results from a required wing area to satisfy takeoff distance requirements and a desired cruise speed equal to or exceeding that of the competition.

The disadvantages are, however, overshadowed by the aircraft's many strengths. The *Airplane* provides more economical travel alternatives than the HB - 40. It is a faster aircraft and can serve one more airport within the AeroWorld market than the HB - 40. It can carry more passengers in fewer flights than the HB - 40 and should thus reduce total fuel costs to its investors over the long term . Finally, it is less costly to operate at its own maximum range and capacity as well as at its maximum range and the HB - 40's maximum capacity than the HB - 40.

POST FLIGHT MANAGEMENT REVIEW: **Airplane**

April 30, 1993

The following observations were made during the flight test validation for this aircraft design. This assessment is obviously quite qualitative and is based primarily upon the pilot's comments and instructor's observations.

1. Take-off performance was very good. Take-off distance estimated at 33 ft.

2. First flight take-off the aircraft was in trim with the C.G. at 27% of the wing chord.

3. Needed full rudder to be able to negotiate the turns in Loftus. If probably was somewhat small since it appeared to have adequate rudder travel.

4. No problems and the aircraft flew very well.

5. Successful validation of basic flight concept. Flew under control through entire closed course at approximately the required loiter speed. Landing and take-off performance was acceptable based upon the requirements.

AIRPLANE Complete Critical Data Summary

Parameter	
DESIGN GOALS:	
V cruise	31 ft/sec
Max # of passengers	70
#passengers-coach	70
# passengers-1st class	0
# crew	4
Max Range at Wmax	12140 ft
Altitude cruise	25 ft
Minimum turn radius	37.4 ft
Max range at Wmin	12520 ft
Maximum TO Weight-WMTO	5.25 lbs
Minimum TO Weight - Wmin	4.85 lbs
Total Cost per Aircraft	$2,094
DOC	$4.90-$5.68
CPSPK(max design conditions)	0.81 cents
BASIC CONFIG.	
Wing Area	9.5 ft2
Maximum TO Weight-WMTO	5.25 lb
Empty Flight Weight	4.85 lb
Wing Loading(WMTO)	9.3 oz/ft2
max length	64 in
max span	9.5 ft
max height	4 in
Total Wetted Area	33 ft2
WING	
Aspect Ratio	9.5
Span	9.5 ft2
Area	9.5 ft2
Root Chord	1 ft
Tip Chord	1 ft
Taper Ratio	1
C mac-MAC	1 ft
leading edge Sweep	0
1/4 chord Sweep	0
Dihedral	8 degrees
Twist(washout)	0
Airfoil section	SPICA
Design Reynolds number	200,000
t/c	11.70%
Incidence Angle root	3 degrees
Hor. pos of 1/4 MAC	x=19 in
Ver. pos of 1/4 MAC	z=3.75 in

WING (Cont'd)	
e-Oswald efficiency	0.75
CDo-wing	0.007
CLo-wing	0.428
Clalpha-wing	4.224 1/rad
FUSELAGE	
Length	64 in
Cross section shape	Rectangle
Nominal Cross Section Area	23 in2
Finess Ratio	9.14
Payload volume	1092 in3
Frontal area	27 in2
CDo -fuselage	0.0247
CLalpha-fuselage	.00444 1/deg
EMPENNAGE	
Horizontal tail	
Area	1.25 ft2
Span	2.5ft
Aspect Ratio	5
Root chord	0.5ft
Tip chord	0.5ft
Average chord	0.5ft
Taper ratio	1
l.e. sweep	0
1/4 chord sweep	0
incidence angle	0
hor. pos. of 1/4 MAC	x=62 in
ver. pos. of 1/4 MAC	z=2 in
Airfoil section	Flat Plate
CLalpha - horizontal	4.563 1/rad
CLde - horizontal	-0.727
CM mac-horizontal	0.5 ft
Vertical tail	
Area	0.833 ft2
Aspect ratio	1.67
root chord	6in
tip chord	6in
average chord	6in
taper ratio	1
l.e. sweep	0
1/4 chord sweep	0
hor. pos. of 1/4 MAC	x=62 in
vert. pos. of 1/4 MAC	z=4.5 in

EMPENNAGE (Cont'd)	
Vertical Tail Airfoil section	Flat Plate
SUMMARY AERODYNAMICS	
Cl max (airfoil)	1.42
CL max(aircraft) w/o flaps	1.28
CL max(aircraft) w/ flaps	1.28
lift curve slope(aircraft)	0.088 1/deg
CDo (aircraft)	0.041
efficiency-e(aircraft)	0.704
Alpha stall(aircraft) w/o flaps	10 degrees
Alpha stall(aircraft) w/ flaps	10 degrees
Alpha zero lift (aircraft)	-4.6
L/D max(aircraft)	11.32
Alpha L/D max(aircraft)	6
WEIGHTS	
Weight total (empty)	4.85 lbs
C. G. most forward-x&y	x=19.36,y=3
C. G. most aft-x&y	x=20.2y=3
Avionics	5.95 oz
Payload-Crew and Pass-max	6.4 oz
Engine & Engine controls	10.3 oz
Propeller	1 oz
Fuel(battery)	14.76 oz
Structure	
Wing	16 oz
Fuselage/emp	20.8 oz
Landing gear	5 oz
PROPULSION	
Propeller Diameter	12 inches
Type of engines	Astro 15
number	1
placement	Nose
Pavil max at cruise	27.3 W
Preq cruise	27.3W
max current draw at TO	12.14 mA
cruise current draw	6.6 mA
Propeller type	Zinger
Propeller pitch	8 in
Number of blades	2
cruise prop. rpm	4621
max thrust	2.86 lbs
cruise thrust	0.82 lbs
battery type	P-90SCR

PROPULSION (Cont'd.)	
number	12
individual capacity	900 mAh
individual voltage	1.2 V
pack capacity	900 mAh
pack voltage	14.4 V
max prop rpm	6281
STABILITY AND CONTROL	
Neutral point	0.575c
Static margin %MAC	0.225c
Hor. tail volume ratio	0.463
Vert. tail volume ratio	0.032
Elevator area	0.68ft2
Elevator max deflection	16 degrees
Rudder area	0.50 ft2
Rudder max deflection	30 degrees
Cm alpha	-0.901
Cn beta	0.105
Cl alpha tail	4.563 1/rad
Cl delta e tail	-0.727
PERFORMANCE	
Vmin at WMTO	19.3 ft/s
Vmax at WMTO	54.3 ft/s
Vstall at WMTO	19.3 ft/s
Range max at WMTO	12140 ft
Endurance @Rmax	7.0 min
Endurance Max at WMTO	8.0 min
Range at Emax	10300 ft
Range max at Wmin	12520 ft
ROC max at WMTO	12.4 ft/s
Min Glide angle	5.05 degrees
T/O distance at WMTO	24.0 ft
SYSTEMS	
Landing gear type	Taildragger
Main gear position	x=20.2 in
Main gear length	x=4.4 in
Main gear tire size	D=1.5in
nose/tail gear position	x=52 in
n/t gear length	3 in
n/t gear tire size	n/a
engine speed control	speed controller
control surfaces	rudder/elev.

ECONOMICS	
raw materials cost	$175.00
propulsion system cost	$107.00
avionics system cost	$285.00
production manhours	100 hours
personnel costs	$1,000.00
tooling costs	$215.00
total cost per aircraft	$2,094.00
Flight crew costs	$0.20
mantenance costs	$0.03
operation costs per flight	$0.23
current draw at cruise WMTO	3.76
flight time-design Range max	0.0926 hours
DOC	$4.90-$5.68
CPSPK (max Range/full)	0.81 cents
Hazardous Waste Disposal	$300.00
# flights/ lifetime	540
Depreciation Expense/flight	$3.88
Total Fixed Subsystems Cost	$404.00
Total Manufacturing Cost	$1,515.00

AIRPLANE DATA SUMMARY IN BRIEF

AERODYNAMICS

Wing Area	9.5 ft^2
$C_{L\alpha w}$	4.224 rad^{-1}
Aspect Ratio	9.5
Span	9.5 ft
Chord	1 ft
Taper Ratio	1
Sweep	None
Dihdral	8 Degrees
C_{do}	0.041
Airfoil Section	Spica
Wing Incidence	5 Degrees

EMPENNAGE

Horizontal Tail Airfoil	Flat Plate
Horizontal Tail Area	1.23 ft^2
$C_{L\alpha t}$	4.563 rad^{-1}
Elevator Area Fraction	0.15
Max Elevator Deflection	$\pm$ 15 Degrees
Vertical Tail Airfoil	Flat Plate
Vertical Tail Area	0.833 ft^2
$C_{L\alpha v}$	2.800 rad^{-1}
Rudder Area Fraction	0.6
Max Rudder Deflection	$\pm$30 Degrees

STRUCTURE

Weight	84.2 oz
Length	64.0 in
Passenger Area Width	7 in
Passenger Area Height	2.5 in

WEIGHT

Total	84.2 oz
Propeller	1 oz
Motor	10.3 oz
Main Gear	3.5 oz
Batteries (12)	14.76 oz
Receiver	0.95 oz
System Battery	2 oz
Servos (2)	1.2 oz
Speed Controller	1.8 oz
Wing	16 oz
Fuselage	17 oz

WEIGHT (Cont'd.)

Passengers	6.4 oz
Floorboard	4 oz
Tailwheel	1.5 oz
Empennage	3.8 oz

PERFORMANCE

Takeoff Distance	24.0 ft
Takeoff Velocity	23.0 ft/s
Cruise Velocity	31.0 ft/s
Cruise Range	12,100 ft
Cruise Endurance	6.8 min
Maximum Range	12,500 ft
Maximum Endurance	8.7 min
Maximum Rate of Climb	12.4 ft/s
Minimum Turn Radius	37.4 ft at 18 Degree Bank

PROPULSION

Engine	Astro 15
Propeller	Zinger 12 - 8
Number of Batteries	12
Battery Pack Voltage	14.4 V
Battery Capacity	900 mah
Motor Cruise RPM	10,990

ECONOMICS

Cost Per Aircraft	$2,094
Maximum DOC	$5. 68
Minimum DOC	$4.90
CPSPK (Max DOC)	$0.0081
CPSPK (Min DOC)	$0.007

EXTERNAL CONFIGURATION OF THE *AIRPLANE*

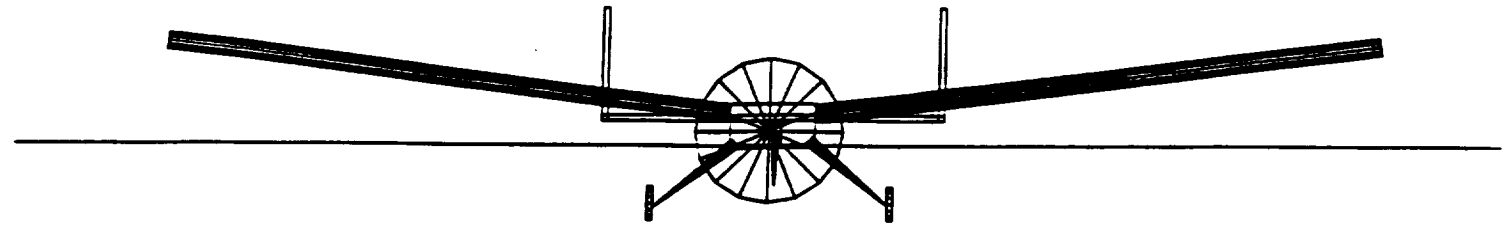

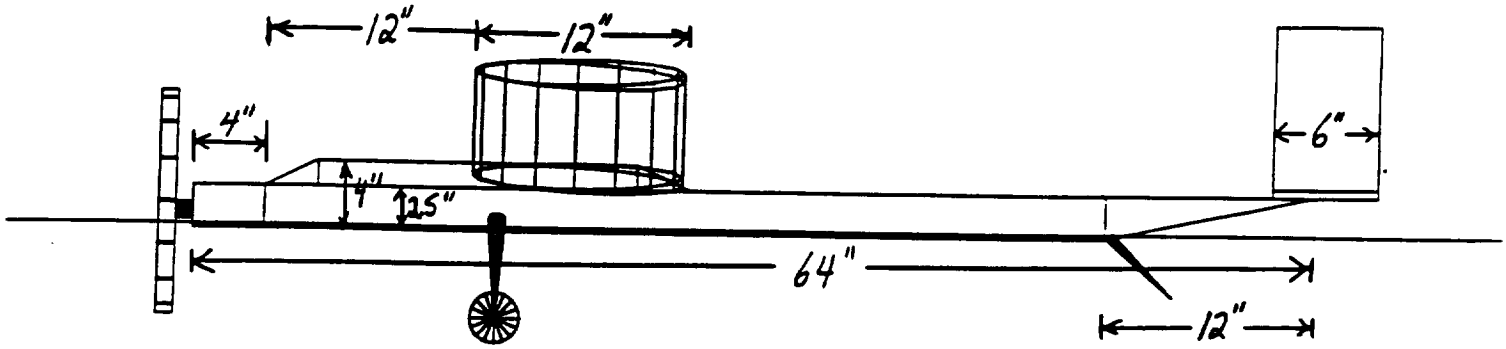

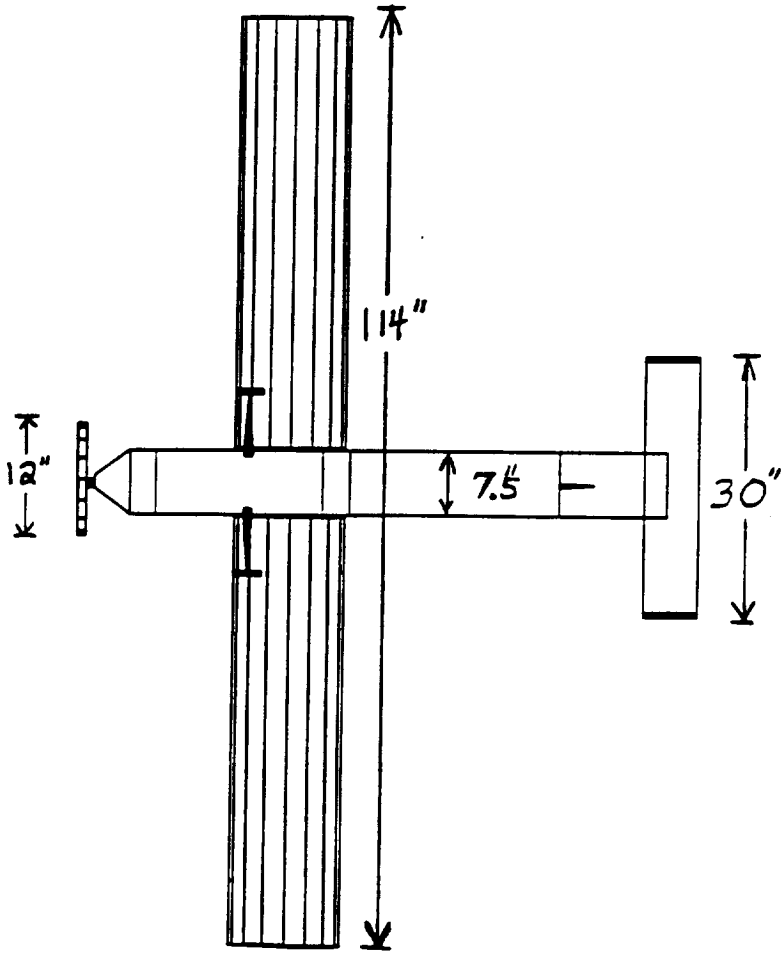

INTERNAL LAYOUT OF THE *AIRPLANE*

○ - passenger
* - flight attendant
● - pilot

1 inch = 8 inches

Level 1

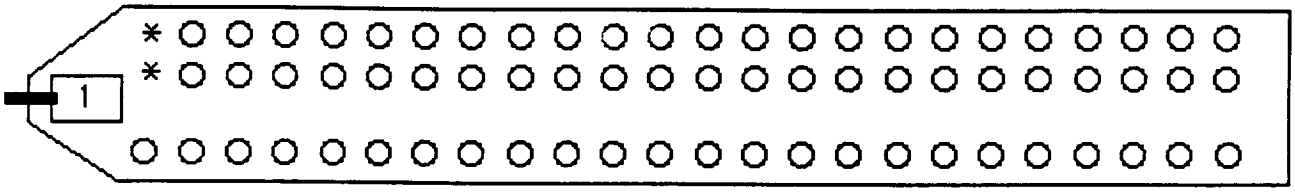

Level 2

Room to move batteries forward/aft for proper c.g. position

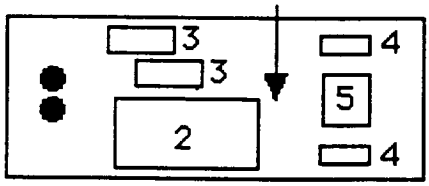

2 - batteries
3 - receiver battery pack/speed controller
4 - servos
5 - receiver

Side

TABLE OF CONTENTS

LISTING OF FIGURES

LIST OF TABLES

1.0 MISSION DEFINITION AND ANALYSIS

AeroWorld currently has one type of commercial aircraft trying to meet a variety of market needs. In order to be more competitive than this existing aircraft, a new design must provide a better profit margin to the companies who buy, fly, and maintain the air fleets. Careful market analysis, goal setting, and concept comparison have been used to ensure that the **Airplane Guys** design group will produce the most economically competitive airplane possible.

1.1 MARKET ANALYSIS AND MISSION SELECTION

Data for the AeroWorld market was provided by G-Dome Enterprises in terms of travel distance between cities, passenger volume, and minimum number of flights per day required between destinations. This market data (Reference 1 - 1) revealed the need for an aircraft with a passenger volume greater than 40 passengers. This aircraft could service the passenger demand in fewer flights than the existing airplane within AeroWorld.

Given the number of passengers traveling between each of the fifteen airports and the distance between each airport, the optimum flights per day for each route was found. The number of passengers and the range for each of these flights yielded a demand density plot as shown in Figure 1-1. The HB-40 when flying only the optimum number of flights per day services the passenger demand enclosed in Box #1. Box #1 shows that the HB-40 can carry a maximum of forty passengers and has a maximum range of 17000 feet. In order for the HB-40 to service all passengers who want to fly between destinations less than 17000 feet apart, the aircraft must fly up to five times the optimum number of flights per day or five aircraft must service the same route. For example, to service the 188 passengers who travel between Airports C and F, the HB-40 must fly five times the optimum number of flights.

FIGURE 1-1
Passenger Demand for Optimum Number of Flights

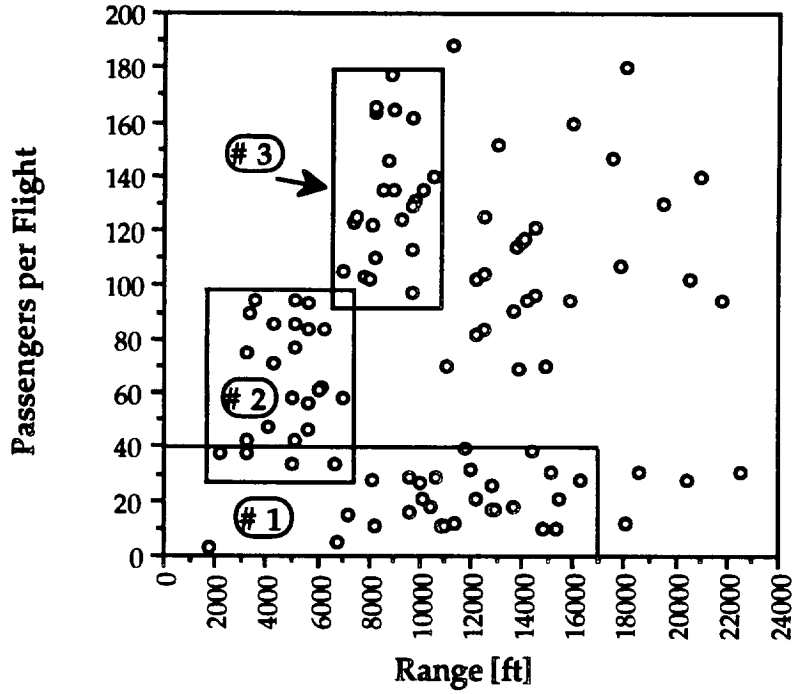

A 188 passenger aircraft could completely satisfy the demand for this route, however would not be filled to capacity on any other route. This assumes that the passenger demand will be equally distributed between all of the flights flown on each route daily.

As can be seen in Figure 1-1, the remaining two boxes define areas of demand densities limited by natural breaks in range and passenger load. Box #2 encloses a demand density of 30 to 100 passengers wishing to fly a maximum of 7000 feet. Similarly, Box #3 includes passengers loads of 100 to 180 passengers wishing to fly a maximum of 10000 feet.

The demand density plot shows the majority of the passengers fly on routes which have ranges up to 10000 feet. In fact, 71% of all the passengers in AeroWorld fly on 53 % of the routes - those routes of 10000 feet or less. The HB-

40 is designed to fly routes up to 17000 feet. However, it becomes expensive to operate at the shorter routes. The cost per seat per thousand feet (CPSPK) for the HB-40 is $.009 at its design range and at full capacity. However, when flying 10000-foot routes at full capacity its CPSPK is $.0153. This represents a 70% increase in CPSPK for the HB-40. An airplane with a design range of 10000 feet could be competitive with the HB-40 by providing service specifically oriented to the shorter routes.

Figure 1-1 also shows an need for a commercial aircraft with a seating capacity greater than 40 passengers. The passenger capacity requirements represented by Box #3 were eliminated from practical consideration based on the large size of the required 800 cubic inch minimum payload volume. An airplane with a passenger capacity of 70 would operate at full capacity for 50% of the routes represented in Box #2 and between 50% and 85% capacity for the other routes contained in the cluster.

In order to service all of the passengers in AeroWorld who require air travel on routes of 10000 feet or less, an aircraft with a 70 passenger capacity would only have to fly 3 times the optimum number of flights for 6 routes. This compares to 5 times the optimum number of flights for the HB-40. Seventy passengers appeared to be a good compromise between satisfying a passenger demand not met by the HB-40 and ensuring high percent seats filled for the majority of the routes with ranges less than or equal to 10000 feet.

1.2 DESIGN REQUIREMENTS AND OBJECTIVES

1.2.1 Design Requirements

The following design requirements were mandated by the Aerospace Design Request for Proposals provided by the upper management of G-Dome Enterprises:

- Minimum passenger volume of 8 in^3 per passenger for coach seating
- Perform a 60 foot radius, steady, level turn at a velocity of 25 ft/s
- Loiter for two minutes
- Design safe life of 50 hours
- Aircraft must takeoff and land under its own power
- Limited to $190 to purchase raw materials
- Install removable radio control and propulsion system in under 20 minutes
- Meet all FAA and FCC regulations for operation
- Must include a two person flight crew
- Must include one attendant per 40 passengers
- A complete safety assessment must be performed
- Can use no more than four servos
- Maximum aircraft altitude is 25 feet

1.2.2 Design Objectives

Airframe Structure and Materials

- Minimize weight of each airplane component such that its total weight does not exceed 5.5 pounds
    - Minimization of weight yields improved performance
    - This represents a 0.5 lb decrease from original DR&O
- Payload volume of 560 cubic inches to accommodate 70 passengers
- Utilize high wing monoplane to simplify wing-fuselage attachment
- Use single-size airfoil sections in non-tapered wing to reduce manufacturing hours
- Design sub-structures to simplify manufacturing process to minimize costs

Propulsion System

- Use electrically powered motor to reduce pollution
- Single engine and propeller configuration to eliminate multiple engine thrust balance
- Propulsion system provide thrust necessary for takeoff and cruise
- Flexible battery placement to control CG location
- Variable throttle control so pilot can regulate flight velocity

Flight Control System

- Elevator to control the pitch of aircraft
- Twin rudders to provide lateral and roll stability
- Dihedral to provide roll stability
- Tail-dragger landing gear provides ground handling as well as wing and fuselage incidence for takeoff
- Two servos to control elevator and rudder deflection and to steer tailwheel

Performance

- Maximum takeoff distance of 24 feet to service 93% of airports
- Cruise speed of 30 ft/s so travel time is competitive with HB-40
    - This represents a new objective not included in original DR&O
- Minimum range of 13000 feet which provides 10000 feet of travel distance and 3000 feet of loitering

Economics

- Total manufacturing cost less than HB-40 to ensure competitiveness

- CPSPK less than $.009 to keep ticket prices comparable to or less than competition
- Maximum total labor hours of 250 to minimize manufacturing costs

1.3 CONCEPT SELECTION

Five different concepts were considered before arriving at a final design concept. These concepts consisted of a delta wing with a canard surface and two pusher propellers, a biplane, a low wing monoplane, and high wing monoplane with a single level as well as a double decked fuselage. Among the considerations were the availability of a data base of a similar concept, the ease of construction, good performance characteristics, and any engineering difficulties which could be predicted.

1. 3. 1 Delta Wing with Canard and Pusher Props

The delta wing and canard configuration as shown in Figure 1-3 has not been attempted in past designs. The reason that this type of concept has never appeared before may be that there are distinct disadvantages associated with this design in the regime of subsonic flight. The advantages associated with a delta wing are normally present when the aircraft travels at supersonic speeds. However, some companies are researching the possibility of subsonic delta wing aircraft. Innovation and ingenuity play a significant role in engineering and while taking risks is sometimes dangerous, these risks must be taken if technology is to improve. This type of design is **not** conventional and therefore this type of design as well as its possible advantages might be overlooked. If a subsonic aircraft (prototype) were designed that could perform well, many companies would be interested in the delta wing concept because a

FIGURE 1-3
The Delta Wing Concept

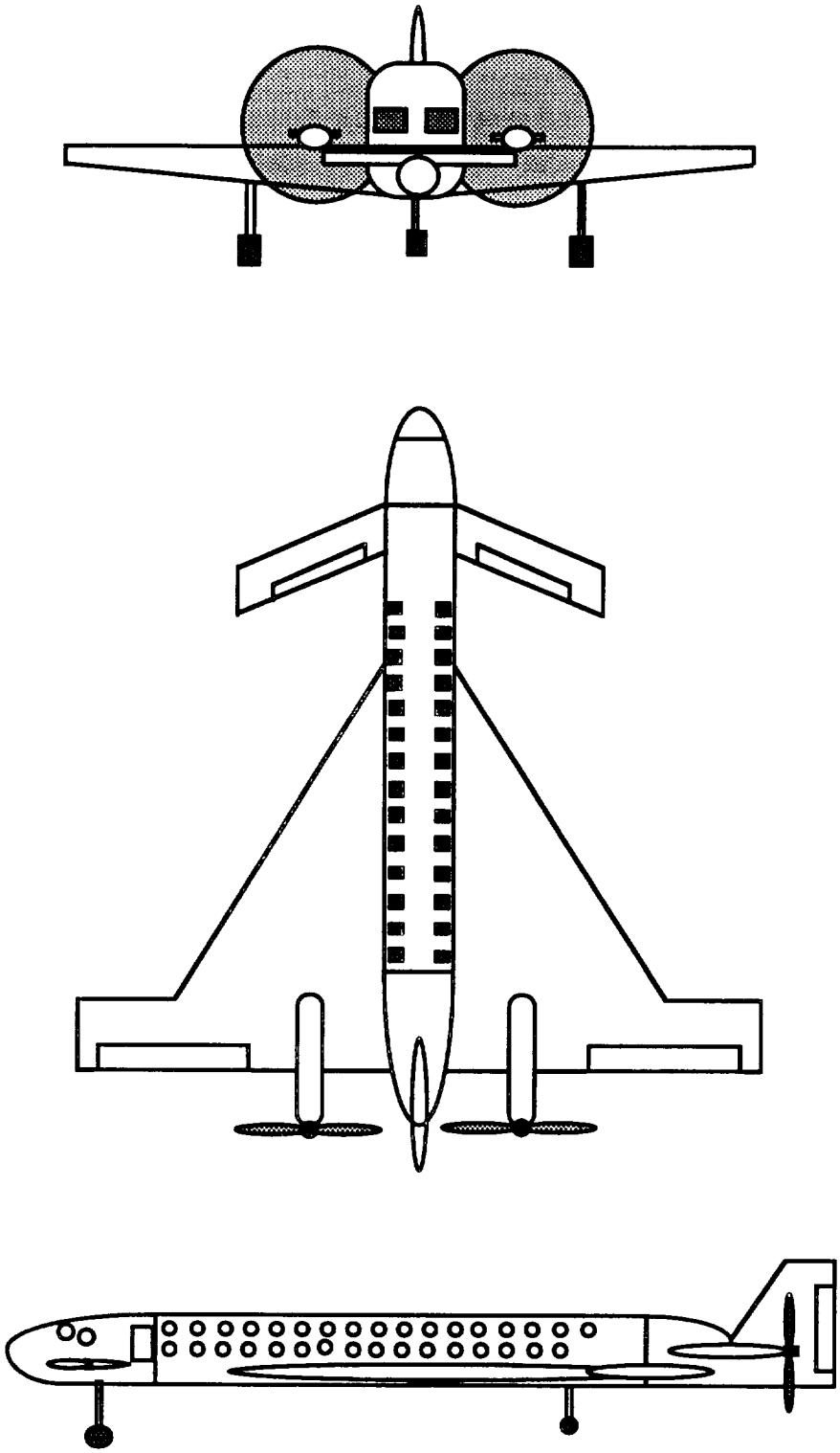

company might be able to implement part or all of the design for a full-size aircraft. On the other hand, if a canard surface is designed properly, it would give a plane better longitudinal control than a regular tail wing. Lastly, pusher propellers are advantageous because the airflow over the lifting surfaces (i.e. canard and wing) is not disturbed and this will help the performance and efficiency of the aircraft.

There are, however, several disadvantages associated with this type of design. There are risks involved with trying something new, and there always exists the possibility that this plane might not fly very well or maybe not at all. No database exists for this type of design, and therefore a starting database would have to be built from scratch. Having too many risks is also undesirable. The plane may not be able to perform a steady, level turn at 25 ft/s with a delta wing because the aspect ratio of a delta wing is generally very low and maneuvering a low aspect ratio plane at low speeds could present a problem. Although the pusher propellers have advantages as stated before, they also have disadvantages. The flow coming off of the trailing edge of the main wing may separate and turbulence may prevail before the flow reaches the propellers. This condition results in a less efficient propeller. Also, the aft section of the fuselage will have to sit high enough so there is sufficient clearance for the propellers.

1.3.2 Biplane

A biplane has been attempted in the past, and therefore there is some data that could be used to evaluate its characteristics. The single-level seating arrangement of 3 passengers/row x 24 rows is shown in Figure 1-4. A biplane is advantageous because it has two wings that produce the lift and therefore the

FIGURE 1-4
Biplane Concept

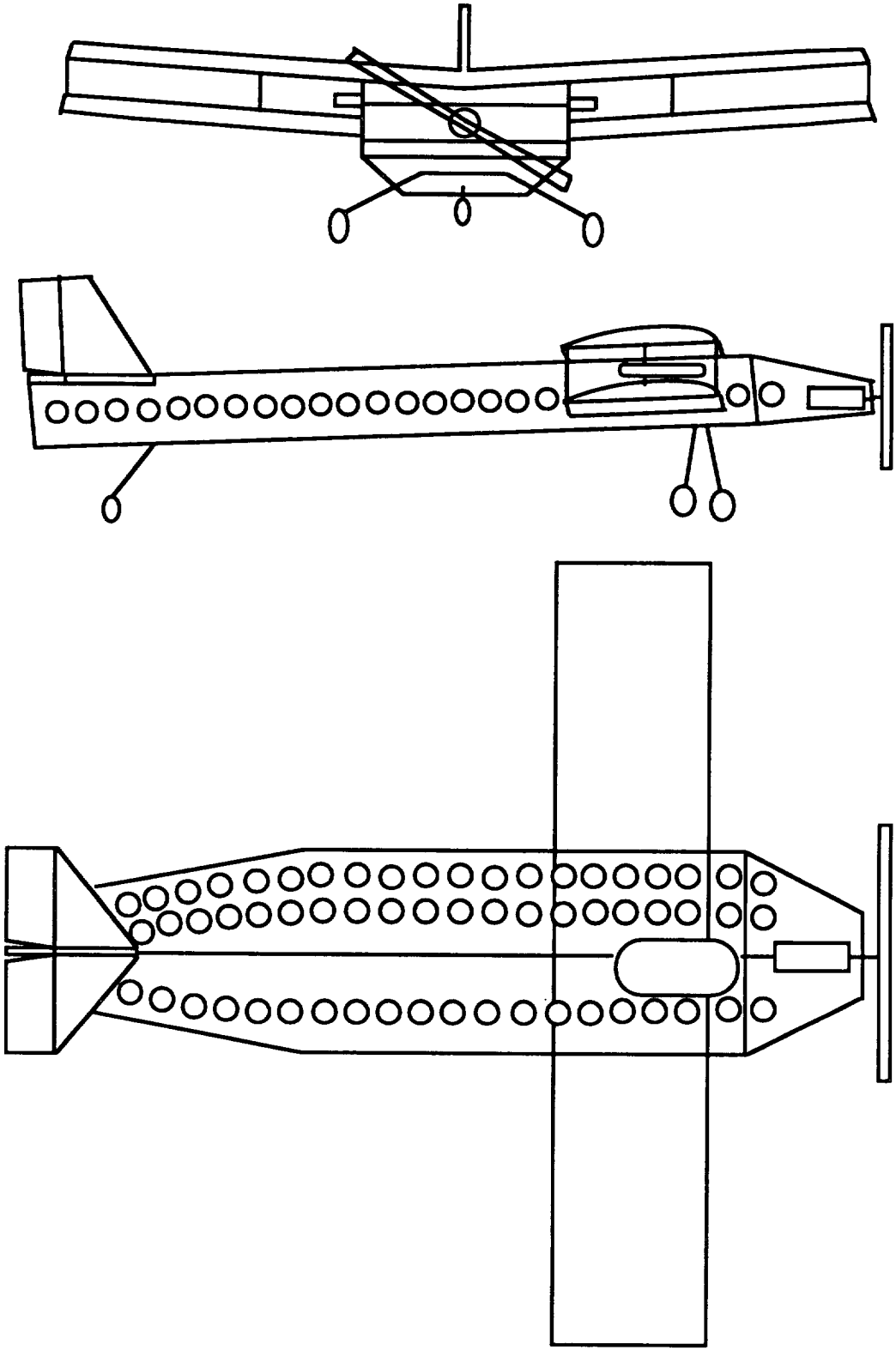

wing span can be reduced. This reduction in wing span will decrease the maximum bending moment at the root, and therefore the structure can be made lighter.

On the other hand, there are significant disadvantages as well. Although the wing span is reduced, there are two wings and this reduction in wing span may not compensate for the increase in weight due to two wings. There might be problems with attaching the lower wing to the center of the fuselage. If the lower wing passes through the fuselage, the problem will consist of separating the passenger compartment and compromising the structural integrity of the fuselage. If the lower wing does not pass through the fuselage, significant structural problems will involve the support of this wing. Although there are two wings producing lift, the lift per area for a biplane is lower than a single wing for reasonably close wing separation distances (i.e. $\approx$ 1 span). Since there are two wings, there will be aerodynamic interference between the them, but it may be difficult to determine those effects accurately.

1.3.3 Low Wing Monoplane

Another concept that was considered was the low wing monoplane which is shown in Figure 1-5. The single-level seating arrangement is 3 pass/row x 24 rows. One of the advantages of this design is easy access to the inside of the fuselage where the batteries and servos are located. Most of the past designs used a high wing monoplane and therefore this type of design would be more unique. A low wing monoplane aircraft is not as statically stable as a high wing aircraft with the same dihedral angle. Therefore a low wing plane would be easier to maneuver.

On the other hand, a removable low wing does not allow easy access to the batteries and servos like the high wing model. A low wing is usually more

FIGURE 1-5
Low Wing Monoplane Concept

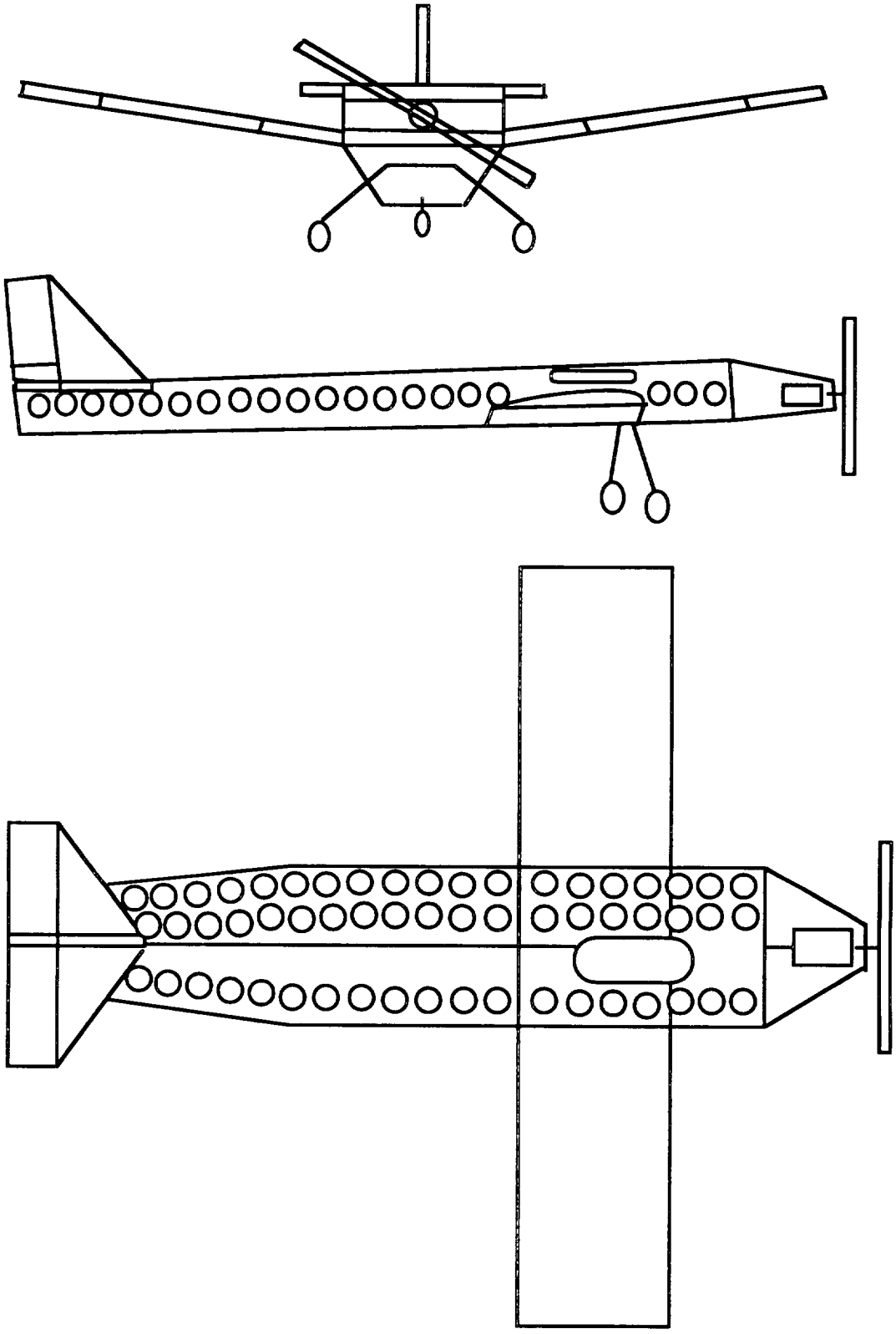

statically unstable than a high wing design, and therefore a low wing needs more dihedral than a high wing to attain the same static stability. Lastly, the database for a low wing design is much smaller than for the high wing model and a large database helps make referencing and comparing results during the design process easier.

1.3.4 High Wing Monoplane with Double Decker Fuselage

A concept similar to this one has been built in the past and is illustrated in Figure 1-6. The seating arrangement is 2 pass/row x 16 rows on the top level and 2 pass/row x 20 rows on the bottom level which totals 72 seats (70 passengers plus two attendants). One of the distinct advantages is a removable high wing design which allows for easy access to the inside of the fuselage for maintenance and battery replacement. By doubling the height of the fuselage, the double decker design will allow the fuselage to remain the same length and width for a larger number of passengers. This design is similar to past designs and therefore an extensive database has been built up which would make an analysis of the validity of the design easy. The construction of this type of design is also fairly straightforward and as such will save money and time.

However, it is clear that this type of design will fly, and therefore there is the large obstacle consists of surpassing the performance and overall cost of the HB-40. The double decker design also creates a larger frontal area on the fuselage and this results in increased drag. The weight of a double decker design is increased by the need to have a strong seating platform between the decks.

1.3.5 The *Airplane*

The final design concept named the Airplane is illustrated Figure 1-7. The *Airplane* is a high wing monoplane with tail dragger landing gear and a

FIGURE 1-6

High Wing Monoplane with Double-Decker Fuselage Concept

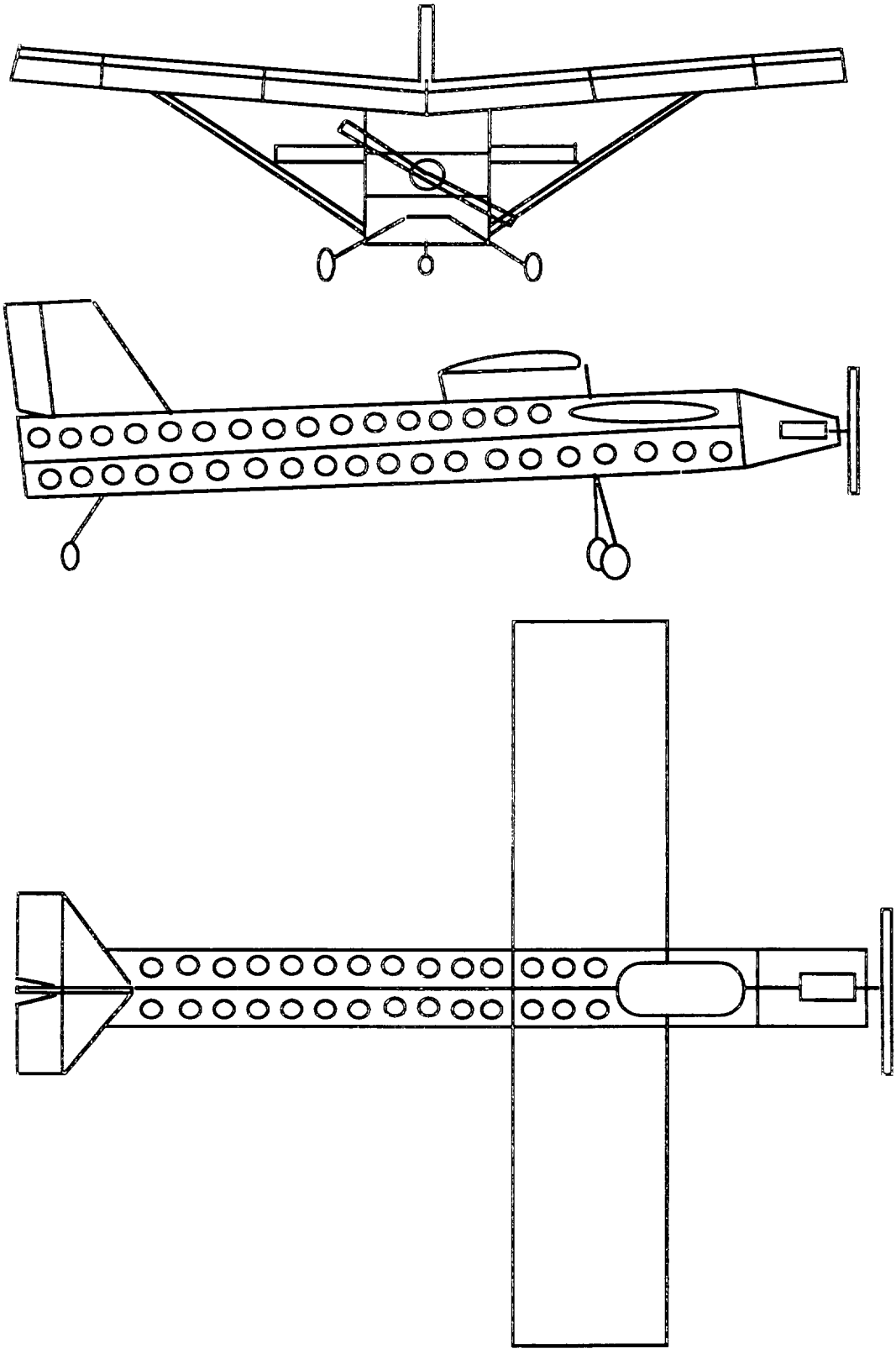

single-level seating arrangement. The wing is rectangular with no taper nor sweep, and the landing gear configuration is a tail dragger.

The seating arrangement as shown in Figure 1-8 was chosen to be 3 passengers/row x 24 rows so that the same fuselage length is maintained while using the flat body of the fuselage as a lifting surface. The 72 seats will allow for 70 passengers plus two flight attendants. One foot of the inside of the fuselage was used for the placement of the servos, the speed controller, the receiver, and the batteries. This design has two control servos: a twin rudder system and an elevator. The fuselage is tapered near the tail which will improve the flow around the two vertical tails. The twin vertical tails are an innovation to further alleviate effects of vortex shedding from the wide fuselage.

However, there are some disadvantages to this design. The seating arrangement could cause a slight imbalance in the weight distribution for which the design must compensate. This wide, long fuselage may create vortices that could interfere with rudder control during the flight. This concept has basically been produced before, and since the design is not very unique except for the twin rudder concept, no new distinct advancements can be made except perfecting this type of design. Finally, this design uses a tail dragger, and therefore it is desirable that the plane be designed so that the tail lifts off the ground first to eliminate tail wheel friction and stresses during takeoff.

The advantages associated with the *Airplane* far outweigh the disadvantages. The first advantage is the twin rudder system which provides greater yaw and roll control than a single rudder system. This type of rudder system also allows for the implementation of a wide fuselage without excessive concern for a loss of directional control due to vortex interference. The long, wide fuselage shape inclined at a small angle of attack could produce some additional lift. The frontal area of this fuselage is slightly less than the double-

decker concept due to less structural parts (i.e. the platform, etc.,) which will result in less drag and reduced weight. This design carries 30 more passengers than the competing HB-40, enabling this aircraft to serve over 50% of the market. Also, in order to cover the market of 140 passengers and 10000 foot range, the HB-40 would have to make four flights to transport these passengers whereas the *Airplane* would only have to make two flights. The tail dragger landing gear gives the aircraft a "natural" angle of incidence on the ground to aid in takeoff performance. Additionally, the single engine concept eliminates the need for balancing thrust at different locations on the aircraft. Finally, the simple, low-risk design concept reduces manufacturing hours and material costs. This reduction in hours and costs is the greatest advantage of the concept since cost is the critical factor in determining the viability of this proposal.

FIGURE 1-7
External Configuration of the *Airplane*

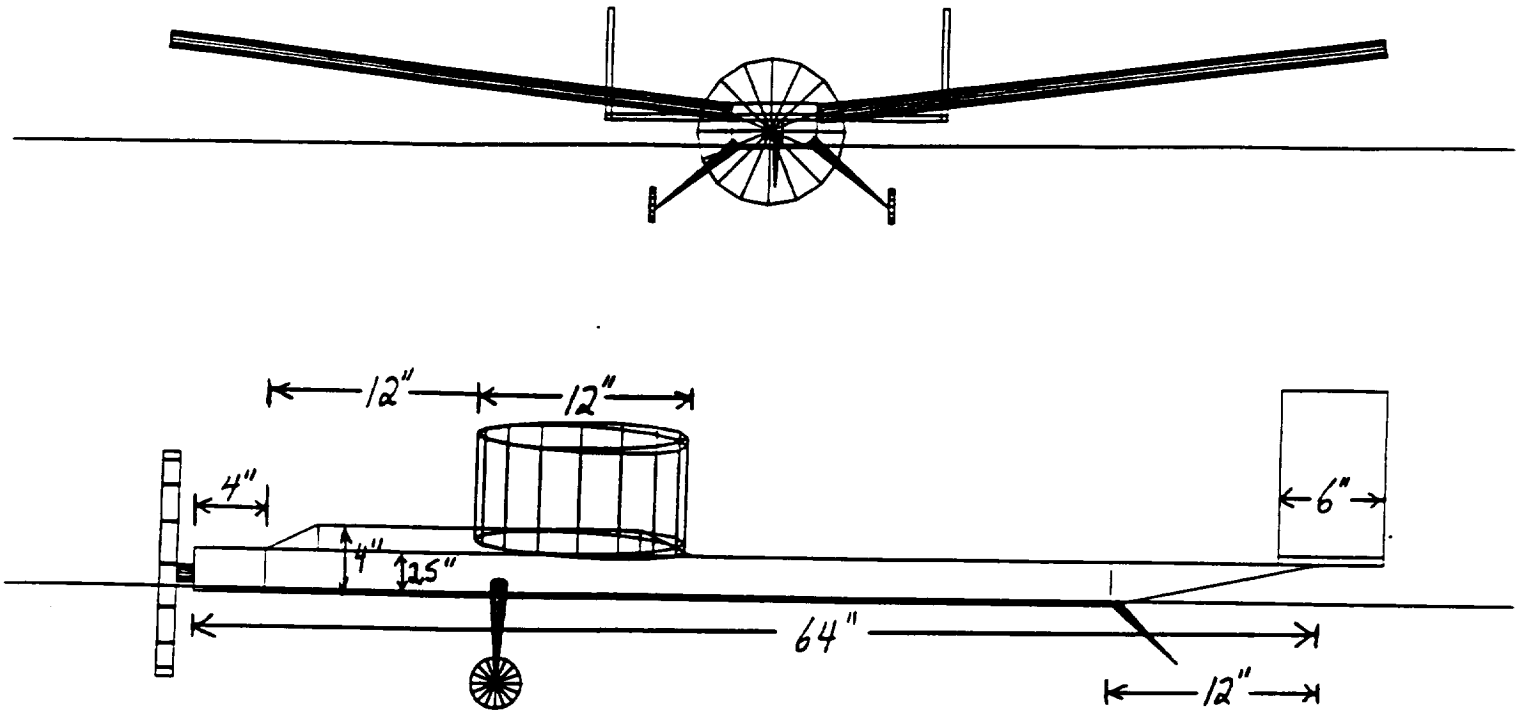

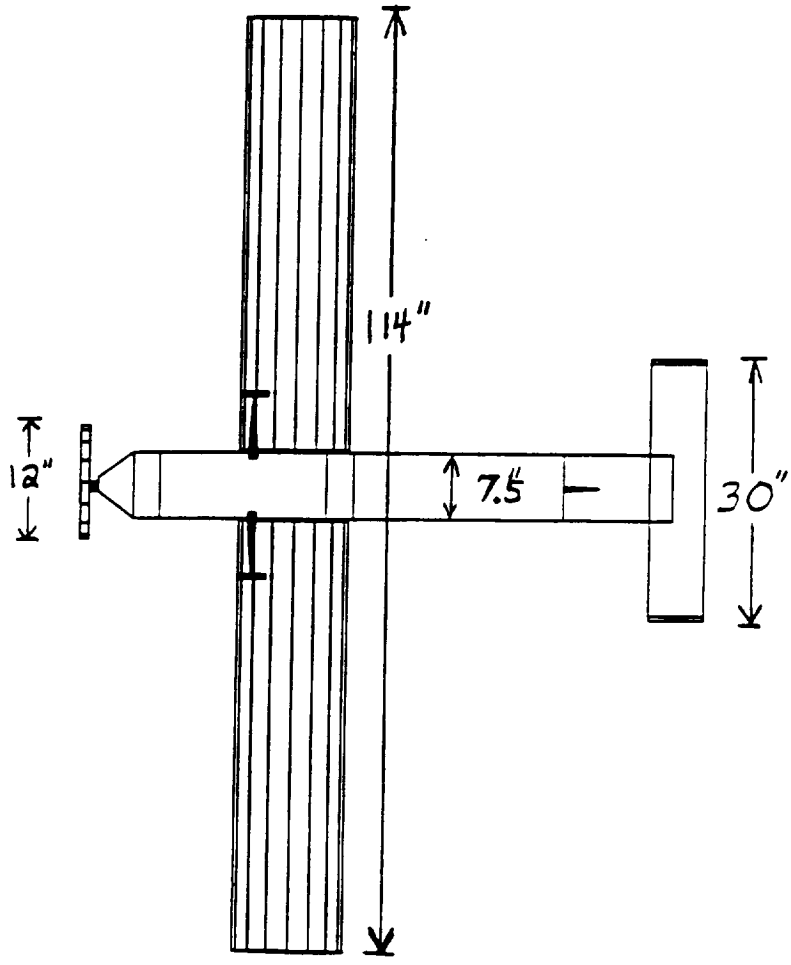

FIGURE 1-8
Internal Configuration of the *Airplane*

○ - passenger
* - flight attendant
● - pilot

1 inch = 8 inches

Level 1

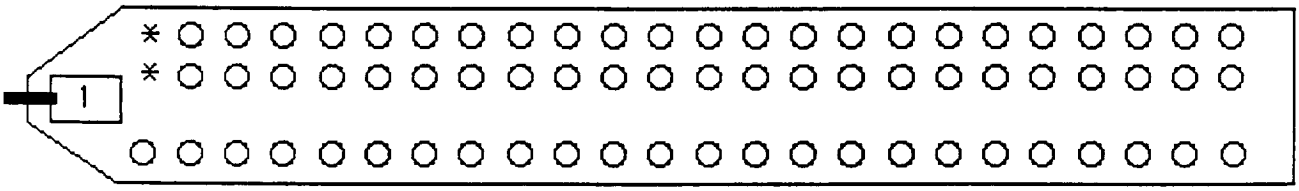

Level 2

Room to move batteries forward/aft for proper c.g. position

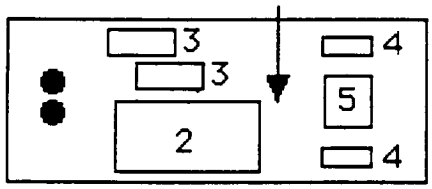

2 - batteries
3 - receiver battery pack/speed controller
4 - servos
5 - receiver

Side

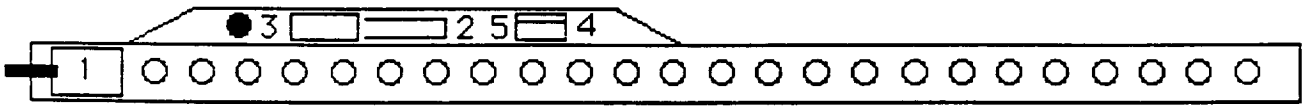

TABLE 1-1
Summary of Concept Selection

Concept	Advantages	Disadvantages
Semi-Delta Wing	- Innovative - Possible drag savings due to streamlined shape	- Not conducive to low speeds - Disturbed flow before props - Rear clearance for props - Lack of data base - Complex wing construction
Biplane	- Reduce wing span - Decrease wing root bending moment	- Difficulty with lower wing attachment - Flow interference between wings - Two wings may increase weight
Low-Wing Monoplane	- Easy access to servos/batteries - Better roll control than high-wing	- Difficulty in wing removal for transport - Less statically stable than high-wing
High Wing Monoplane Double-Decker	- Substantial data base available - Wing is easily removable	- More drag due to large frontal area - Fuselage manufacturing complexity
The *Airplane*	- Simple design - Wide, flat fuselage acts as lifting body - Twin rudder provides more lateral control	- Vortices from fuselage may interfere with rudder control - Potential weight imbalance from passenger placement - Not highly innovative

REFERENCES

1 - 1. "Market Data," *AE 441: Aerospace Design Class Handout*, Spring 1993.

TABLE 1-1
Summary of Concept Selection

Concept	Advantages	Disadvantages
Semi-Delta Wing	- Innovative - Possible drag savings due to streamlined shape	- Not conducive to low speeds - Disturbed flow before props - Rear clearance for props - Lack of data base - Complex wing construction
Biplane	- Reduce wing span - Decrease wing root bending moment	- Difficulty with lower wing attachment - Flow interference between wings - Two wings may increase weight
Low-Wing Monoplane	- Easy access to servos/batteries - Better roll control than high-wing	- Difficulty in wing removal for transport - Less statically stable than high-wing
High Wing Monoplane Double-Decker	- Substantial data base available - Wing is easily removable	- More drag due to large frontal area - Fuselage manufacturing complexity
The *Airplane*	- Simple design - Wide, flat fuselage acts as lifting body - Twin rudder provides more lateral control	- Vortices from fuselage may interfere with rudder control - Potential weight imbalance from passenger placement - Not highly innovative

2.0 AERODYNAMICS

2.1 AIRFOIL SELECTION

The process of airfoil selection began with a list of requirements and information which were deemed necessary to make the process a success. The following items were investigated:

* Thickness of the section to withstand the required loads
* The design Reynolds Number
* Stall characteristics
* Maximum lift coefficient
* Drag characteristics
* Moment coefficient
* Manufacturability

Airfoils with thicknesses in the range of eleven to thirteen percent chord provide the highest lifting characteristics at low Reynolds Numbers (reference 2-1). This range of thicknesses, with a chord of approximately one foot (the average airfoil chord length from the data base for similar aircraft), would be sufficiently thick to easily hold beams of any of the considered materials to support the required loads. As analyzed with bending moment calculations and material data, the primary spar dimensions will easily fit within the wing. With the thickness requirement, the number of possible airfoils, taken from *Airfoils at Low Speeds* (reference 2-2), was reduced to nine. Airfoils with similarly high maximum lift coefficients yet lower or higher than eleven to thirteen percent thicknesses were considered exceptions to the trend and were also investigated.

Next, the design Reynolds Number was calculated so that the proper data/graphs from (reference 2-2) could be determined. From the data base it was seen that the average chord length of previous designs was about one foot; this

was used to initially determine an approximate Re, though not to determine the design chord length. The design cruise speed of 31 ft/s (21.1 mph) and an estimated design altitude of sea level (because of the low cruise altitude of the design) were used to complete the calculation:

$$Re^* = 9324 \cdot V(mph) \cdot c(feet) = 197000$$

*reference 2-1

This result made the lift estimations fairly accurate because one group of tests on the airfoils (reference 2-2) were done at Reynolds Numbers at or near 200000.

The stall characteristics of the airfoils at the design Reynolds Number were then examined. A fairly high yet reasonable stall angle requirement of greater than ten degrees was established because of the way in which the aircraft would be flown. The pilot will be flying the plane for the first time and will not have much time to familiarize him/herself with the control characteristics. With a higher stall angle, there is more room for pilot error, especially at the critical conditions of takeoff and landing. Ten degrees was chosen because this was a good cut-off point to narrow down the airfoils regarded while leaving a sufficient number for investigation in the other areas of interest. There were approximately seven airfoils which met the stall angle requirement.

The airfoil lift characteristics were definitely a priority in the selection process. In order to determine the coefficients necessary, it was first required to roughly size the wing and determine the minimum speeds at which the aircraft would fly. This was partially completed on a trade study with weight varying between our preliminary limits of 4.5 - 5.5 pounds and wing loading varying between nine and eleven ounces per square foot. It was found that a wing planform area of between nine and ten square feet would guarantee a wing loading near the lower end of the limits. For the minimum speeds, the group had set a takeoff velocity goal of less than 25 ft/s so that the takeoff roll could be

reduced to below 24 feet enabling the plane to fly into and out of more airports (the HB-40 takeoff speed was calculated at 25.5 ft/s with a roll of 26.5 feet). The speed and wing area were used to determine that the total aircraft would have to generate a lift coefficient of at least 1.0 to takeoff. Because the total lift coefficient of the aircraft is lower than that of the section due to 3-D effects, it was determined, using the computer application *Wing Design* , that the section must have a maximum lift coefficient of at least 1.2 in order to guarantee a wing 3-D lift coefficient of 1.0. This narrowed our selection down to six airfoils: the Clark-Y, E193 MOD, Spica, E214, Wortmann, and SD7032.

The C_{D_o} of each remaining airfoil was then tabulated for final comparison and selection. Drag, as further explained in Section 2.4, becomes as significant as lift because its magnitude determines the power required to operate the aircraft. The C_{D_o}'s for the airfoils investigated are shown in table 2-1 below.

A section moment coefficient near zero was desired. With a lower coefficient, the tail would require less trim to overcome the pitching moment of the wing to insure airplane stability; hence, less trim drag would be accrued. (reference 2-1.) All of the airfoils considered had similarly low moment coefficients, and a lack of background information on the topic made it impossible to assess how significant the differences were in terms of trim requirements. Thus, the near- zero moment coefficient goal was placed as a lower priority.

The significant data for the remaining airfoils is tabulated below (at a Reynolds Number near 200000):

TABLE 2-1
Comparison of Airfoil Characteristics

AIRFOIL	MAXIMUM Cl	C_{D_0}	STALL ANGLE
CLARK-Y	1.2	0.014	10°
E193 MOD	1.2	0.014	10°
SPICA	1.42	0.03	14°
E214	1.3	0.02	10.5°
WORTMANN	1.6	0.032	11°
SD7032	1.3	0.02	11°

Manufacturablity was the final consideration. It was seen by looking at previous designs that airfoils with flat lower surfaces allowed the monokote to more easily retain the airfoil shape between ribs, thus increasing performance predictability because of the consistency in shape. Also, a flat bottom airfoil would be easier to manufacture, especially in accurately carving the airfoil ribs from a pattern on a sheet of balsa. The Spica airfoil was the only of the above airfoils to have a flat underside. It also had the highest stall angle and the second highest maximum section lift coefficient. Therefore, the SPICA was chosen as the *Airplane's* airfoil section. The airfoil Cl/α curve is shown in Figure 2-1.

FIGURE 2-1
Section Lift Coefficient vs. Alpha
Spica PT/Re = 202300

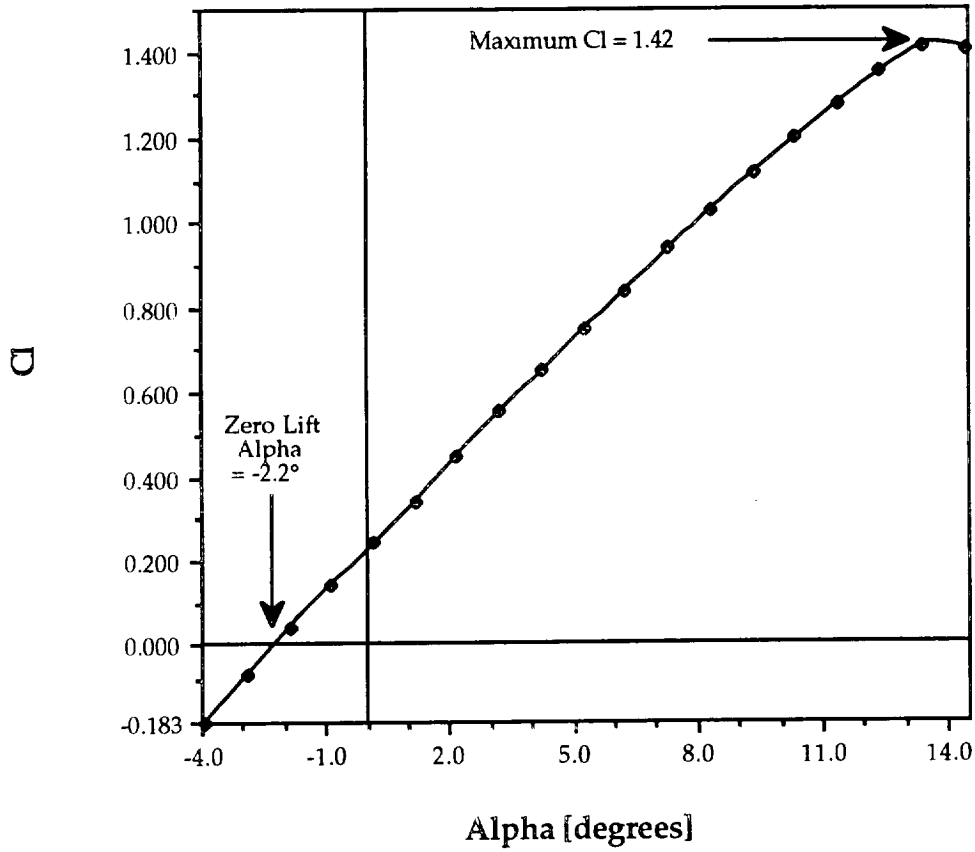

2.2 WING DESIGN

Because of the choice of a high lift airfoil, it was desired to design the wing with a sufficiently high aspect ratio in order to minimize the induced drag. The importance of the chord length as related to the design Reynolds Number was also considered; the performance of the airfoil improves with increased Re. It was decided that the chord would be held at one foot to provide the desired Reynolds Number without decreasing the aspect ratio.

As stated in Section 2.1, the goal for wing loading was between nine and eleven ounces per square foot. With improved weight data and engine/battery information, the weight estimate became more precise with a maximum of 5.25

pounds. It was decided that a span of 9.5 square feet would give a sufficiently high aspect ratio (9.5) and a (more than) sufficiently low wing loading of 8.84 ounces/sq. ft. This smaller load will lead to more weight advantages in the structure of the wing and wing attachment configuration.

It was decided that for ease of manufacturing and lack of significant aerodynamic gains, (reference 2-3) for the cruise condition, the wing would have no sweep, taper, or twist. The wing design has 8° of dihedral in order to provide sufficient roll stability. The wing will be mounted at an incidence of 3° in order to offer a low aircraft cruise angle of attack (< 2°) with little required trim.

2.3 AIRCRAFT LIFT ESTIMATION

The program LinAir 1.49 was used in order to estimate the lift of the entire aircraft. Only the contributions from the wing and horizontal tail were modeled. Though the *Airplane*'s fuselage will provide some lift due to it's width, any lift contributions from the fuselage were deemed insignificant when compared to the forces of the lifting surfaces. Also, any lift generated by the fuselage in actual flight will enhance the performance of the aircraft because of the added, unpredicted lifting contribution and will certainly not cause any problems which could have been predicted by the LinAir model.

The design was carefully modeled with the proper number of panels on each surface so that they would line up and give accurate results. The program input files, results, and a schematic of the model are shown in Appendix A. Also, the Cl vs. Cd for the airfoil was plotted and a curve was fit to it in order to obtain the CD# coefficients (see Appendix A) for the airfoil description and modeling in LinAir. The same was done for the tail using data from flat plate experiments at half the design Reynolds Number (the horizontal stabilizer chord is half the wing chord). As suspected, 3-D effects caused the maximum lift coefficient of the

aircraft (1.28) to be less than that of the airfoil section (1.42). The C_{Lmax} occurred at an aircraft angle of attack of 10°, the configuration at which the section lift coefficient of the root of the wing on the LinAir model fell just under the maximum section lift coefficient of the Spica. The aircraft C_L/α curve is shown in Figure 2-2.

FIGURE 2-2
Complete Aircraft CL/Alpha Curve

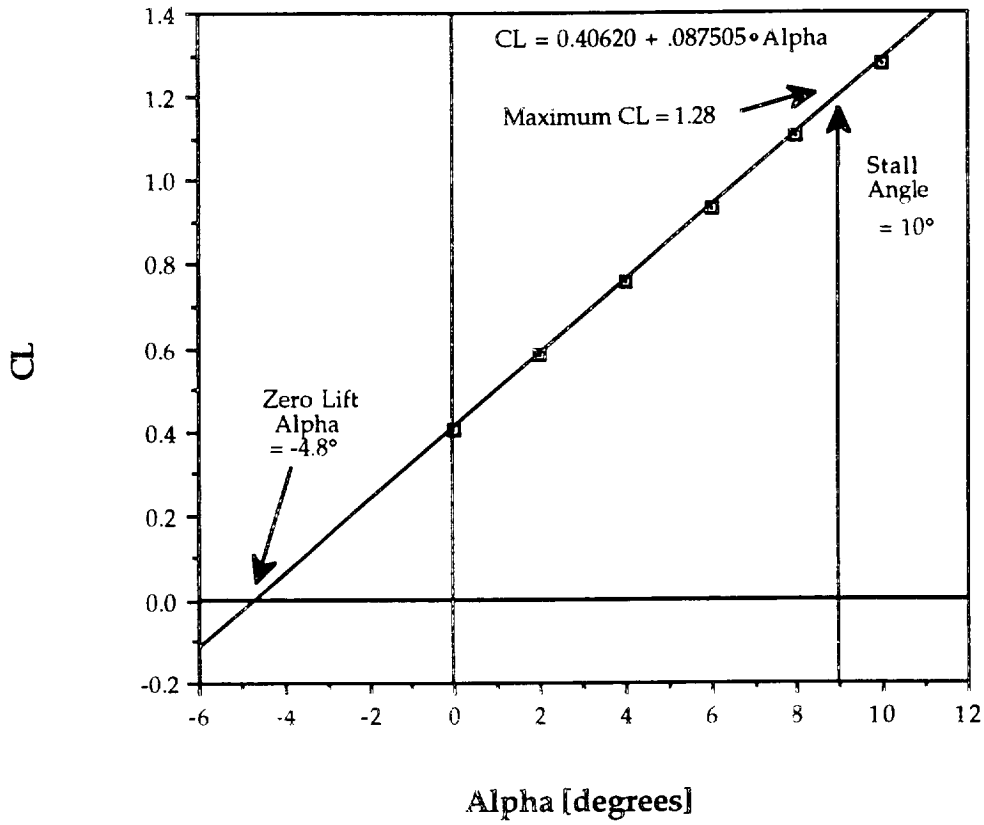

2.4 AIRPLANE DRAG

Drag determination played an integral role in the *Airplane* design process. An estimate of its value was necessary in order to begin to select the propulsion system for the aircraft. Drag is also related to the range and endurance of the plane in that it dictates the power required. Although low drag is desired when

designing a plane, other considerations took priority in the case of the *Airplane* design. The design of the fuselage and landing gear, which are large contributors to the overall drag, were governed mainly by such objectives as ease in manufacturing, structural integrity, and passenger accommodation, and not by drag minimization efforts. However, accurate drag predictions were required throughout the design process.

To determine the aircraft drag, both the profile and induced drag were estimated. These two values added together account for the overall drag as follows:

$$C_D = C_{Do} + \frac{C_L^2}{\pi\, AR\, e}$$

The first term is the profile drag. This was estimated using a component build-up method as presented in reference 2-4. Each airplane component's drag coefficient was determined either from reference 2-4 or reference 2-5. The areas on which the component drag coefficients were based to determine the overall C_{Do} were determined and used in the following formula:

$$C_{Do} = \frac{1}{S_{ref}} \sum C_{D\pi} A_{\pi}$$

The S_{ref} term refers to the wing area, which is 9.5 square feet for the *Airplane*. As explained in reference 2-4., the component $C_{D\pi}$'s were based on particular areas, i.e., the frontal area for the fuselage. Table 2-2 below lists the values used in the build-up process, the percentage of the total C_{Do} of each component, the totals, and the references from which the values were obtained.

TABLE 2-2
Component Drag Buildup

Component	$C_{D\pi}$	A_π [ft^2]	$\frac{C_{D\pi}A_\pi}{S_{ref}}$	% of C_{Do}	Reference
Wing	.007	9.5	.007	19.6	2-4.
Fuselage	.9	.208	.0197	55.1	2-5.
Vert. Tail	.008	1.25	.0011	3.1	2-4.
Horiz. Tail	.008	.833	.0007	1.9	2-4.
Front Gear	1.0	.0668	.007	19.6	2-5.
Rear Gear	0.2	.0122	.00026	.7	2-5.
Total	N/A	N/A	.0357	100	N/A

The area listed for the vertical tail represents the sum of the areas of the two vertical tails on the *Airplane*. Using these values, the $\sum C_{D\pi} A_\pi$ is 0.340 and the C_{Do} is therefore .0357. According to the material from reference 2-4, an additional 15% should be added to this profile drag to account for interference and roughness. This yields an airplane profile drag coefficient of .041. This value is reasonable based on comparison with existing aircraft of similar geometry.

The induced drag is a function of the lift coefficient squared, the Oswald efficiency factor (e), and the wing aspect ratio. The *Airplane* has an aspect ratio of 9.5. To determine e, the following equation was used (reference 2-6.):

$$\frac{1}{e} = \frac{1}{e_{wing}} + \frac{1}{e_{fuselage}} + \frac{1}{e_{other}}$$

where e_{other} is 20 and e_{wing} and $e_{fuselage}$ are determined from empirical data (graphs) for rectangular wings and fuselages (reference 2-7.). From the graph in reference 2-7, e_{wing} is approximately 0.75. For the fuselage, e is 26.9. The overall e is therefore .704. Using this value and the equation for the induced drag yields the drag polar, a function of C_L^2:

$$C_D = 0.041 + 0.0476\, C_L^2$$

Figure 2-3 shows the graph of the aircraft drag as a function of C_L.

FIGURE 2-3
Drag Polar

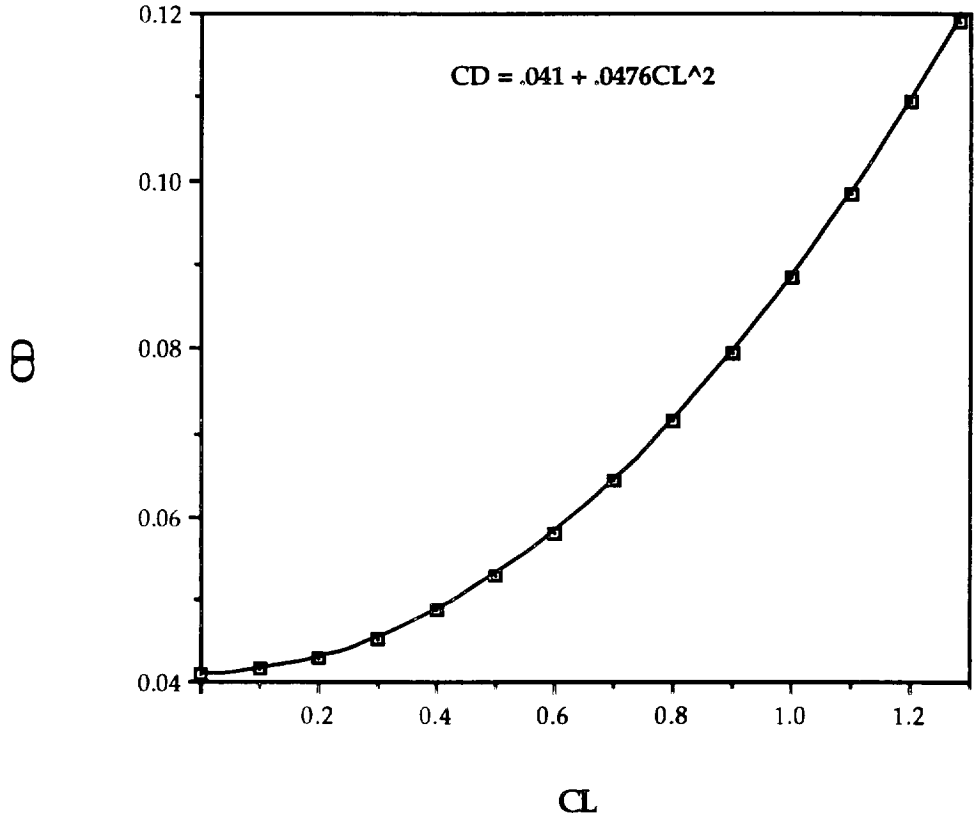

Figure 2-4 shows the aircraft C_L/C_D vs. C_L. This is an extremely important plot in analyzing the efficiency of the aircraft. As can be seen, the cruise L/D lies at 9.5 and the maximum L/D is 11.3. Ideally, the two should be

equal so that at the cruise condition, the configuration at which the *Airplane* spends most of its flight time, the aircraft is most efficient for reduced costs and increased range. The *Airplane* sacrifices some efficiency with its large planform area in order to meet the takeoff requirement of 24 ft. and to cruise slightly faster than the competition.

FIGURE 2-4
Entire Aircraft CL/CD VS. CL

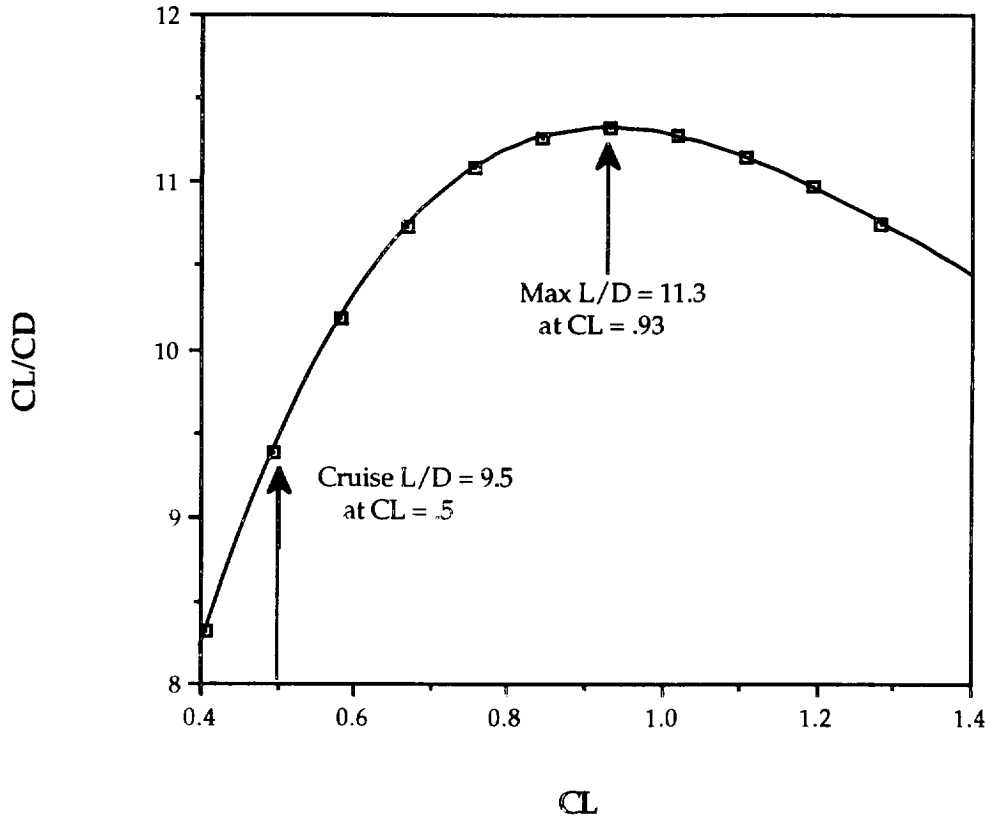

At the cruise velocity of 31 ft/sec, the required lift coefficient for the 5.25-pound *Airplane* is .5, corresponding to a contribution to overall drag due to this lift of .0119. This is less than half of the parasite drag contribution, indicating that parasite is the area to target if drag minimization were of concern.

REFERENCES

2-1. Crawford, Donald R. A Practical Guide to Airplane Performance and Design. Crawford Aviation, California, 1981

2-2. Selig, Michael; Donovan, John F. and Fraser, David B. Airfoils at Low Speeds. H. A. Stokely Publisher, Virginia, 1989

2-3. Hoerner, Sighard F. and Borst, Henry V. Fluid-Dynamic Lift. Liselotte A. Hoerner, New Jersey, 1975

2-4. Nelson, Robert "Subsonic Drag Breakdown Method", University of Notre Dame, Indiana, 1989

2-5. Hoerner, Sighard F. Fluid Dynamics Drag. Published by author, New Jersey, 1958

2-6. Jensen, Daniel "A Drag Prediction Methodology for Low Reynolds Number Flight Vehicles", University of Notre Dame, Indiana, February 1990

2-7. Nelson, Robert. Flight Stability and Automatic Control. McGraw Hill Book Company, New York, 1989

3.0 PROPULSION SYSTEM

3.1 PROPULSION SYSTEM REQUIREMENTS

In order to meet performance requirements, the *Airplane* requires a propulsion system which is lightweight, yet still provides enough power to take-off in a short distance. The Design Requirements and Objectives (see Section 1.2) outlined four objectives for the propulsion system:

* Should be electrically powered to reduce environmental pollution
* One motor and propeller must provide sufficient power for aircraft to avoid complex multiple engine thrust balance
* Battery pack(s) should have flexible placement requirements
* Propulsion system should have variable throttle control

Certain performance, structural, and economic objectives which effect the selection of the propulsion system were also established in the DR&O:

* Must provide enough power so the aircraft can take off in 24 feet
* Must have sufficient fuel so the aircraft can fly a distance of 13000 feet
* Sustain a minimum cruise velocity of 30 ft/s
* Must be lightweight to help meet weight objective
* Must be inexpensive to help reduce overall manufacturing costs

3.2 MOTOR AND PROPELLER SELECTION

With these requirements in mind, three motors and six different propellers were evaluated to determine which combination produced power available in the same range as the power required of the aircraft. Other considerations were weight, price, and fuel requirements. Because of time constraints, existing propulsion components were analyzed instead of attempting to design new subsystems. Towards this end, the Astro FAI 05, the Astro 15, and the Astro 25

motors were evaluated, as well as Zinger 10, 11, and 12 inch diameter propellers. Tables 3-1 and 3-2 list the types of motors and propellers evaluated in the initial stage of the propulsion system selection process. It should be noted that cost and weight differences for the propellers were found to be negligible.

TABLE 3-1
Motor Size and Pertinent Data

Motor	Weight (oz)	Cost	Kv	Kt	Tloss
Astro FAI05	6.5	$103.00	.000437	.5948	1.487
Astro 15	7.5	$107.00	.000796	1.1344	1.5850
Astro 25	11.0	$174.00	.001125	1.5433	2.3613

** the source of this information can be found in Appendix B-1

TABLE 3-2
Propeller Diameter and Pitch

Zinger 10 Series	Zinger 11 Series	Zinger 12 Series
10 - 4	11 - 5	12 - 4
10 - 6	11 - 7	12 - 6

In the process of evaluating these and other Zinger propellers, a new permanent data base was established for AeroWorld containing the details of each propeller's chord, thickness, and performance estimation under varying conditions. The program, "Notre Dame Propeller Program" (Reference 3-1), was used with the option of using simple blade element theory to perform the propeller performance analysis. The chord and thickness of each Zinger propeller were measured, and the propeller airfoil was assumed to be a low Reynolds number airfoil. The radial pitch of the propeller was calculated by:

$$\beta = \tan^{-1} [\text{pitch} / (2 \pi r)]$$

The performance characteristics for each propeller (efficiency, coefficient of thrust, and coefficient of power) are presented in the data base as a function of the advance ratio. This data base is included in Appendix B-2.

From initial calculations of power available it was determined that the Zinger 10-4 and 10-6 propellers could not provide sufficient power for the aircraft. These propellers were not included in further analysis. The motors were evaluated using the recommended battery pack capacities and voltages. As can be seen from Figure 3-1, all three motors exceeded the power requirement of 27.3 Watts. Increasing the diameter of the propeller increased the total power available.

FIGURE 3-1
Power Available for Various Motor and Propeller Combinations

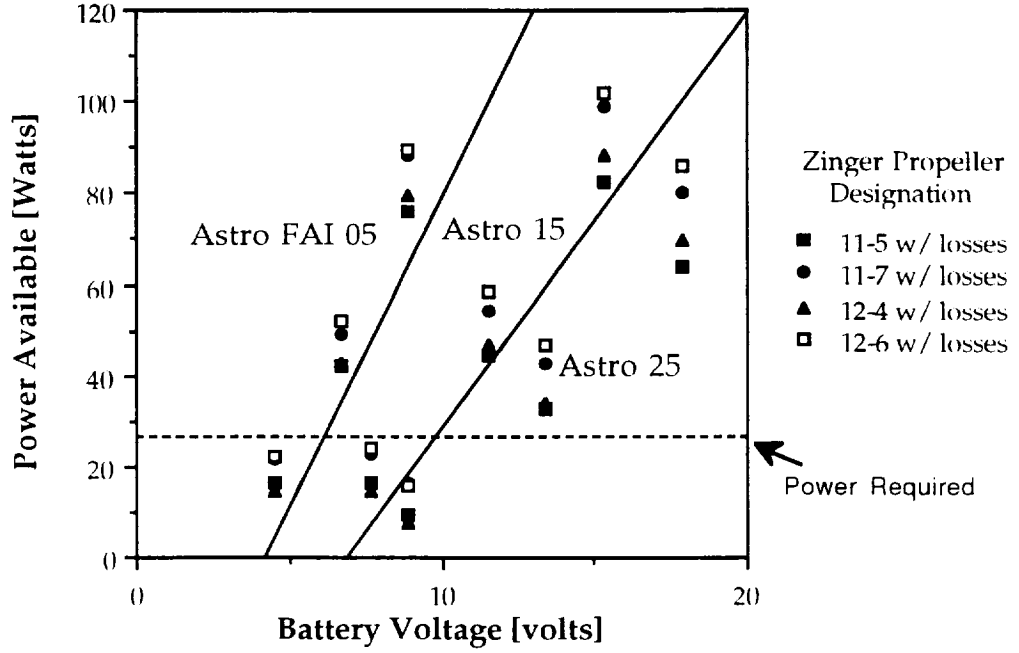

Power available was calculated using a spreadsheet method described by Reference 3-2. The algorithm representing this spreadsheet method and a copy of the spreadsheet can be found in Appendix B-3. Increasing the diameter and pitch of the propellers resulted in an increase in the current draw of the propulsion system. The Astro FAI 05 motor was found to produce only 10% less power available than the Astro 15 but required a much higher current draw (Figure 3-2).

FIGURE 3-2
Current Draw for Various Motor and Propeller Combinations

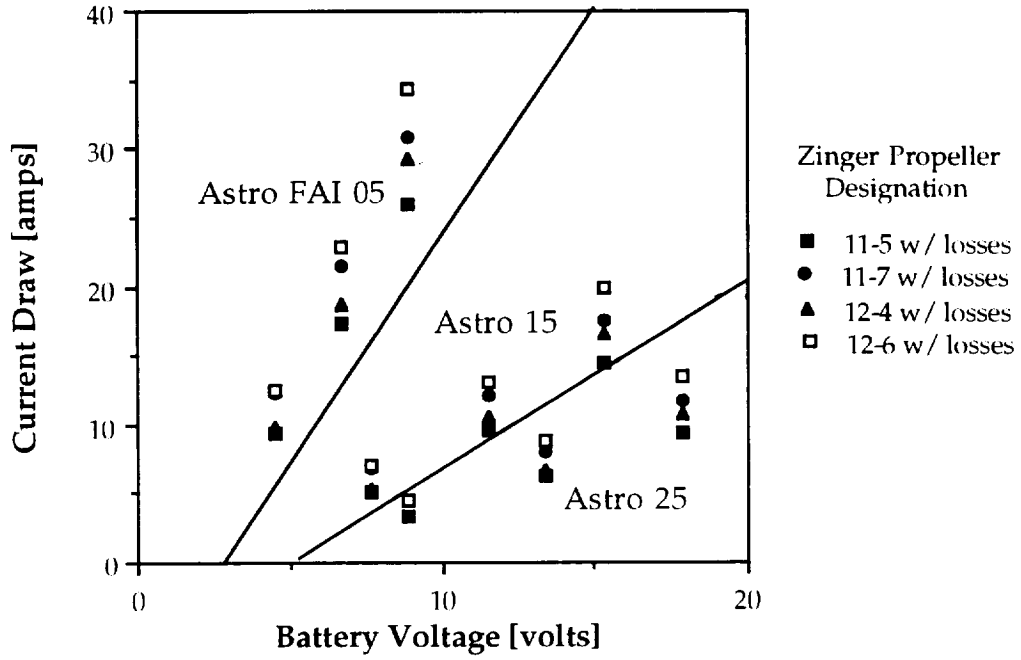

The Astro 25, on the other hand, had a very small current draw; but weighed and cost significantly more than the Astro 15 or the Astro FAI05. A final comparison of the three motors is given in Table 3-3. As can be seen from this table the Astro 15 had the best characteristics overall.

TABLE 3-3
Motor Comparison

Motor	Cost	Weight	Current	Power
FAI 05	Excel	Excel	Poor	Poor
15	Excel	Excel	Fair	Fair
25	Poor	Poor	Fair	Excel

Thus the Astro 15 using the Zinger 11- 7 propeller was chosen as the motor for the *Airplane*. Using the Fortran code, "Takeoff Performance"(Reference 3-3), it was confirmed that the propulsion system was capable of meeting the takeoff distance requirement.

After the motor was acquired, it was discovered that the actual gear ratio of the Astro 15 was significantly different than the data base had suggested. After this change was made to the "Takeoff Performance" analysis program it was found that the chosen propulsion system no longer met takeoff distance requirements. Continued propeller performance analysis revealed that propeller pitch had a greater impact on takeoff performance than propeller diameter. As can be seen in Figure 3-3, the Zinger 12 - 8 propeller provided enough thrust for the *Airplane* to takeoff within the required distance. The next best take off distance was achieved by the Zinger 13-8. This propeller, however, did not meet the minimum takeoff distance requirement. The propeller efficiency of the Zinger 12-8 propeller is given in Figure 3-4.

3.3 BATTERY PACK SELECTION

Twelve 800 milliamp hour batteries were selected as the ideal battery pack for the *Airplane*. This battery pack provided sufficient voltage (14.4 volts) to the motor for takeoff and enough current to meet the range objectives and loiter requirements. However, based on the limited types of batteries available in

FIGURE 3-3
Takeoff Distance for the Astro 15 Motor

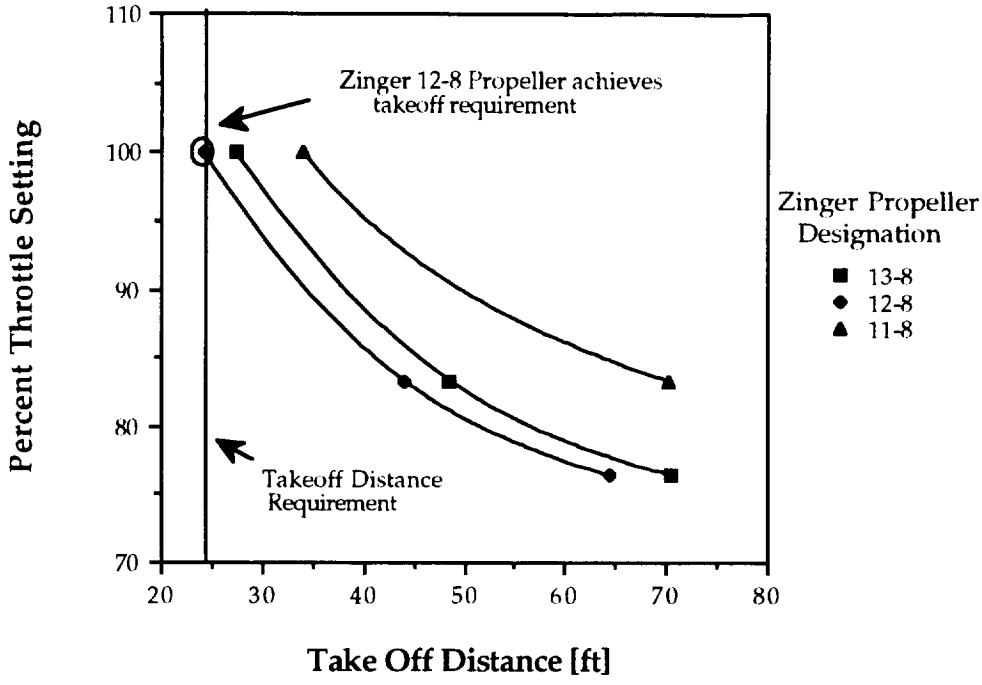

FIGURE 3-4
Zinger 12 - 8 Propeller Efficiency
(including induced velocity and tip losses)

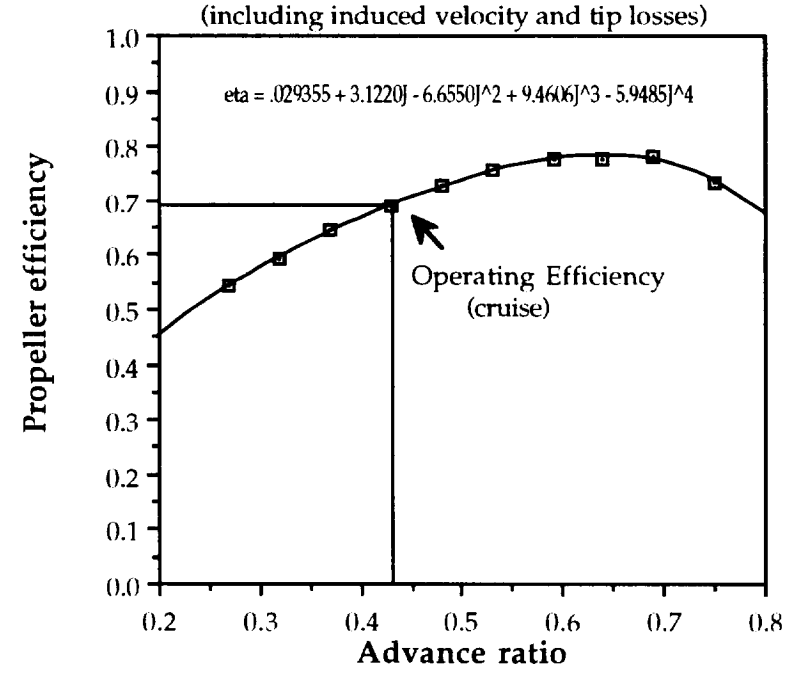

AeroWorld, a selection had to be made between 900 milliamp hour and 600 milliamp hour batteries. It was found that the 600 milliamp hour battery pack would not meet the range objectives, therefore the 900 milliamp hour battery pack was selected. This resulted in an approximately 1.8 oz weight increase from the 800 milliamp hour battery pack. Twelve P-90SCR Ni-Cad batteries (each with a voltage of 1.2 volts) connected in series were selected as the final battery pack for the propulsion system. This pack provides a maximum battery voltage of 14.4 volts and a total of 900 milliamp hours of current. At $3.00 per battery, this battery back was the least expensive of all listed possibilities. At 1.23 ounces per battery, the total weight for the battery pack was determined to be 14.76 oz; 17.6% of the total weight of the aircraft. The battery pack has a maximum current discharge rate of 18 amps, however the maximum current draw of the propulsion system does not exceed 12.3 amps at throttle.

3.4 PROPULSION SYSTEM CHARACTERISTICS

The propulsion system chosen for the *Airplane* meets all of the requirements listed in Section 3-1. The basic propulsion system characteristics can be found in Table 3-4. Actual aircraft performance information using this propulsion system can be found in Section 6.

TABLE 3-4
Summary of Propulsion System

Type of Motor	Astro 15 (Gear Ratio = 2.38)
Propeller Designation	Zinger 12 - 8
Number of Batteries in Pack	12
Battery Pack Capacity	900 milliamp hours
Battery Pack Voltage	14.4 volts

A complete breakdown of the propulsion system, including component cost and weight can be found in Table 3-5. Since the transmitter is kept on the ground, its weight is not included in the total propulsion system weight of the aircraft.

TABLE 3-5
Propulsion System Components

Component	Type	Weight (oz)	Cost
Motor	Astro 15	7.5	$107.00
Propeller	Zinger 12 - 8	1.0	$2.00
Battery Pack	P-90SCR (12 batteries)	1.23 oz per battery 14.76 oz for pack	$36.00
Speed Controller	Tekin	1.66	$50.00
Servos	Futuba S133 (2)	1.8	$70.00
Receiver	Futuba	.95	$35.00
Receiver Batteries	Futuba	2.0	$10.00
Transmitter	Futuba	not important	$75.00
		Total Weight: 28.67 oz	**Total Cost: $385.00**

3.5 MOTOR CONTROL AND INSTALLATION

The propulsion system incorporates a speed controller which allows the pilot to control the voltage across the motor, thus effectively changing the power available from the motor and hence the velocity of the aircraft. In order to take off at the maximum weight configuration of 5.25 lb, the pilot must use 100% throttle. After achieving altitude, the pilot may then throttle back to approximately 55% throttle a maintain the design cruise velocity. In order to climb, the voltage across the motor must be increased. This requires an increase in the throttle setting. Similar action must be taken during a turn in order to maintain altitude.

The motor will be installed in the nose of the aircraft. The battery pack, speed controller, and receiver will be clustered together in the body of the

aircraft. Since these components of the propulsion system make up most of the weight of the aircraft, keeping them together will simplify the establishment of the correct center of gravity. A wiring diagram for the propulsion system is given in Figure 3-5.

3.6 PROPULSION SYSTEM FINAL CONSIDERATIONS

Meeting the takeoff requirement for the aircraft and trying to minimize the weight of the propulsion system were the driving factors in selecting all of the components of the system. All propulsion system requirements have been met by the selected propulsion configuration. However, if the actual constructed weight of the aircraft is any greater than the design 5.25 lb, the minimum takeoff distance objective of 24 feet will not be met. For the one airport in AeroWorld with a runway of 24 feet, the *Airplane* has no factor of safety. However, for the other 13 airports included in the mission objective, the *Airplane* has a takeoff factor of safety of 1.5 to 1.7. Only one airport is in danger of not being served.

FIGURE 3-5
Equipment Configuration

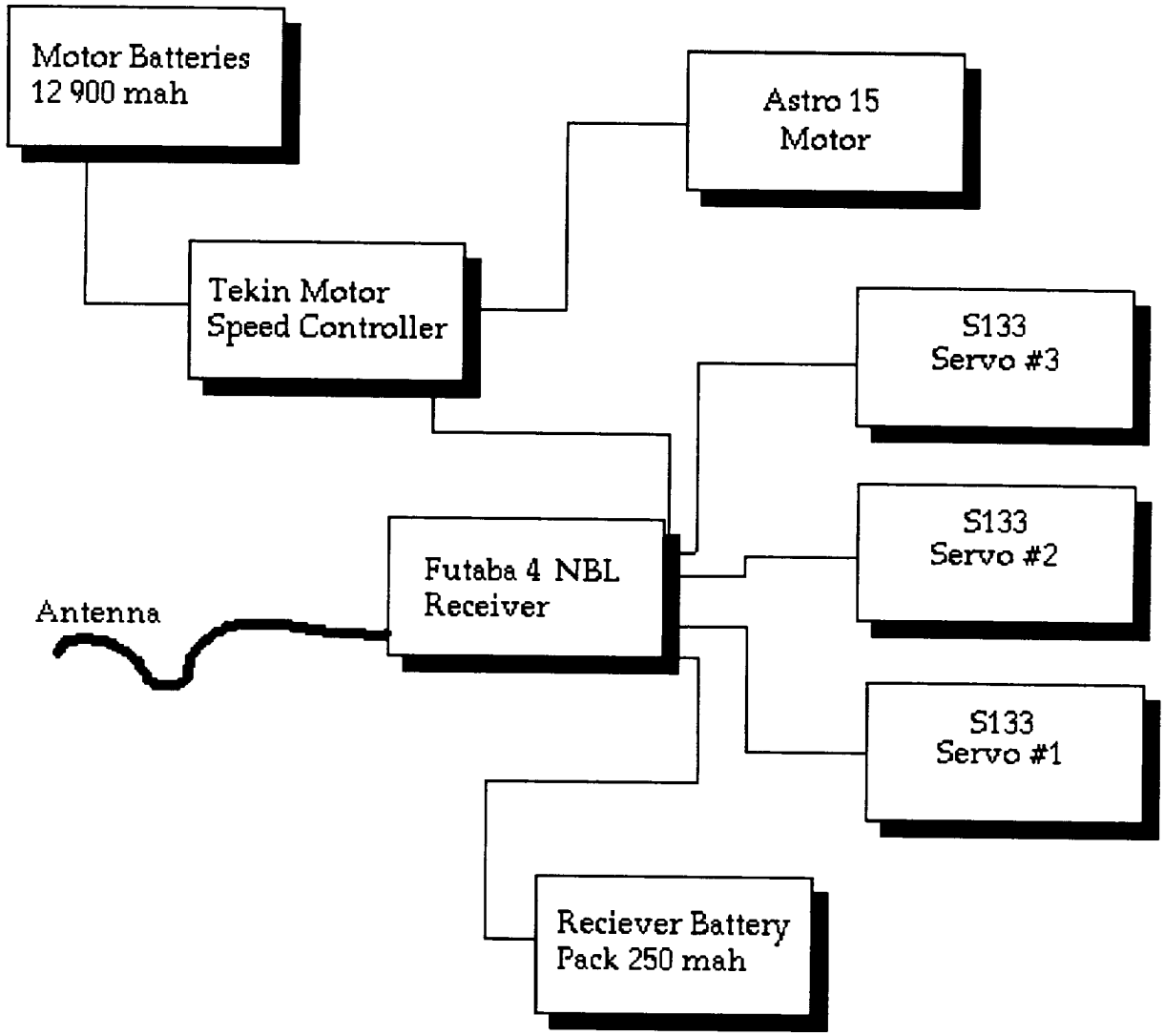

REFERENCES

3.1 Young, Barry, "The Notre Dame Propeller Program", University of Notre Dame

3.2 Dunn, P., "RPV Performance" Excel computer program (modified), AE 454 Propulsion class, University of Notre Dame, 1992

3.3 Batill, S., "Takeoff Performance" Fortran computer program, University of Notre Dame, 1991

4.0 STRUCTURES and WEIGHTS

4.1 *THE AIRPLANE* LOADING

The performance envelope in which the *Airplane* is able operate is depicted in the Velocity-Load Factor (V-n) diagram, Figure 4-1. The V-n diagram includes the stall limits for the aircraft with and without passengers.

FIGURE 4-1
V-n Diagram
For Empty and Maximum Weight

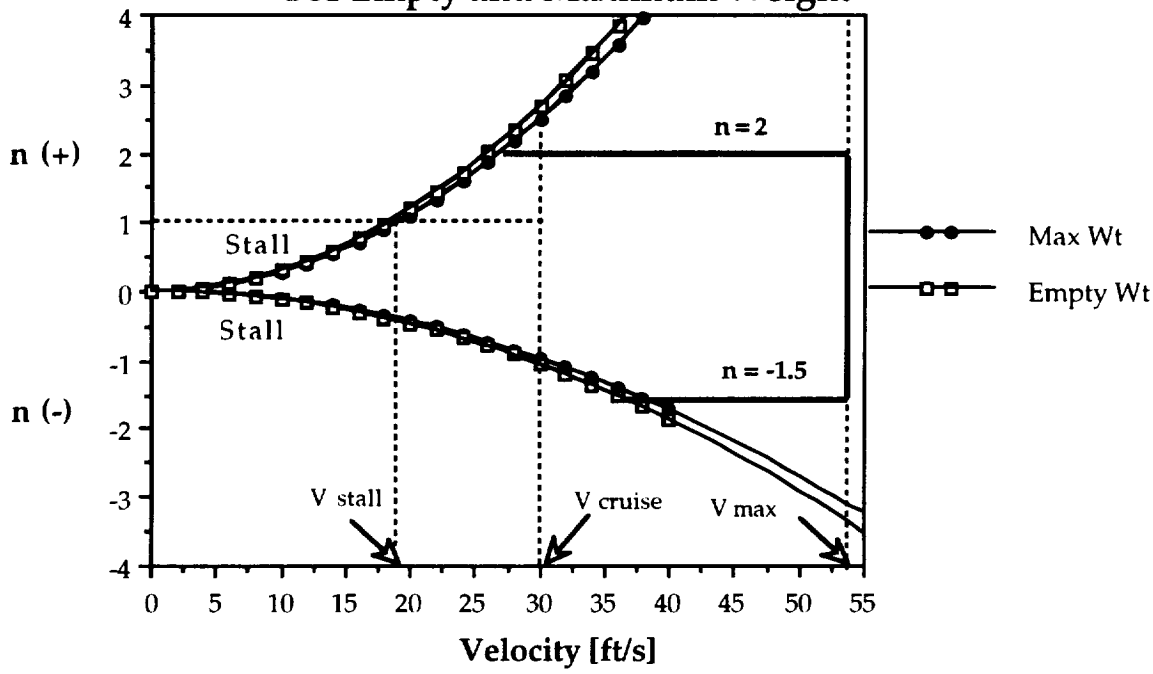

Based on the maximum lift coefficient achieved by the airplane (1.28), the minimum C_L of -0.5, and standard sea level atmospheric conditions (ρ = .00238 lb/ft^3), the stall limits of the diagram were established according to the following relation:

$$n_{max/min} = \frac{1}{2} \rho \frac{S}{W} C_{L_{max/min}} V^2$$

The two extreme weight conditions of the aircraft are 5.25 pounds with 70 passengers and 4.86 pounds without passengers. These two possible aircraft weights do not change the stall limits significantly, as shown in the V-n diagram.

The *Airplane* has a maximum straight and level flight velocity of 54 ft/sec. This is based on power available and power required data at maximum battery voltage. In determining loading limits that the aircraft needed to withstand structurally, several flight maneuvers were considered. In order to cope with possible emergency situations it was estimated that the pilot may need the aircraft to perform sustained turns at high bank angles at velocities in excess of the cruise speed. Calculations of the resulting load factors yielded a limit load of 1.3. This is the load factor experienced by the plane while performing a 45 foot radius turn at approximately 35 ft/sec and a bank angle of 39 degrees. This maneuver is much more structurally demanding on the aircraft than the anticipated and required maneuvers. Performance requirements set by management stipulated a 60 ft radius turn at 25 ft/s. An ultimate load factor of 2.0 was set in order to account for these types of emergency flight maneuvers and to allow for a 1.5 factor of safety.

The *Airplane* is not expected to experience any negative loads during flight since it is not designed to perform inversion maneuvers or to fly in an environment with gusts of any kind. If, however, during takeoff or landing the aircraft stalls or crashes from some height above ground, some negative loads may occur if the landing gear does not absorb the energy associated with the fall and the aircraft 'bounces', travelling vertically upward. It was estimated that the plane could fall from no more than approximately five feet and be expected to maintain its structural integrity. Free-fall of the 5.25 pound plane from this height and assuming 30% of the momentum is conserved after a 0.1 second

collision between the landing gear and the ground yielded a negative load limit of approximately -1.5. This is merely an estimate of what was a reasonable 'crashing' height for an aircraft to withstand.

These limiting loading situations dictated requirements for the Airplane Guys manufacturing team in order to ensure structural integrity during all flight phases and any unexpected maneuvers. Note the cruise velocity is indicated on Figure 4-1. It intersects the straight and level flight load condition (where n=1) well within the flight envelope. Thus, there is no danger of approaching any of these loading limits unless the pilot directs the *Airplane* to perform unexpected or demanding maneuvers.

4.2 FLIGHT AND GROUND LOADS

4.2.1 Ground Loads

While on the ground the *Airplane* will be required to maneuver during taxi, takeoff and landing. The ground loads of the *Airplane* were estimated from the weight and position of all the aircraft components All were analyzed as concentrated loads except the payload, fuselage and passenger floorboard weights, which were analyzed as distributed loads. For this analysis, the aircraft was constrained at the main gear and tail wheel location. The resulting shear and bending moment diagrams appear as Figures 4-2 and 4-3.

FIGURE 4-2
Shear Force Diagram: Ground Loads

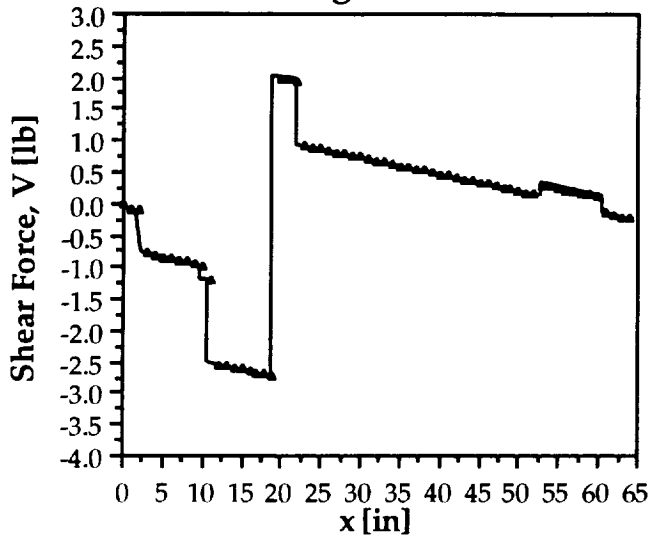

FIGURE 4-3
Bending Moment Diagram: Ground Loads

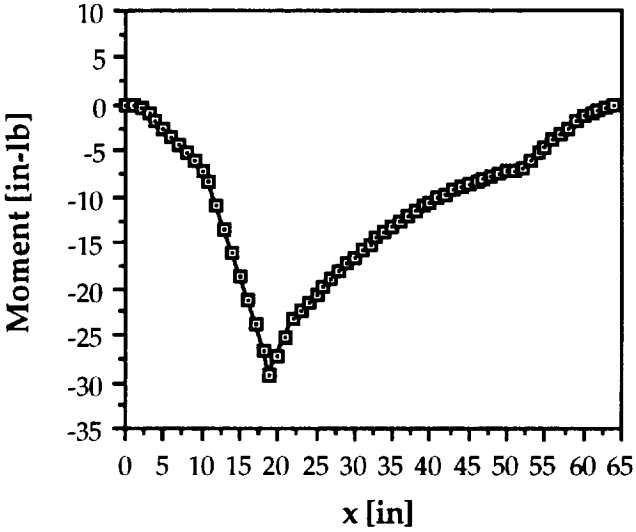

The largest ground loads that must be sustained are those associated with landing. An estimate of the landing force for a fully loaded weight condition is 8.2 pounds. This is based on the impulse formula:

Ft=mv

where the decent rate of 5 ft/sec and an impulse time of 0.1 seconds were estimated. This corresponds to a landing load estimate of 1.6. The landing gear will absorb much of the energy of the landing and will be attached to the fuselage where wood that is stronger than balsa, such as plywood, will be used. The design of the landing gear is discussed later in this chapter.

4.2.2 Flight Loads

During flight, the wing will carry much of the loads. While flying at the limit load of 1.3, the wing for a 5.25 pound aircraft will produce 6.8 pounds of upward force. This lift distribution will create a maximum bending moment about the root chord of 110.3 in-lbs. Figure 4-4 shows this bending moment as a function of distance along the span (Ref. 4-1)

FIGURE 4-4
Wing Bending Moment

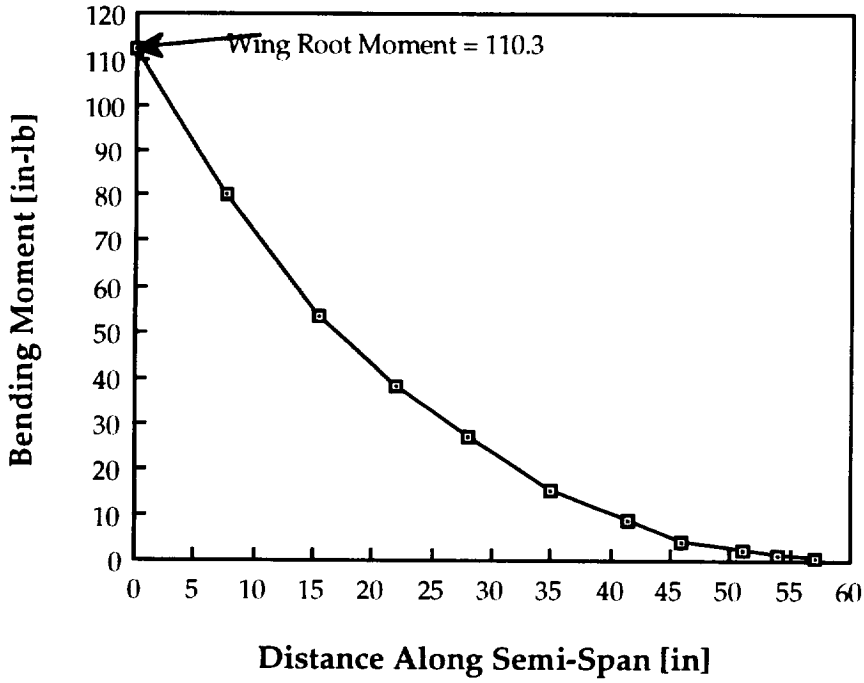

4.3 STRUCTURAL COMPONENTS

The structural design for the main components of the *Airplane* was based on existing plans of other flight worthy aircraft of similar scale and configuration, including the competitor, the *Hot Box*.

4.3.1 The Fuselage

The fuselage is mainly a truss structure comprised primarily of balsa wood. The use of trusses provides strength without the use of a lot of wood, which would add weight. As depicted in the scaled three-view schematic of the *Airplane*, Figure 1-7, the fuselage length is 64 inches, the width is 7.5 inches, and the height is 2.5 inches. At the front, the fuselage has a 2 foot long section providing an additional 1.5 inches of height. This is where the wing is attached and where the majority of the propulsion system is housed. The 70 passengers and 4 crew members require a floorboard. This will be made of balsa, the lightest available material, with holes ("chairs") cut out. Because many past airplanes have been over-designed (Ref. 4-2), few supports beyond those required to maintain the shape of the fuselage when the skin is added will be used. This is important since weight minimization was a primary objective for the design. The MonoKote, which is a heat-shrinkable film to be used as the aircraft skin, will provide additional strength to withstand flight and ground loads. Figure 4-5 is a schematic of the proposed fuselage truss-structure layout.

FIGURE 4-5
Fuselage Structure: Side and Top Views

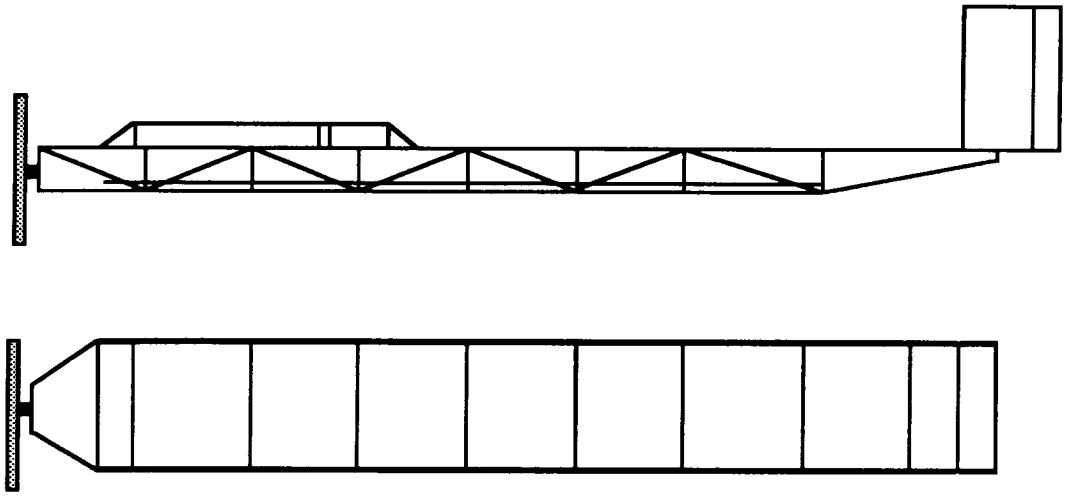

The fuselage can be modeled as a beam which is subjected to both concentrated and distributed loads. These loads are due to the aerodynamic forces and the components making up the overall weight of the aircraft: passengers, avionics, propulsion system, landing gear, and the empennage. The longerons are the members that support the bending loads during flight and were considered the most important structural part of the fuselage. There will be four longerons forming the basic rectangular shape of the fuselage and they will be made of spruce. Section 4-3 includes the factors influencing the selection of materials for the structure of the *Airplane*. For a given direct stress due to bending capacity, a longeron made of spruce can have a cross-sectional area nearly 2.5 times smaller than the area required for balsa (Ref 4-2). This was an important consideration for the Airplane Guys because the fuselage is only 2.5 inches tall in some sections and large pieces of wood would infringe on the volume available for payload, propulsion and avionics equipment, and repair/work access. Thin plywood sections will be used to support parts of the subsystems that are heaviest or need to be screwed into the wood. Some of these

components include the motor and landing gear attachments. Again, section 4-3 includes the advantages of plywood.

The volume requirement for the passengers as dictated in the Request for Proposals and the space requirements for all equipment on board drove the design of the fuselage structure. In addition, the fuselage needed to be designed with an internal configuration which would accommodate movements of fuel (two battery packs, each with six batteries in series) such that the center of gravity was at the desired location.

4.3.2 The Wing

The wing structure will be made of balsa SPICA airfoil shapes and a single spar at approximately 30% of the chord (Ref. 4-3). Based on the designs of existing aircraft, the airfoils can be made slightly lighter by cutting out much of the wood, leaving only the outline shape of the airfoil. In addition to the spar, the MonoKote skin will provide added strength to the extent that keeping the airfoil shape should drive the structural design of the wing (Ref. 4-1). The *Airplane* is a high-wing aircraft. The wing will be attached using a spruce/plywood slot assembly. It is at this attachment point that an emphasis on strength is important since the material used in the assembly will be subjected to the large bending moment (110 in-lb). The wing will be attached such that it is flush with the top of the fuselage, thus eliminating the additional drag that would have been incurred had the wing simply been set on top of the fuselage. The wing is 9.5 ft^2 with a chord length of 1 ft.

The spar will be made from spruce since it will carry the loads due to bending in flight, as discussed in section 4.2.2. A study of existing RPV aircraft with wing areas of at least eight square feet indicated that a single spar would provide enough strength to support the bending moment. To estimate the size of

the spar and determine if a web is necessary, a spar stress analysis was performed using the TK Solver Plus equations (Ref. 4-4) and input values listed in Appendix C. The analysis is based on cantilevered beam theory and assumes a uniform lift distribution over the wing. In this case, the spar is cantilevered at its midspan location. For spars made of spruce, the maximum allowable stress including a factor of safety of 2 is 3100 psi. Figure 4-6 shows the variation in spar axial stress as the spar cap width and height are varied for the case when no web is used. Figure 4-7 shows the same stress/spar size relationship for a wing including a web. The graphs each note the allowable stress limit for spruce. The limit set at a spar height of .25 inches is due to the observation that increasing the height beyond this value yields no significant decrease in the spar stress. Note that when a web is used (the web used for these data is made of 1/16 inch thick balsa), all but one combination of spar cap dimensions satisfies the maximum stress requirement. The data in both Figures 4-6 and 4-7 represent the case when the aircraft is operating at its limit load factor, 1.3. Figure 4-8 depicts how the weight of the spar varies with different spar dimensions.

FIGURE 4-6
Stress in Wing Spar vs. Spar Cap Dimensions: No Web

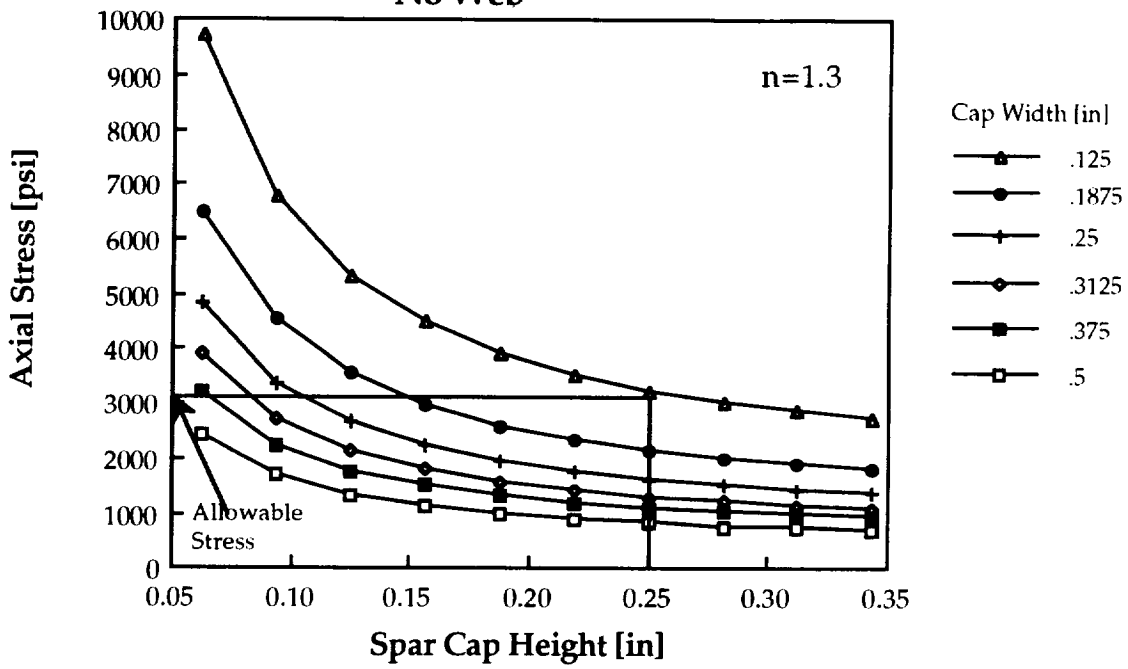

FIGURE 4-7
Stress in Wing Spar vs. Spar Cap Dimensions: With Web

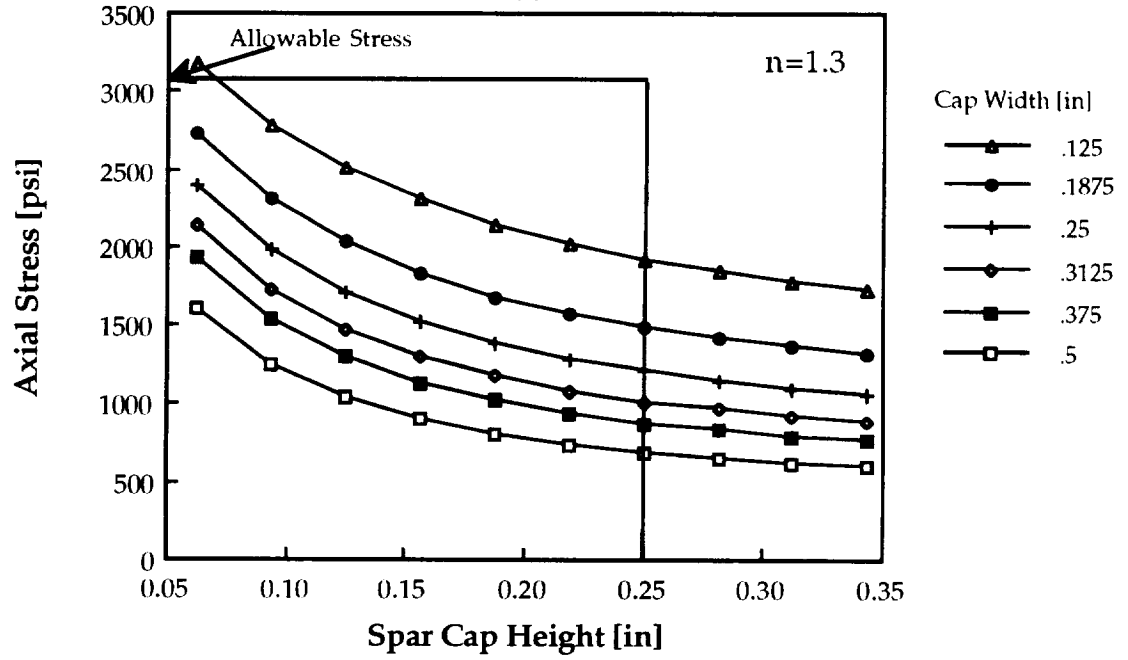

FIGURE 4-8
Spar Weight vs. Spar Cap Dimensions

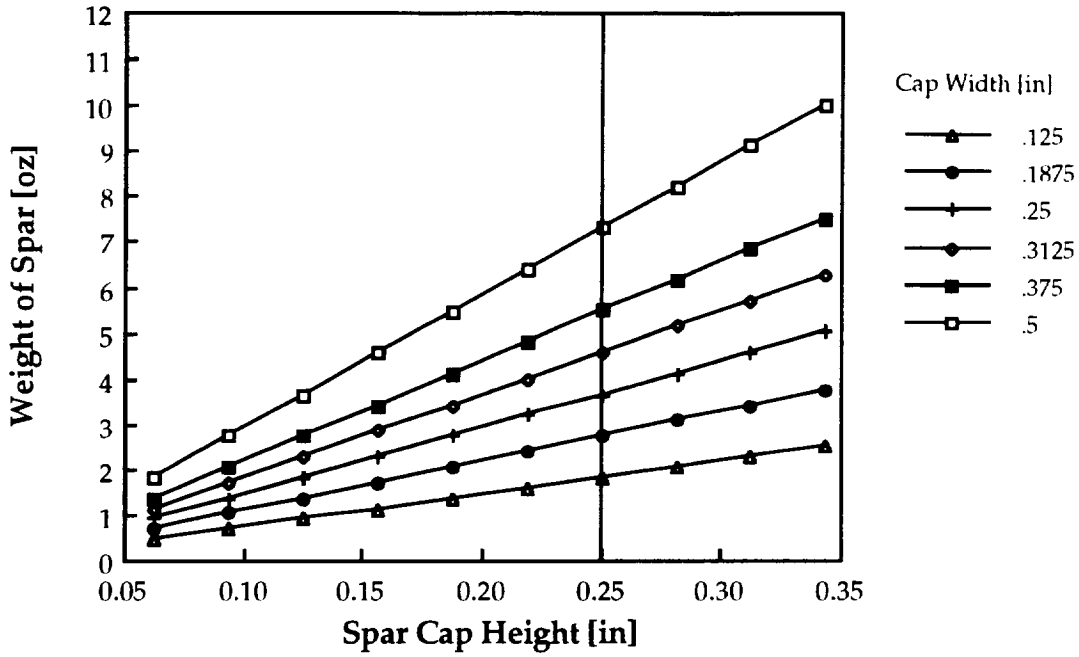

Figures 4-6 through 4-8 provide guidelines for choosing the optimum sized spar caps to satisfy the stress requirements as well as to minimize the weight. The graphs indicate that the use of a web reduces the required size of the spar caps. A web of the size and material used in this analysis would add only 0.7 ounces to the wing weight but would reduce the weight of the spar cap. Although Figure 4-7 (with web) would allow choices for spars with all width-height combinations except one, the choice of spar dimensions is 3/16 inches width by 1/8 inch height. Dimensions smaller than this seemed unreasonable when compared to previous aircraft. Also, for ease in manufacturing, the web may not run the length of each semi-span continuously so that it can be attached to the spar between ribs. Thus, a no spar smaller than the size mentioned will be considered.

The TK Solver Plus analysis for the spar assumed that the ribs were spaced 4 inches apart. This appears to be a reasonable spacing to ensure that the airfoil shape is maintained once the MonoKote is shrunk around the wing structure (Ref. 4-2).

4.3.3 The Empennage

The horizontal and vertical tails are flat plates. They will be constructed using rectangular pieces of balsa arranged in a right triangle truss design. All tail surfaces have rectangular planforms. Again, MonoKote will be used as the skin and will also serve as the hinges for the elevators and the rudder, which are attached at the trailing edges of the tails. This is the hinging method used in many existing aircraft and is a good manufacturing method because it eliminates the gap between the tails and the control surfaces. Past experience indicates that it also provides ample rigidity so that the surfaces are effective controllers. The sizing of the tails and control surfaces was determined such that the aircraft would be stable and controllable in flight. The required tail sizes will be easily manufactured since balsa is available in lengths greater than those required by the tail surfaces.

4.4 MATERIALS SELECTION

Of the many materials available for use in constructing the *Airplane*, only wood and MonoKote were seriously considered. Wood is the material of choice because it is readily available, inexpensive, lightweight, and strong enough to handle the stresses expected for the *Airplane*. Existing aircraft of the same relative size and weight made of wood have successfully taken off, flown, and landed in the same environment in which the *Airplane* will operate. Several types of wood were considered: Balsa, spruce, and birch plywood. These were used

in specific structural applications depending on the strength desired. A summary of the data available for these woods appears below in Table 4-1 (Ref 4-5).

TABLE 4-1
Material Properties

Material	Density (oz/in^3)	σ_{xx}, max (psi)	σ_{yy}, max (psi)	τ_{xy}, max (psi)
Balsa	0.0928	400	600	200
Spruce	0.256	6200	400	750
Birch Plywood	0.370	2500	2500	2500
MonoKote	.000125 (lb/in^2)	NA	NA	NA

Balsa is the lightest of the woods, and, as noted previously, has adequate strength to justify its use in the majority of the aircraft structure. Plywood is useful because it can be purchased in thin sheets and can carry loads along two perpendicular axes. Spruce will be used where extra strength is needed, as in the spar and longerons. This will be done sparingly since low weight is one of the most important objectives of the *Airplane* design. Low-weight balsa will be employed in the structure whenever its strength is adequate. Existing aircraft structures that maintained their structural integrity, even in landing, provided justification for this limited use of woods stronger that balsa.

As pointed out in Chapter 1, in order to keep the cost per seat per 1000 feet (CPSPK) as low as possible, minimizing the costs involved in manufacturing is of great importance. This economic consideration is another reason to minimize the use of woods other than balsa since balsa is the least expensive of all the woods considered.

4.5 THE LANDING GEAR

The *Airplane* has a tail-dragger type landing gear configuration. The main gear will be attached beneath the center of gravity and the tailwheel will easily be used for ground control by mechanical coordination with the rudder deflection. This configuration causes the tail to lift off the runway and to rotate about the forward gear during takeoff. The tail dragger need not include a wheel to provide adequate ground handling (Ref 4-2). Rather, a solid metal tube will extend from the fuselage and be bent such that approximately one inch of tubing drags along the ground. This will eliminate the weight associated with a wheel and will not cause a large drag penalty at takeoff since it lifts off the ground within seconds.

The important factors that were considered in the forward landing gear design were placement, both with respect to the c.g. and separation distance between the tires, material properties of the strut, type and size of the wheels used, and the height of the landing gear. The propeller is 12 inches in diameter, so the driving objective for the gear is to keep the propeller from hitting the ground. The main gear will be attached at and angle of 15 degrees ahead of the c.g. This ensures that the gear is not too far forward, thus creating a moment arm that is so large the airplane lift is unable to cause the tail to rotate during takeoff. (Ref. x) Based on the landing gear on the *Hot Box*, a wheel diameter of 1.5 inches is adequate. Figure 4-9 indicates these geometric requirements for the gear.

FIGURE 4-9
The *Airplane* Landing Gear

Main Gear : Front Strut Required Geometry

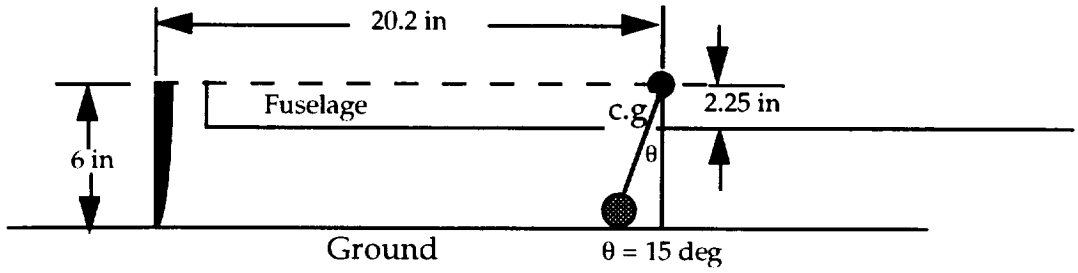

6 " - 2.25 " - 1.5 " = 2.25 " is the vertical height required from the front struts

The geometric distances pictured in Figure 4-9 represent the minimum lengths. It was determined that an additional 2 inches should be added to the distance required by the 6 inch prop radius to be certain that the prop will not strike the ground at any time. This two inches allows for some deflection of the forward landing gear in the vertical direction. The deflection will be limited by attaching a steel wire with 1 inch slack between the forward wheels. For takeoff, it was determined that the aircraft needed to be at a 5.5 degree incidence angle. This, in conjunction with the 8 inch height requirement of the prop, dictated that the tail rod provide 3 inches of height at 52 inches from the nose. Further study of the plane geometry yielded the landing gear configuration as seen in Figure 4-10.

FIGURE 4-10
Proposed Landing Gear

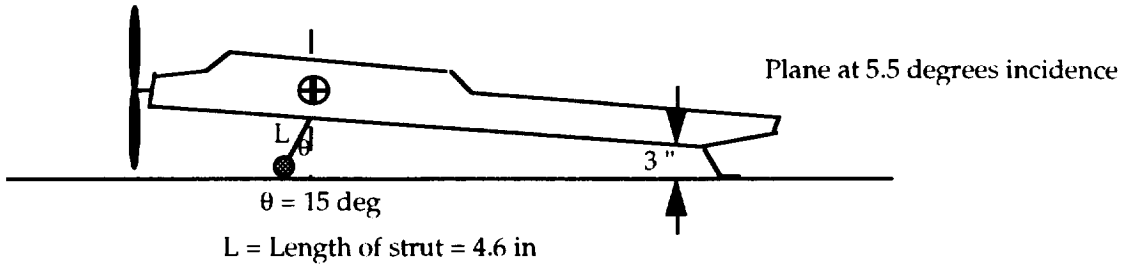

Front View:

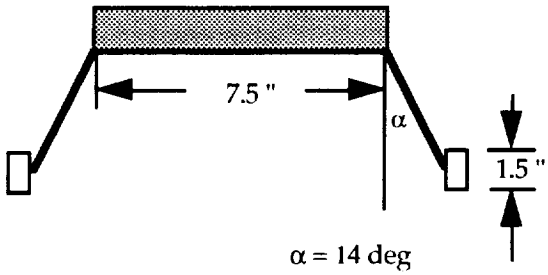

The angles and lengths indicated in the figure will provide enough stability and height to allow the plane to takeoff, rotate, and operate on the ground. The struts will most likely be constructed using a piece of steel tubing, bent to yield the desired configuration. However, an analysis of the materials available, beyond the examination of the gears in the data base, has not been completed.

4.6 AIRCRAFT WEIGHT AND CG LOCATION

An early, and very important segment of aircraft design is the weight estimation. The aircraft should be as light as possible to diminish high power requirements, takeoff distances and fuel costs for operation. Consequently, minimizing the weight is a key consideration in driving the design of the aircraft.

4.6.1 Weight Estimation

The final estimate of total weight of the aircraft is 5.25 lb. The component breakdown for the aircraft is shown in Table 4-2. A graphical representation of component weight percentages is depicted in Figure 4-11. The highest percentages of weight belong to the fuselage and wing. The empennage size and weight are closely related to the aircraft center of gravity. A c.g. closer to the aerodynamic center of the wing reduces the necessary tail surface sizes for stability and control of the aircraft.

TABLE 4-2
Component Weight Breakdown for the *Airplane*

Component	Weight (oz)	X (in)	Weight Percentage
Propeller	1	0	1.2
Motor	10.3	2	12.2
Main Gear	3.5	19	4.2
Batteries	14.76	8.91	17.5
Receiver	0.95	8.91	1.1
System Battery	2	8.91	2.4
Servos (2)	1.2	8.91	1.4
Speed Controller	1.8	8.91	2.1
Wing	16	22	19.0
Fuselage	17	28	20.2
Passengers	6.4	28	7.6
Floorboard	4	28	4.8
Tailwheel	1.5	52	1.8
Empennage	3.8	60	4.5
Horizontal Tail	2.0	60	2.4
Vertical Tails	1.8	60	2.1

FIGURE 4-11
Graphical Representation of Weight Components

(For numerical weight percentages see Table 4-2)

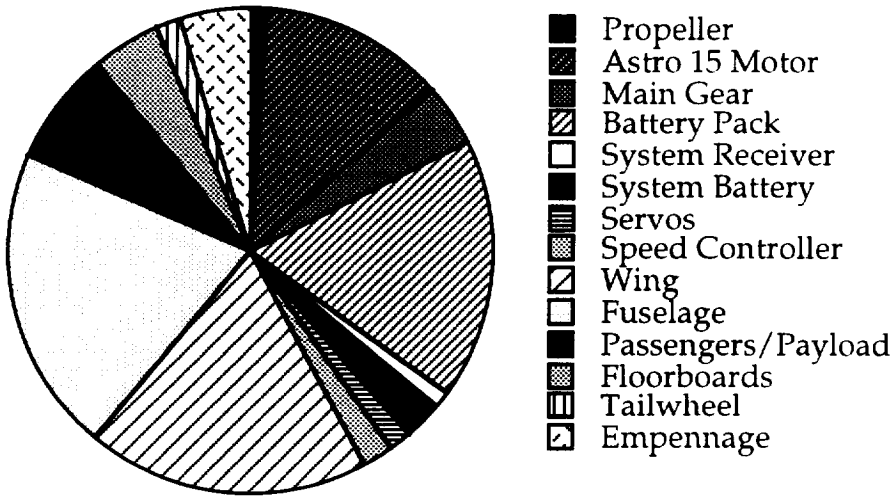

The initial estimate of the total weight of the *Airplane* was 5. 6 lbs. The main reasons for its current value (5.25 lb.) are that the propulsion system has been selected and its weight finalized and the tail surface size has decreased because of more advantageous c.g. placement. The estimates of propeller and landing gear weights are averages calculated from a large database of past RPVs (Refs. 4-6 - 4-13). The wing, empennage, and fuselage estimates were also made in this fashion. From the database, component weights were plotted against their corresponding area or volume in order to develop an approximate functional relationship between substructure sizes and their estimated weights. Changes in wing area, for instance, can be immediately compensated for in terms of weight with this type of estimation.

4.6.2 Center of Gravity Travel and Location

The center of gravity is an important concept in terms of weight and stability and control of an aircraft. The internal layout of the *Airplane* was driven by a required fuselage length to carry 70 passengers plus crew as well as engine placement in the nose of the aircraft. Known weights, consisting of the batteries, receiver, system battery, servos, and the speed controller, were lumped together in a "package" representation. The weights of these components are all fairly certain and will be acting at very nearly the same location along the fuselage. After a configuration for the remainder of the aircraft was devised, this package was maneuvered along with the wing to determine c.g. location. An important factor in determining c.g. location is the static margin. For RPVs, the static margin should not be less than 0.2. Figure 4-12 depicts the relationship between the c.g. location and static margin for the current size of the aircraft. An upper limit of 0.3 was placed on the static margin so that the aircraft would have some maneuverability and not be too stable.

FIGURE 4-12
Limitations of Center of Gravity Placement by Static Margin

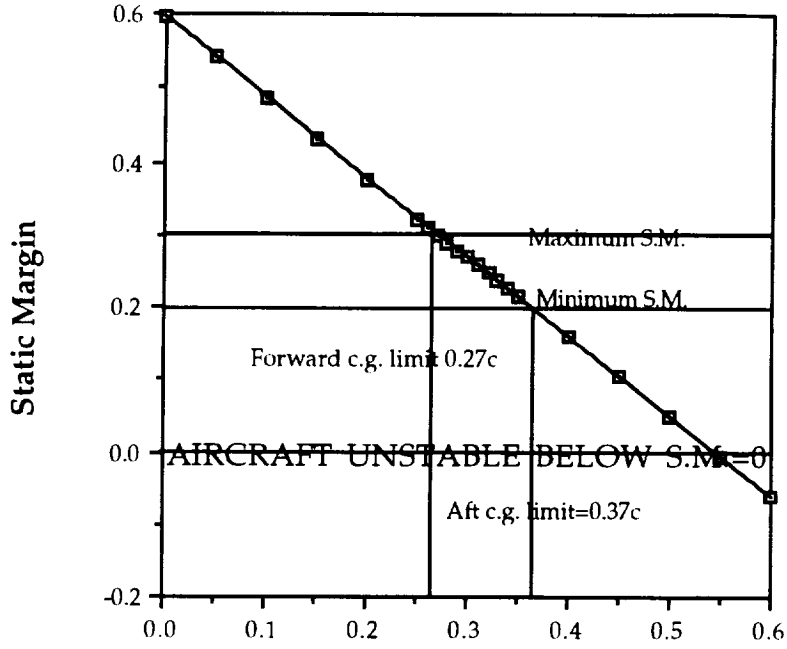

Section 5.0 discusses the importance of static margin and c.g. location in terms of stability and control. The c.g. of the aircraft lies at 20.2 in. (0.35c), just aft of the wing aerodynamic center at 19 in (0.25c). The package is located at x = 8.91 in. Should the weights of some of the more undetermined components cause the center of gravity to shift such that the longitudinal stability of the aircraft would break down, the battery / control package is allowed six inches of forward travel to move and compensate for the shift.

A further concern about the aircraft weight is the travel of the center of gravity for different numbers of passengers on a given flight. Figure 4-13 indicates that if passengers are seated exclusively from front to rear of the aircraft the empty weight center of gravity location is at 30 % chord. As more rows are

filled in the front of the fuselage, the center of gravity travels to its forward most position at 28 % chord.

FIGURE 4-13
Weight-Balance Diagram for Front to Back Seating

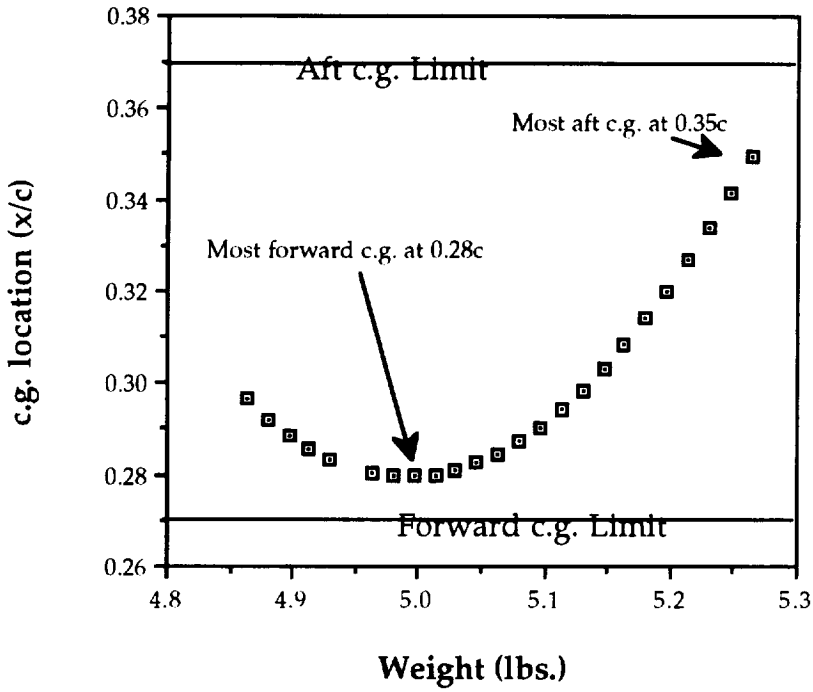

This occurs when the aircraft is carrying approximately 25 passengers. As more rows are filled to the capacity level of 70 passengers, the center of gravity travels rearward until it reaches its aft-most position at 35 % of the chord. Figure 4-13 indicates that for front - to - back seating of the *Airplane*, the center of gravity location stays within the limits set forth by the static margin requirements. The seating plan and the respective c.g locations are therefore appropriate.

REFERENCES

4-1. Cashin, Tim, WINGLOAD Computer Program, ARROW 227 Final Design Proposal, Department of Aerospace and Mechanical Engineering, University of Notre Dame, May 1992, Appendix A.

4-2. Mergen, Joe, verbal consultation with the Airplane Guys Design Group, March 1993.

4-3. Swift, Richard, *SWIFTOS User's Guide*, University of Notre Dame, November 1990, p. 31.

4-4. Bontempi, Bose, Brophy, Cashin, Kanarios, Ryan, Peterson, ARROW 227 Final Design Proposal, Department of Aerospace and Mechanical Engineering, University of Notre Dame, May 1992, Table I.1, p. I-6.

4-5. Cashin, Tim, TK Solver Plus Program,

4-6. *Design Proposal for the Hotbox.* May 1991.

4-7. *Design Proposal for the Stealth Biplane.* May 1990.

4-8. *Design Proposal for the Penguin.* May 1990.

4-9. *Design Proposal for the Valkyrie.* May 1991.

4-10. *Design Proposal for the El Toro.* May 1991.

4-11. *Design Proposal for the Pale Horse.* May 1991.

4-12. *Design Proposal for the Screem-J4D.* May 1990.

4-13. *Design Proposal for the Sky Shark.* May 1989.

5.0 STABILITY AND CONTROL

5.1 SYSTEM REQUIREMENTS

Stability of an aircraft without the highest of technologies is essential if it is to remain humanly controllable in the air for any substantial length of time. An aircraft is stable when it possesses longitudinal (pitch) stability, lateral or yaw stability, and roll stability. All of these features must be incorporated into the design concept of the aircraft. This leads to the following series of requirements for the *Airplane*:

* The aircraft must be able to maintain steady and level flight at all ranges of velocities and flight conditions.
* Longitudinal, or pitch, stability must be accomplished by an aft horizontal tail with elevator, as set forth in the design concept
* Yaw stability must be accomplished by a dual vertical tail/rudder system because of the tendency of a wide fuselage to create vortices that interfere with a single vertical tail at a conventional placement in the rear of the fuselage.
* Roll stability, in the absence of ailerons, must be accomplished by a combination of wing dihedral and rudder deflection.
* The rudder/dihedral combination must be able to bank the aircraft and satisfy the turn requirement of a 60 foot radius turn at 25 ft/s.
* The maximum deflections of the rudder and elevator must be capable of being produced by the respective servo.

This section discusses the methods used to satisfy the above requirements.

5.2 LONGITUDINAL STABILITY

Longitudinal stability of an aircraft requires that the particular aircraft trim at any angle of attack within its particular range of flight speeds and attitudes. This, of course, implies that the pitching moment coefficient of the aircraft, Cm, is equal to zero at the desired angle of attack. In order for the aircraft to be considered stable, the slope of the pitching moment coefficient with respect to angle of attack (Cm_α) must be negative. Futhermore, the intercept of this graph must be positive if the aircraft is to cruise at a positive angle of attack.

This slope was subsequently quantified by slopes that are used for general aviation and other types of aircraft. These values were obtained in Appendix B of Reference 5 - 1. These values were compared to the pitching moment curve slope of the *Hotbox*, found inReference 5 - 2. Based on the above information and that corresponding to other aircraft of similar size and weight, it was determined that a slope of around -0.901 1/rad was satisfactory for the *Airplane*. This number was chosen as a compromise between the different slope values. Furthermore, the slope is practical in that it does not require an excessive elevator deflection ($\delta \sim 16$ degrees) to trim near stall (see Figures 5-4a and 5-4b). The necessary intercept is one at which the elevator deflection will be approximately zero at cruise. The main reason for zero elevator deflection is to keep the drag at a minimum at the cruise condition. Three components contribute to the slope and intercept and thus the aircraft's longitudinal stability: the fuselage, wing, and horizontal tail.

5.2.1 Fuselage Contribution

The fuselage of an aircraft generally has a destabilizing effect on longitudinal stability. Reference 5-1 states that the fuselage makes a positive contribution to Cm_α and a negative contribution to Cm_o. Reference 5-1 also

outlines Multhopp's method for estimating these contributions. The method involves breaking down the fuselage into small increments(Δx) of some average width (w_f) and using wing geometry and characteristics to determine the fuselage contribution. The equations are as follows:

$$C_{mof} = \left(\frac{(k2-k1)}{36.5Sc}\right) \sum_{x=0}^{x=lf} w_f{}^2 \left(\alpha_{ow} + i_f\right) \Delta x$$

$$C_{m\alpha f} = \left(\frac{1}{36.5Sc}\right) \sum_{x=0}^{x=lf} w_f{}^2 \frac{d\varepsilon_u}{dx} \Delta x$$

Values for (k2-k1) and $d\varepsilon_u/d\alpha$ were given in Reference 5-1. Multhopp's method yielded the following values for fuselage contribution:

$$C_{mof} = -0.009$$

$$C_{m\alpha f} = 0.125 \frac{1}{rad}$$

5.2.2 Wing Contribution

The wing makes a significant contribution to the longitudinal stability of the airplane. The contribution of the wing is influenced by three main parameters. These parameters include the type of airfoil used for the wing, the wing aspect ratio (and therefore wing geometry), and the center of gravity location. The influence of these parameters are shown below in the equations for $C_{m\alpha w}$ and C_{mow}, given in Reference 5-1.

$$C_{m_{ow}} = C_{m_{acw}} + C_{L_{ow}}\left(\frac{x_{cg}}{c} - \frac{x_{ac}}{c}\right)$$

$$C_{m_{\alpha w}} = C_{L_{\alpha w}}\left(\frac{x_{cg}}{c} - \frac{x_{ac}}{c}\right)$$

One parameter, the 2-D lift curve characteristics for the type of airfoil chosen , is important in determining the three-dimensional wing lift curve slope. This is obvious from the following formula, where a_0 is the 2-D lift curve slope.

$$a = \frac{a_0}{1 + \frac{a_0}{\pi AR}}$$

The SPICA airfoil was chosen for the *Airplane* because of its high-lift characteristics at relatively low Reynolds numbers. The equation above indicates that the second parameter, wing aspect ratio, also affects the wing contribution. A higher aspect ratio leads to a larger three-dimensional lift curve slope. It is, however, important to realize that these two parameters are generally chosen for aerodynamic characteristics and not stability considerations.

The final parameter, c.g. location, is crucial to the wing's contribution to stability. The center of gravity for the *Airplane* has always been located behind the aerodynamic center of the wing. Therefore, the wing has a destabilizing effect due to its positive contributions to moment curve slope. The effect of center of gravity location on Cm_α is shown in Figure 5-1. In order to minimize the wing's destabilizing effect, it is essential that the aircraft's center of gravity be as close to the wing aerodynamic center as possible. The final center of gravity location for maximum takeoff weight is located at 0.35c. This location was chosen because the current layout is the most efficient in terms of total fuselage volume, the static margin at this location is favorable, and this location enables

front to back seating in the aircraft without moving the center of gravity ahead of the aerodynamic center as well as practical elevator deflections for trim near stall The maximum weight values for wing contribution are as follows:

$$C_{m_{ac_w}} = -0.0877$$

$$C_{m_{\alpha_w}} = 0.4224 \frac{1}{rad}$$

FIGURE 5-1
Pitching Moment Slope vs. Area Ratio

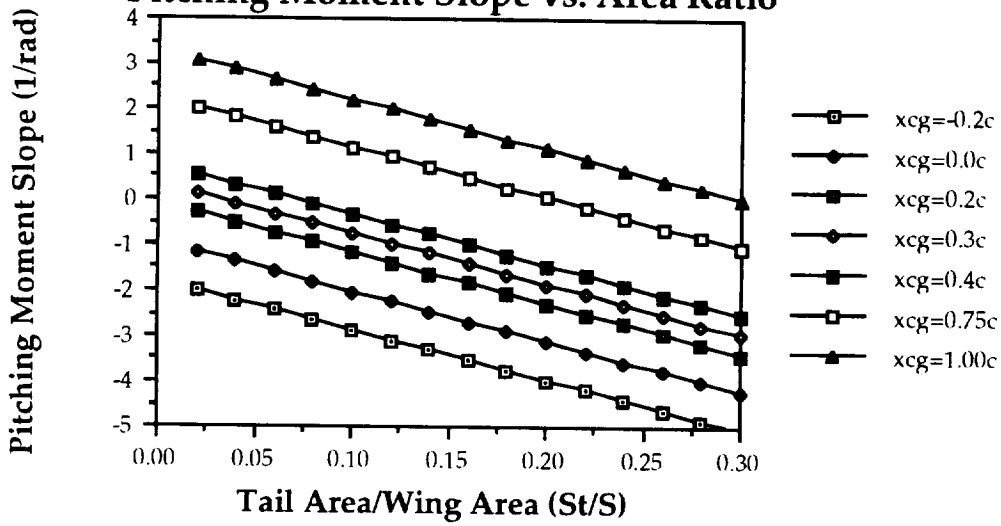

5.2.3 Horizontal Tail

The horizontal tail is the surface used to overcome the destabilizing effects of the wing and fuselage in order to provide longitudinal stability. Its contribution is also determined by three main parameters: the horizontal tail volume ratio, the downwash angle at the tail, and the tail incidence angle. These factors are visible below in the formulas given in Reference 5-1.

$$C_{m_{ac_t}} = \eta V_h C_{L_{\alpha_t}} \left(\varepsilon_0 + i_w - i_t \right)$$

$$C_{m_{\alpha_t}} = \eta V_h C_{L_{\alpha_t}} \left(1 - \frac{d\varepsilon}{d\alpha} \right)$$

The horizontal tail volume ratio is defined as follows:

$$V_h = \frac{S_t l_t}{Sc}$$

A very important value in the volume ratio is the moment arm to the horizontal tail (l_t). The moment arm is a function of center of gravity location and aircraft layout. Again, c.g. location is vital to the longitudinal control of the aircraft. The tail dimensions are important parameters to tail contribution in the same way that wing geometry was important to wing contribution. A flat plate was chosen as the section for the horizontal tail because of its simplicity, enabling the aircraft to be assembled in a more economical fashion, than if a contoured thin airfoil was used.

The downwash plays an important role in longitudinal stability. It, in some ways, dictates the effectiveness of the tail surface. Downwash can be estimated from finite-wing theory and the assumption of an elliptic lift distribution. The formulas are presented in Reference 5-1 and are as follows:

$$\frac{d\varepsilon}{d\alpha} = \frac{2C_{L\alpha w}}{\pi AR}$$

$$\varepsilon_o = \frac{2C_{Lwo}}{\pi AR}$$

These estimations were used to predict the downwash effect at the tail and, in effect, help size the tail using the desired Cm_α of approximately -0.901 1/rad. There was an attempt to model downwash on LinAir, but the results obtained did not compare favorably to those from the assumption of elliptic lift distribution. The $d\varepsilon/d\alpha$ value from LinAir was nearly one-half of the value

obtained from that of the estimations in Reference 5-1. A conservative choice was made to use the larger value.

The incidence of the tail also plays an important role in determining the intercept contribution of the horizontal tail. The wing incidence is set by aerodynamic requirements and the downwash angle is a function of the wing characteristics. The method used, as mentioned earlier, is to determine the required tail incidence so that the elevator deflection is at a minimum at the cruise condition. This cruise condition occurs at an aircraft angle of attack of 1.3 degrees. The tail is mounted at 0 degrees angle of attack, which leads to an elevator deflection of about 0.6 degrees at cruise. The final tail numbers are in Table 5 - 1:

TABLE 5 - 1
Horizontal Tail Aerodynamic And Size Parameters

C_{mot}	.1225
$C_{m\alpha t}$	-1.448 rad^{-1}
Tail incidence	None
Horizontal Tail Volume Ratio, V_H	0.464
Tail Surface Area, S_t	1.25 ft^2
Tail Chord, c_t	0.5 ft
Tail Moment Arm, l_t	3.53 ft
Tail Aspect Ratio, AR_t	5.0
$C_{L\alpha t}$	4.35 rad^{-1}

The slope and intercept of the pitching moment coefficient curve for an aircraft are simply the arithmetic sums of the contributions of the fuselage, wing, and tail to each value. The final values for slope and intercept for this aircraft are:

$$C_{m\alpha} = -0.9006 \frac{1}{rad}$$
$$C_{m_0} = 0.0288$$

The graph for Cm vs. α is shown in Figure 5-2 for most forward and aft c.g. locations. The most aft center of gravity location for the *Airplane* is at a full payload capacity and is located at 0.35c. Because the *Airplane* will be seated from front to back, the most forward c.g. location is 0.28c. This occurs when only 21 passengers are on board. The importance of c.g. location is also noted in Figure 5 - 2.

FIGURE 5-2
Cm vs. Alpha for extreme c.g. locations

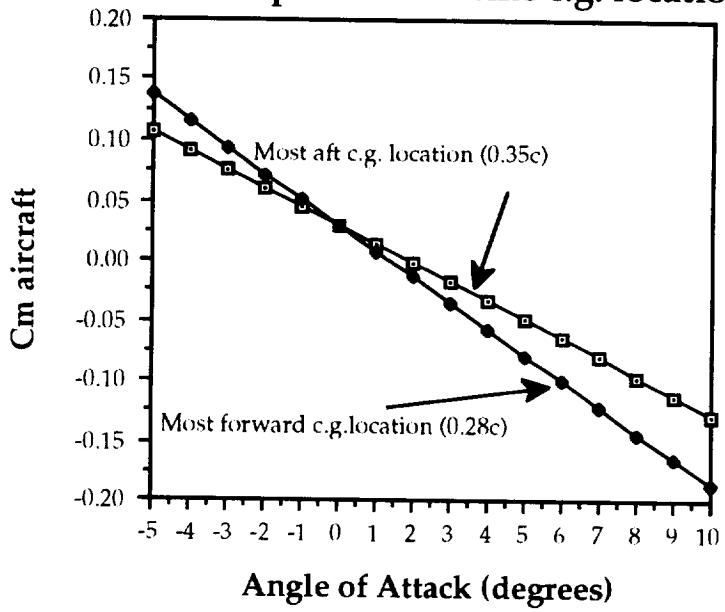

5.2.4 Neutral Point and Static Margin

The neutral point is defined as the point where the aircraft is neutrally stable. It is an aft limit for center of gravity placement. A c.g. location beyond this point will result in an unstable aircraft. The formula for calculating the neutral point, obtained from Reference 5-1, is:

$$\frac{x_{np}}{c} = \frac{x_{ac}}{c} - \frac{C_{m\alpha f}}{C_{L\alpha w}} + \eta V_h \frac{C_{L\alpha t}}{C_{L\alpha w}}\left(1 - \frac{d\varepsilon}{d\alpha}\right)$$

The center of gravity location itself plays a crucial role in determining the neutral point of the aircraft, as the moment arm l_t is an influencing term in the tail volume ratio. Obviously, the neutral point is also affected by wing and tail characteristics.

The static margin, defined below, is a crucial number in the area of longitudinal stability.

$$S.M. = \frac{x_{np}}{c} - \frac{x_{cg}}{c}$$

In most airplanes, the static margin should be in the neighborhood of 0.05 to 0.10 for the aircraft to be considered stable. Past experience, however, has shown that a static margin around the 0.20 to 0.25 region is necessary in RPV's. This is due to the fact that the pilot is not in the aircraft, causing a longer aircraft response time to signals or inputs. The center of gravity location must be chosen so that the static margin is at least 0.2 and the neutral point is at a location which the aircraft center of gravity will never be under any mode of operation and weight distribution. A center of gravity location of 0.35c was selected with this in mind. Other factors were, as mentioned earlier, most efficient layout in terms of fuselage volume and ability to keep the center of gravity behind the aerodynamic center to minimize necessary elevator deflections to trim the aircraft. The final values for the *Airplane* design at maximum weight are:

$$\frac{x_{np}}{c} = 0.575$$
$$S.M. = 0.225$$

5.3 LONGITUDINAL CONTROL

Longitudinal control is needed in every aspect of a flight, beginning with rotation for takeoff. It is necessary to trim at any angle of attack and speed within the flight envelope at different c.g. locations. Finally, longitudinal control is essential in flaring the airplane to complete a successful landing. Control of the pitching moment of an aircraft is accomplished by means of an elevator as part of the horizontal tail. The moment coefficient changes with elevator deflection in the following manner:

$$C_m = C_{mo} + C_{m\alpha}\alpha + C_{m_{\delta e}}\delta_e$$

$$C_{m_{\delta e}} = -\eta V_h C_{L\alpha t}\tau$$

$Cm_{\delta e}$ is known as the elevator control power and is related to the ratio of the elevator area to the horizontal tail area. The parameter τ is the flap effectiveness parameter, which is a function of the ratio of elevator to tail area. The relation is given in Reference 5 - 1.

The elevator was designed with three ideas in mind. First, the sensitivity of the aircraft must not be too great to pilot input that it causes the plane to oscillate. This sets a limit on the elevator control power. Based on studies done on the *Airplane* and the values presented in Reference 5-1 for general aviation aircraft, the elevator control power should not exceed -1.0 rad^{-1} in magnitude. This has a direct relation to the size of the elevator. Second, the elevator must be able to trim the aircraft at the stall angle for landing purposes. Landing occurs slightly above the stall speed, but trimming at stall builds in some factor of safety. The design of the elevator was based on the most forward c.g. location, which is 0.28c. At this location, the elevator deflection needed to trim at or just below stall is a maximum. The maximum elevator deflection is related to the

incidence angle of the tail for a particular aircraft configuration. Figure 5-3 depicts this situation for the most forward c.g. location of the *Airplane*. The final design consideration was that the maximum elevator deflection must be within the capability of the servomotor. It was determined from the database that a maximum deflection of approximately 15 degrees or less was clearly within the realm of possibility.

FIGURE 5-3
Elevator Deflection to Trim at Stall vs. Tail Incidence

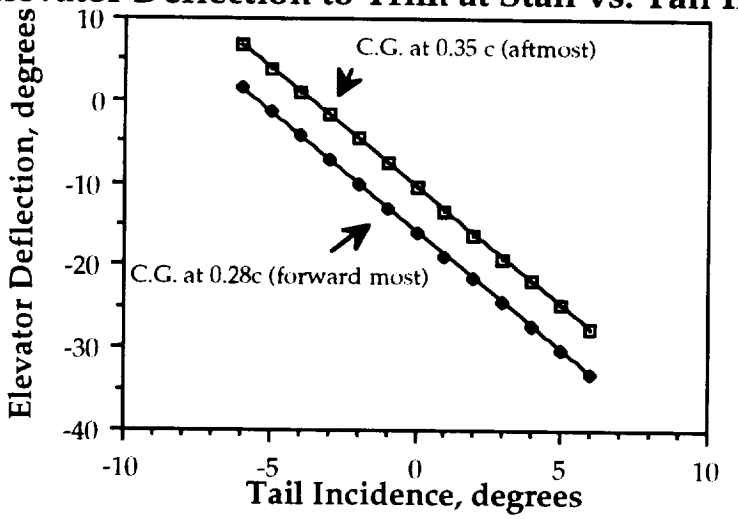

Taking into account all design considerations, it was determined that an elevator control power of approximately -0.75 would be appropriate. The flap effectiveness parameter τ was determined from the elevator control power. Round numbers were then used for ease of manufacturing to yield the final design of the elevator shown in Table 5 - 2. The results of the elevator design are shown in Figures 5-4a and 5-4b, where the effect of elevator deflection is plotted against aircraft angle of attack for the most aft and forward c.g. locations.

TABLE 5 - 2
Elevator Control Surface Summary

Elevator Control Power, $C_{m\delta e}$	-0.727 rad^{-1}
Flap effectiveness, τ	0.36
Control Surface Area Ratio, S_e/S_t	0.15
δ_e cruise	0.6 degrees
δ_e max	$\pm$ 15 degrees

FIGURE 5-4a
Effect of Elevator Deflection (aft c.g. location)

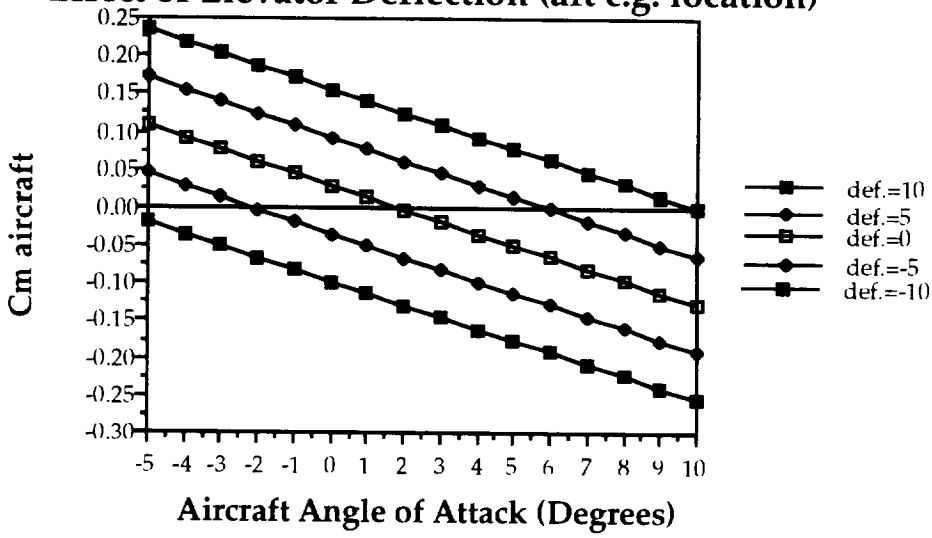

FIGURE 5-4b
Effect of Elevator Deflection (forward c.g. location)

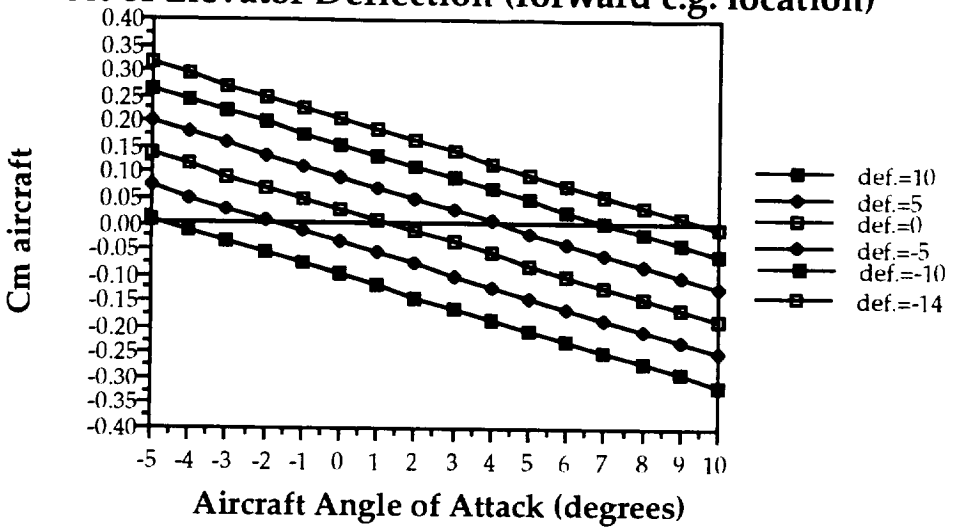

5.4 LATERAL OR DIRECTIONAL STABILITY

Directional stability is defined by the aircraft's ability to return to an equilibrium state about its vertical (yaw) axis of rotation. In the event of an induced sideslip angle, β, it is desired that the aircraft will move toward this equilibrium state rather than diverging more and more rapidly away from it. As the sideslip angle is defined to increase in positive magnitude as the aircraft rotates about its yaw axis in the negative sense, it is a design criterion that the moment induced by such an angle of sideslip be in a positive, restoring sense. Similarly, if a negative angle of sideslip is induced as the aircraft yaws in the positive sense, the restoring moment must necessarily be in the positive sense. This direct relationship between the sideslip angle and the necessary restoring moment leads to the underlying directional static stability condition (Reference 5 - 1)

$$C_{n_\beta} > 0$$

C-2

The stability derivative, C_{n_β}, is comprised of contributions from the wing - fuselage as well as the aircraft vertical tail. Of these, the most dominant contribution comes from the vertical tail, where (Reference 5 - 1)

$$C_{n_{\beta_v}} = V_v \eta_v C_{L_{\alpha_v}} \left(1 + \frac{d\sigma}{d\beta}\right)$$

and

$$\eta_v \left(1 + \frac{d\sigma}{d\beta}\right) = 0.724 + 1.53 \frac{S_v}{S} + 0.4 \frac{z_w}{d} + 0.009 AR_w .$$

Figures 5.5 - 5.6 show the sensitivity of the coefficient to several of the design variables upon which it depends.

FIGURE 5-5
Variation of Cn Beta with Wing Aspect Ratio

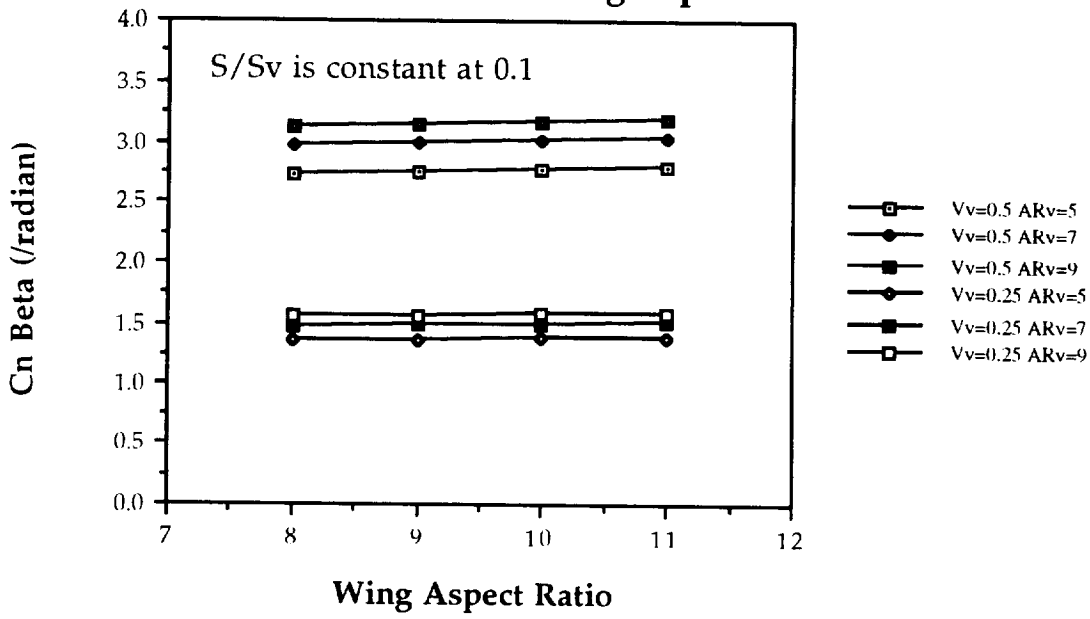

FIGURE 5-6
Variation in Cn Beta with Vertical Tail Volume Ratio

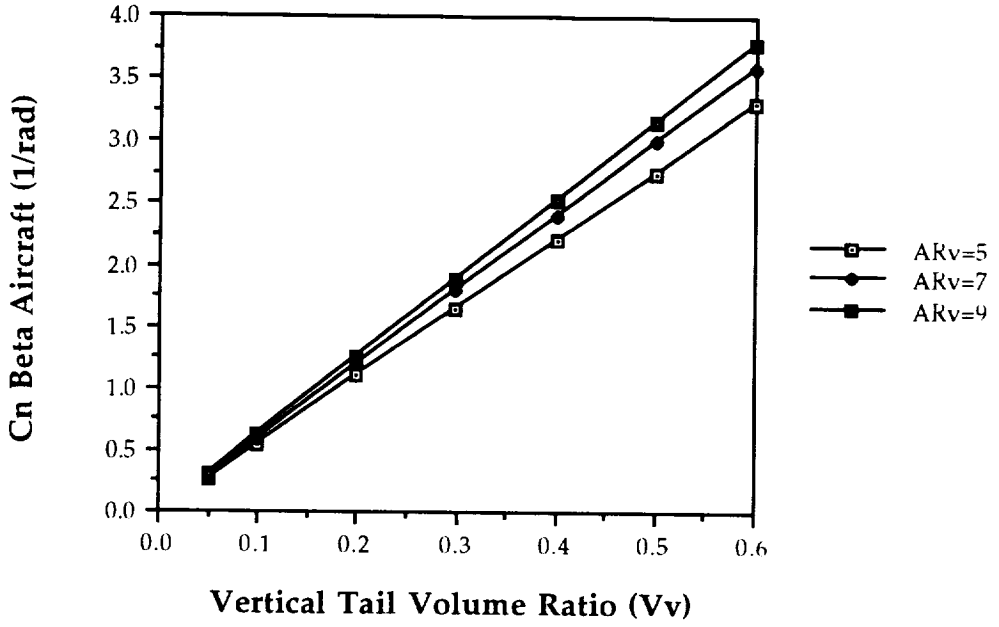

From these, it may be readily observed that C_{n_β} shows notable improvement with changes in the vertical tail volume ratio and tail aspect ratio (which drives the tail lift curve slope), but negligible variation with changes in the wing aspect ratio.

5.5 LATERAL OR DIRECTIONAL CONTROL

For the aircraft to be at all useful it is necessary that the pilot be able to control its direction. For the *Airplane*, this is accomplished by the incorporation of a movable control surface, or rudder, within the vertical tail. The rudder can be deflected by the pilot to produce the desired yaw moment. For this aircraft, the rudder will also be used in conjunction with wing dihedral to create a rolling moment in the absence of ailerons. The amount of yaw control provided by the

rudder is driven by the size of the tail, the relative size of the rudder and the angular deflection of the rudder according to (Reference 5 - 1)

$$C_{n_{\delta r}} = -\eta_v V_v \frac{dC_{Lv}}{d\delta r}$$

$$\frac{dC_{Lv}}{d\delta r} = C_{L_{\alpha v}} \tau$$

The quantity, τ, the flap effectiveness, is related to the area fraction that the rudder occupies on the vertical tail according to Fig. 2.20 in Reference 5 - 1.

A parametric sensitivity study of rudder control power is presented in figure 5 - 7 and shows that the rudder control influence on aircraft yaw increases significantly both with increasing overall tail area as well as with the ratio of rudder to tail area. This reflects the dependence of the yaw moment developed upon the sideways "lift" force acting on the vertical tail surface. Lift force, of course, is proportional to the surface area and increases as a function of the airfoil camber.

FIGURE 5-7
Yaw Control Power vs. Control Surface Area Ratio

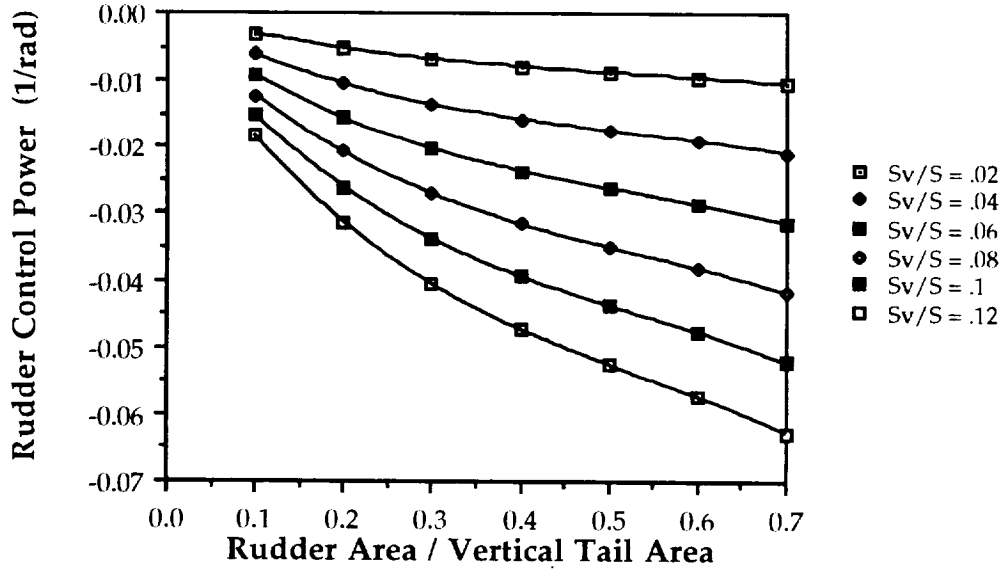

5.5.1 Roll Control Without Ailerons

As stated previously, the rudder will be used together with wing dihedral to roll the aircraft in order to turn rather than in conjunction with ailerons to simply coordinate a turn. Indeed from a neutral condition, if the pilot desires to turn the aircraft he may deflect the rudder to create a sideslip angle which, in tandem with the dihedral effect, results in the production of a net rolling moment on the aircraft. From a method introduced in Reference 5 - 3, the sideslip angle associated with a step rudder input may be computed using the following equation,

$$C_n = C_{n_\beta}\beta + C_{n_{\delta r}}\delta r$$

where $C_n = 0$ at the trim condition. Once sideslip angle has been determined, the roll moment coefficient may be subsequently computed from the following,

$$C_l = C_{l_\beta}\beta + C_{l_{\delta r}}\delta r.$$

This equation reflects not only the contribution of the rudder control to the rolling moment but also, the effect of the wing dihedral which is the driving factor behind the sideslip contribution to aircraft roll.

5.5.2 Sizing Stabilizer and Control Surfaces

Figures 5.8 - 5.10 were used to compare the maximum amount of roll produced by commonly sized ailerons (8 - 15 % of the wing surface) with the maximum moment producible by coupling the rudder and dihedral effects . The

FIGURE 5-8
Aileron Contribution to the Roll Moment Coefficient

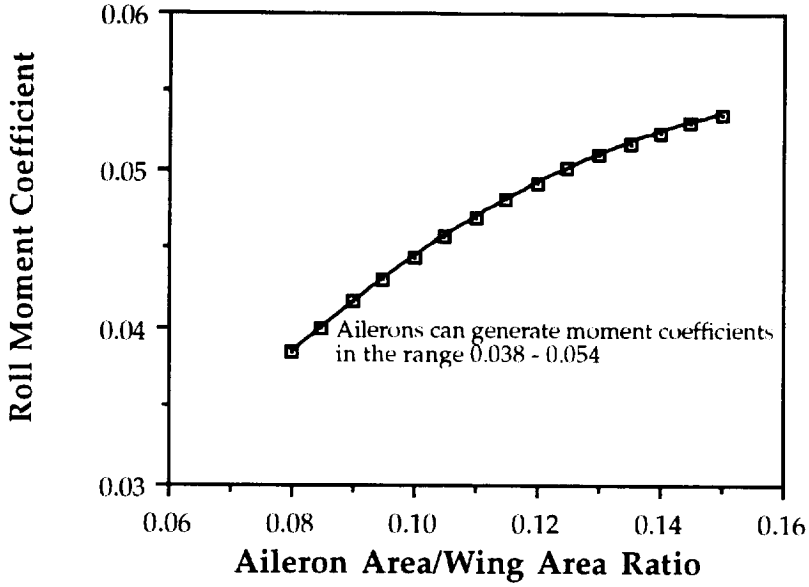

final configuration shown reflects a decision based on a trade study which charted the effects of both wing dihedral and vertical tail size for a given rudder control surface fraction on the overall rolling moment coefficient. The study showed that, while increasing wing dihedral induced marked improvements in roll moment generation, increased vertical tail area induced an opposing effect. It is proposed that the *Airplane* have a dihedral angle of eight degrees combined with a S_V/S_W o f 0.088 as determined in yaw static stability analyses to produce a rolling moment coefficient at maximum deflection of approximately 0.04 which falls in the lower end of the moment regime producible by ailerons.

FIGURE 5-9
Roll Moment Coefficient Generated by Rudder and Dihedral

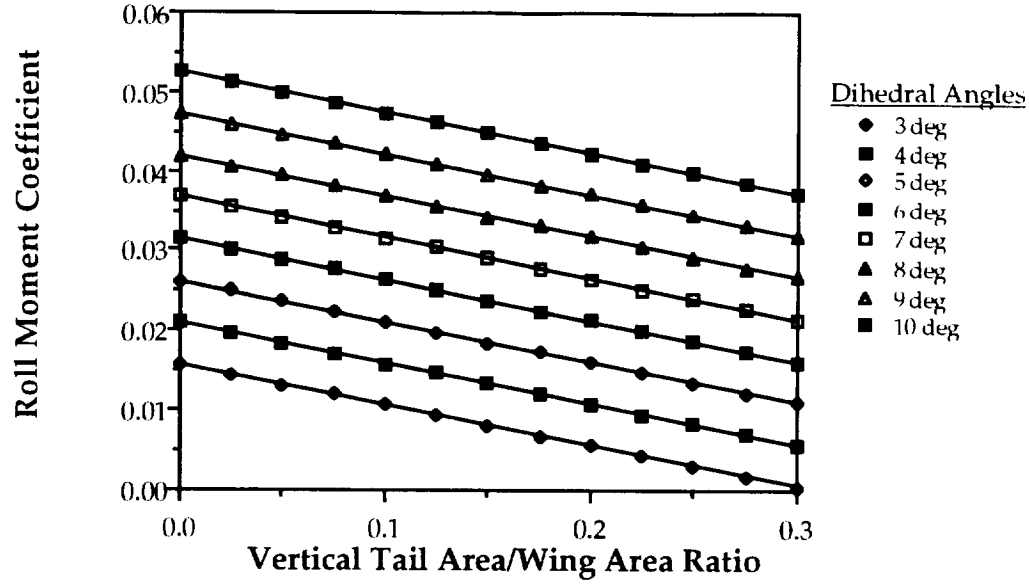

FIGURE 5-10
Rolling Moment vs. Rudder Deflection

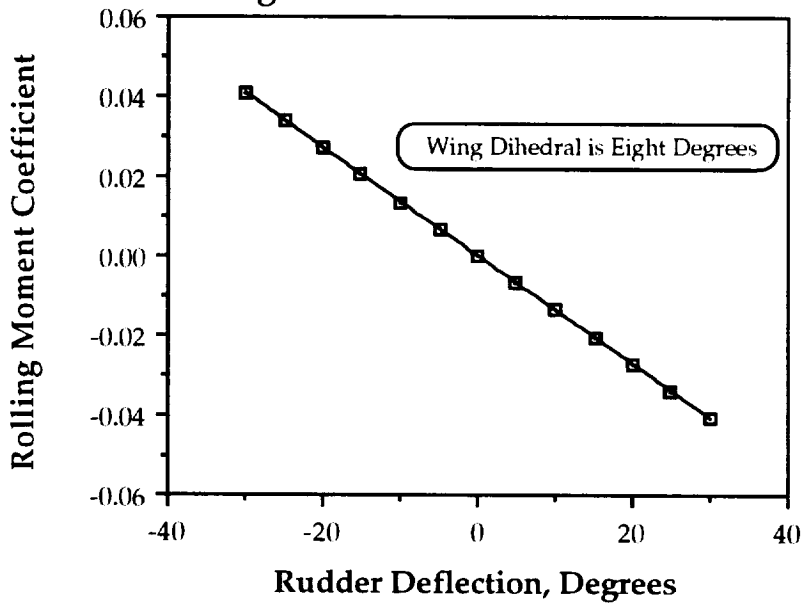

The *Airplane* incorporates a twin vertical tail design concept. This is done in tandem with aft fuselage tapering to remove the directional control surfaces from the effects of the vortices shed by the wide passenger section of the

fuselage. The tail surfaces were ultimately sized using a baseline aircraft layout with a fixed tail moment arm and fixed wing geometry. The aforementioned directional stability criterion then guided the sizing for a value of C_{n_β} comparable to those of previously designed aircraft of similar weight and geometry as well as to the general aviation aircraft presented in Reference 5 - 1. For the accompanying tail volume ratio, the rudder surface fraction was then chosen to achieve a similarly specified $C_{n_{\delta r}}$. Underlying this choice of rudder control power, is the constraint that the aircraft not react to quickly or violently for the pilot to react. Conversely, it must not react so slowly that a necessary maneuver is undertaken to late to expedite a particular route or avoid a midair collision. The distribution of the tail surface area in terms of aspect ratio was based upon values suggested in Reference 5 - 4.

The final tail and rudder geometric characteristics and their associated stability derivatives are as follows:

TABLE 5 - 3
Geometric Parameters Of *Airplane* Twin Vertical Tail

Total Vertical Tail Area, S_V	0.833 ft^2
Vertical Tail Span, b_V (each)	0.833 ft (10 in)
Vertical Tail Chord, c_V (each)	0.5 ft (6 in)
Vertical Tail Volume Ratio, V_V	0.033
Vertical Tail Aspect Ratio, AR_V	1.67
Rudder Area Fraction (each)	0.6
Maximum Rudder Deflection	±30°

TABLE 5 - 4
Lateral Stability Derivatives

C_{n_β}	0.105 rad^{-1}
$C_{n_{\delta r}}$	-0.072 rad^{-1}
C_{l_β}	-0.124 rad^{-1}
$C_{l_{\delta r}}$	0.0095 rad^{-1}

A final concern for aircraft stability during a turn is the induced angle of attack on the wing during the maneuver. This change may be approximated as (Reference 5 - 1)

$$\Delta\alpha = \beta\Gamma,$$

that is, the product of the sideslip and dihedral angles. For the *Airplane* configuration, a maximum rudder deflection of 30 degrees would result in a 20.5 degree sideslip which, with the eight degrees of dihedral would induce an angle of attack shift of 10.7 degrees. Noting that the wing is mounted at a three degree incidence, such a shift would bring the aircraft very close to the stall angle of attack, 14 degrees. This would call for a slight stick forward input from the pilot just a bit after the rudder actuation during sharp turning maneuvers in order to reduce the chance of stall.

REFERENCES

5 - 1. Nelson, Robert O., *Flight Stability and Automatic Control*, Mc Graw - Hill Book Company, New York, 1985.

5 - 2. *Proposal for Design of the Hotbox*, 1991.

5 - 3. *Proposal for Design of the Drag 'N' Fly*, 1990.

5 - 4. Lennon, A. G., *R/C Model Airplane Design*, Motorbooks International, Wisconsin, 1986.

6.0 PERFORMANCE

Performance is a very critical part of aircraft design. Any successful aircraft must have good performance qualities. These qualities must comfort the passengers as well as the pilot, and an aircraft with good performance will not only save the passengers money. Burning fuel efficiently and safely helps the environment as well. For this design, however, the main concern with performance is meeting the requirements of takeoff, performing a steady, level turn, and landing within a given distance. Meeting the range and endurance requirements were also important factors and were critical to catering to the target segment of the AeroWorld market.

TABLE 6-1
Performance Characteristics

Takeoff Distance	24.0 ft
Takeoff Thrust	2.67 lb
Battery Drain @ takeoff	6.54 mahr
Takeoff Velocity	23.0 ft/s
Minimum Velocity	19.3 ft/s
Maximum Velocity	54.3 ft/s
Stall Speed	19.3 ft/s
Maximum Range @ Wmax	12100 ft
Maximum Endurance @ Wmax	8.0 min
Maximum Range @ Wmin	12520 ft
Maximum Endurance @ Wmin	8.7 min
Endurance @ Max Range	7.0 min
Range @ Max Endurance	10300 ft
Maximum R/C @ Wmax	12.4 ft/s
Maximum (L/D)	11.3
Cruise (L/D)	9.5
Cruise Range @ Wmax	12140 ft
Cruise Endurance @ Wmax	6.8 min
Minimum Glide Angle	5.05 degrees
Minimum Sink Speed	1.74 ft/s
Landing Distance	52.4 ft
Minimum Radius of Turn	37.4 ft @ bank angle=18 deg

Note: All of the values on previous page for range and endurance exclude the two minute loiter.

6.1 TAKEOFF PERFORMANCE

The takeoff distance of an aircraft is a very important parameter because this value will constrain an aircraft to serving only certain airports in AeroWorld. The propeller has a strong influence upon the takeoff distance and therefore it must be selected carefully. It is desired that the *Airplane* can takeoff over a range of lift coefficients, weights, and battery voltages in the event that it does not always operate at its design (full) capacity. The selected propulsion system will allow the takeoff distance to be 24 feet. This allows the aircraft to takeoff from the targeted 14 out of 15 cities in AeroWorld. The size and capacity of the batteries also have a strong influence on the takeoff performance of the *Airplane*. Since only 0.7 % of the battery pack current is exhausted during takeoff (i.e. 6.5 mahr out of the 900 mahr) , a sufficient battery charge is left after takeoff in order to complete the other phases of the mission which are cruising, turning, landing, and loitering.

In order to compute the performance characteristics during takeoff, a Fortran code was used [Reference 6-1]. Table 6-2 shows an example of input and output using this program.

TABLE 6-2
Input and Output for "Takeoff Performance" program

Input:

Weight	5.25 lb
Planform Area	9.5 ft^2
Cl @ takeoff	0.404
Cd @ takeoff	0.0488
Prop. Diameter	1.0 ft

Battery Voltage		14.6 volts
K_T		1.134
K_V		0.000796
J	Cp	Ct
0.000	0.100	0.0299
0.220	0.0989	0.0410
0.280	0.0860	0.0430
0.340	0.0799	0.0430
0.400	0.0729	0.0430
0.450	0.0649	0.0410
0.510	0.0579	0.0390
0.570	0.0480	0.0359
0.630	0.0379	0.0309
0.680	0.0270	0.0250
0.740	0.0150	0.0179
0.800	0.0030	0.0099

Output:

Time to Takeoff	2.10 sec
Takeoff Velocity	23.3 ft/s
Takeoff Distance	24.0 ft
Takeoff Thrust	2.67 lb
Battery Drain	6.54 mahr
Current Draw	12.44 amps
Max. Motor Power	280.8 watts

These results of the takeoff performance analysis show that the *Airplane* will satisfy the takeoff requirements.

6.2 RATE OF CLIMB

A plot of power available and power required versus velocity for a full range of power settings is shown in Figure 6-1. From this figure, it can be shown that V_{max} = 54.3 ft/s and V_{min} = 19.3 ft/s = V_{stall}, because the plane stalls before the two power curves intersect at the lower end of the graph. From Figure 6-2, at a velocity of 35 ft/s and at the full throttle condition and at full payload capacity, a maximum rate of climb of 12.4 ft/s can be achieved. When there are no passengers, the maximum rate of climb is 13.1 ft/s. The rate of climb is as follows:

$$R/C = (T - D)\, V/\, W = (P_{av} - P_{req})/W$$

Other important parameters are the minimum sink speed and the minimum glide angle. These can be determined by the following relationships from Reference 6-2:

$$(R/S)min = (2\, W/\rho\, S)^{0.5}\ [C_D\ /\ C_L{}^{1.5}]_{min}$$

$$\gamma_{min} = \text{minimum glide path angle} = \arctan\,[1/(C_L/C_D)_{max}]$$

FIGURE 6-1
Power Required and Power Available for Flight Regime

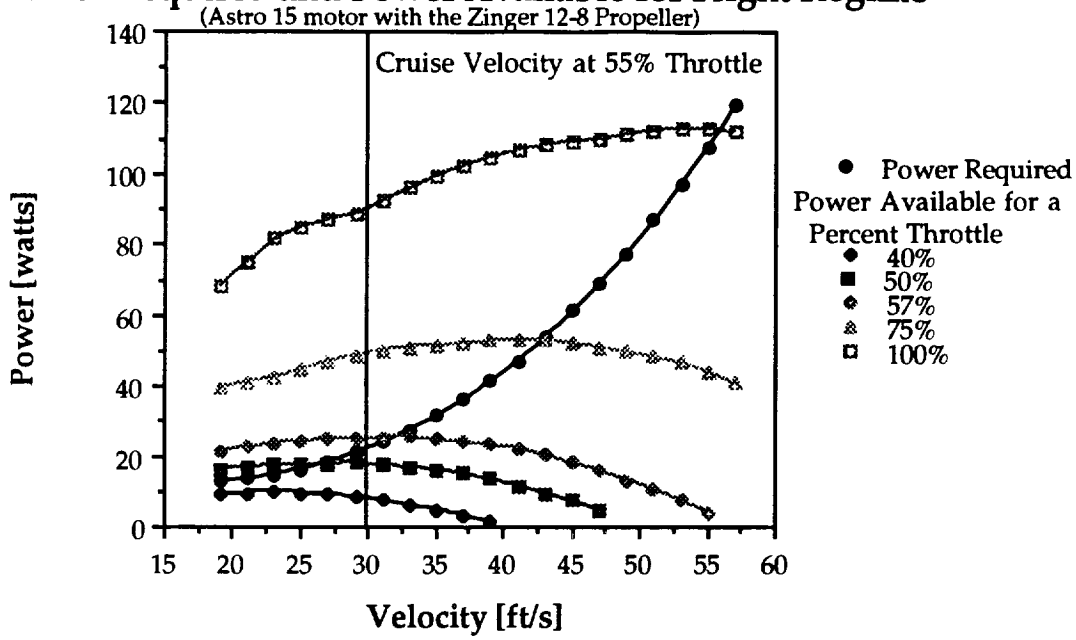

FIGURE 6-2
Maximum Rate of Climb and Maximum Velocity

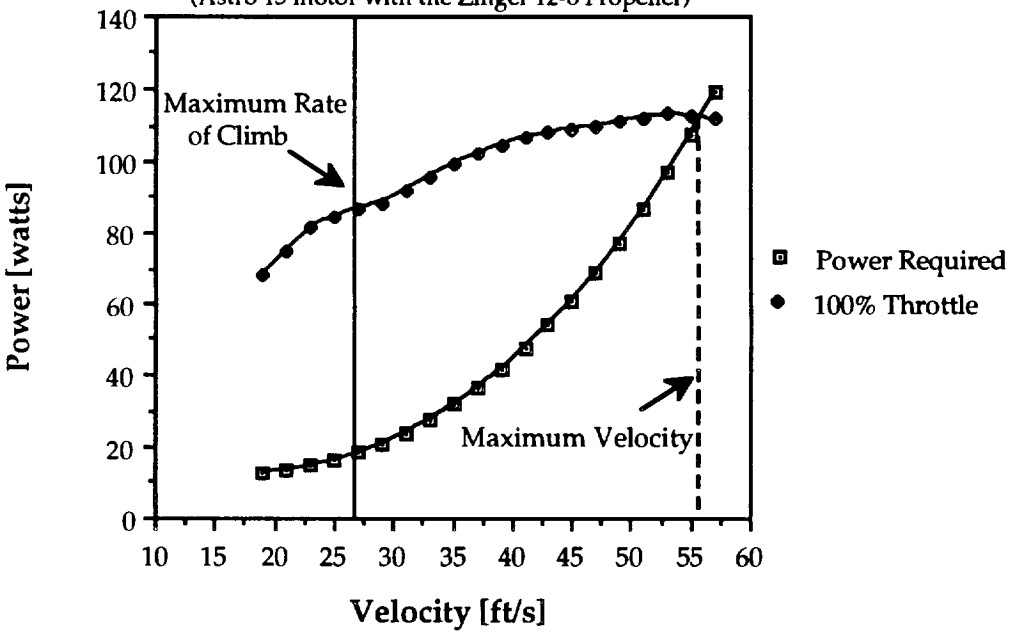

6.3 LEVEL TURN PERFORMANCE

The main requirement for turn performance is that the aircraft must perform a sustained, level 60 ft radius turn at a flight speed of 25 ft/s. The main parameters in the steady level turn are the bank angle and the related load factor. The relationship is as follows:

$$n = 1/\cos(\phi)$$

A plot of this relationship is shown in Figure 6-3. The load factor increases with increasing bank angle, but the pilot probably will not bank the aircraft at more than 30 degrees in order to keep the passengers comfortable and hence the load factor should be less than 1.2. This value for the load factor is important because it must be incorporated into the structural considerations of the aircraft.

FIGURE 6-3
Load Factor vs. Bank Angle

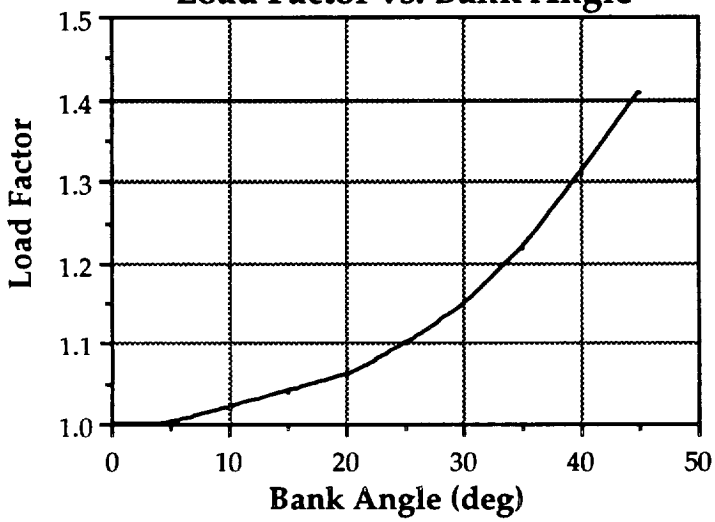

The turn radius is another parameter in a steady level turn that should be examined. It can be determined from the following relationship:

$$R = V^2 / g * \tan(\phi)$$

A plot of the turn radius as a function of bank angle at four different flight speeds is shown in Figure 6-4. The radius of the turn is very sensitive to the bank angle whereas the velocity affects the radius in a much less significant fashion. This figure gives an indication of maneuverability (i.e. radius of turn) versus control input. It is desired that the aircraft turns efficiently and smoothly in order to comfort the passengers. For the requirements of a 60 ft radius at 25 ft/s, the required bank angle is 18 degrees, and the load factor is 1.05.

FIGURE 6-4
Turn Radius vs. Bank Angle
(at various speeds)

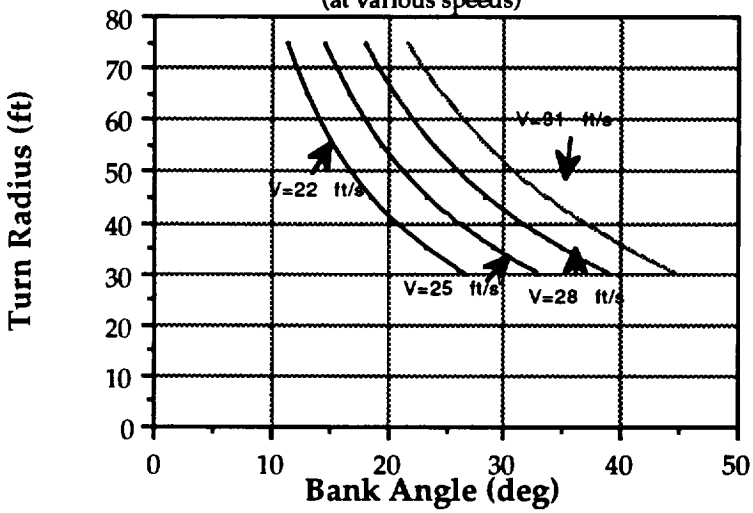

Another important relationship occurs between the lift coefficient and the bank angle, and this plot is shown at three different flight speeds in Figure 6-5. The relationship is as follows:

$$C_l = \frac{W/S}{q \cos(\phi)}$$ where q = dynamic pressure = $0.5 \rho V^2$

At small bank angles, the lift coefficient is not very sensitive to changes in the bank angle. Beyond 15 degrees of bank, the lift coefficient begins to increase more sharply with an increase of bank angle. From this plot, it is evident that at a velocity of 25

ft/s and a bank angle of 18 degrees, the turn requirement flight conditions, the lift coefficient is approximately 0.8.

FIGURE 6-5
Lift Coefficient vs. Bank Angle (W=5.25 lb)
(at various speeds)

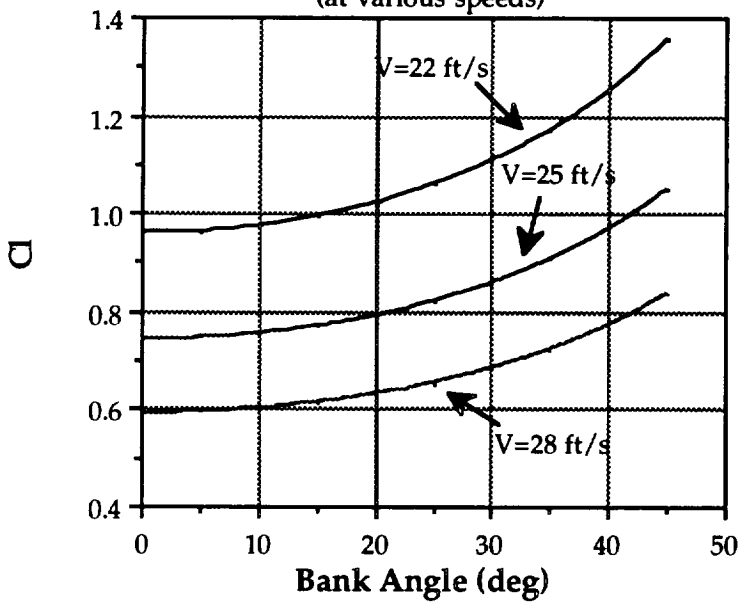

6.4 RANGE AND ENDURANCE

The *Airplane* has a maximum lift to drag ratio of 11.3. The range and endurance versus velocity are shown in Figures 6-6 and 6-7, respectively. **All of the following values for range and endurance exclude the necessary two minutes for loitering.** From this figure, the maximum aircraft range is 12520 ft and the endurance at maximum range is 7.0 minutes. At the cruise velocity of 31 ft/s, the lift to drag ratio decreases to 9.5, and the range and the endurance have values of 12140 ft and 6.8 minutes, respectively. Normally the maximum range for a propeller-driven aircraft occurs at (L/D)max, where the drag is a minimum. However, for remotely piloted vehicles this generality does not apply. On the other hand, maximum endurance for propeller-driven aircraft occurs at minimum power, and this generality seems to apply to RPV's as well.

The values for range and endurance were found using a modified version of the RPV program in Excel [Reference 6-3].

FIGURE 6-6
Range vs Velocity
(enough reserves for two min. loiter @ 1.2 of max endurance)

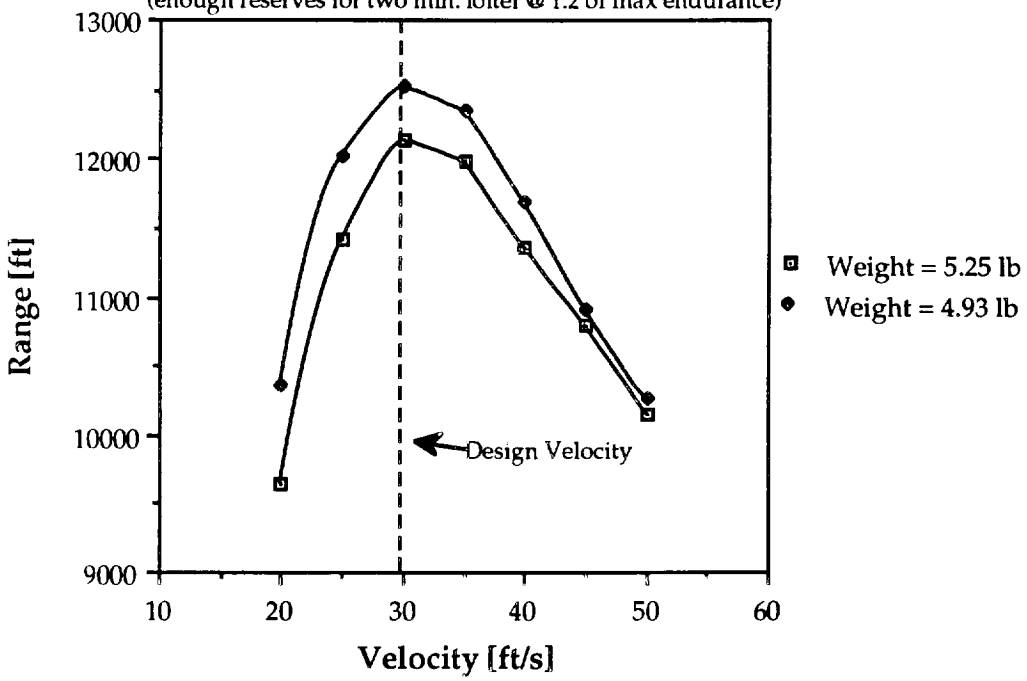

FIGURE 6-7
Endurance vs Velocity
(enough reserves for two min. loiter @ 1.2 of max endurance)

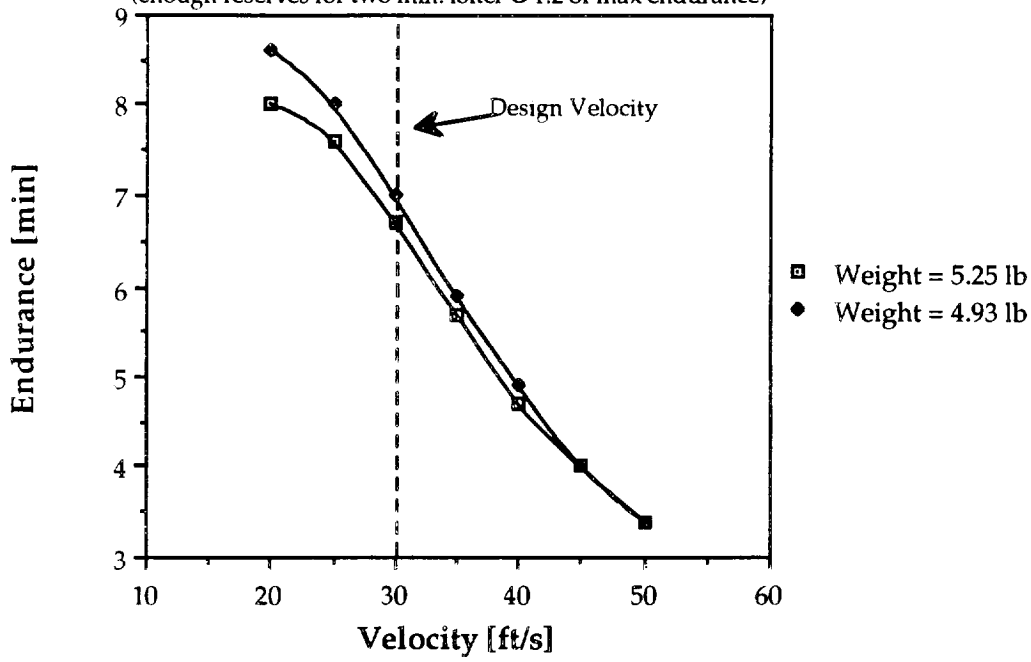

6.5 RANGE VS. PAYLOAD

The range of an aircraft will increase as the payload decreases, and this is depicted in Figure 6-8. This plot was made at the cruise speed of 31 ft/s, and it reveals that at 100% capacity the range is 12140 ft and at 0% capacity the range is 12520 ft. Since our range requirement of 10000 ft is exceeded, the pilot will be able to make more than 10 attempts at a landing if the excess range is not used to fly further. The extra mahr and hence extra range will also provide the aircraft with current for ground handling, taxi, and runway delays.

FIGURE 6-8
Range vs. Payload
(not including the two minute loiter range)

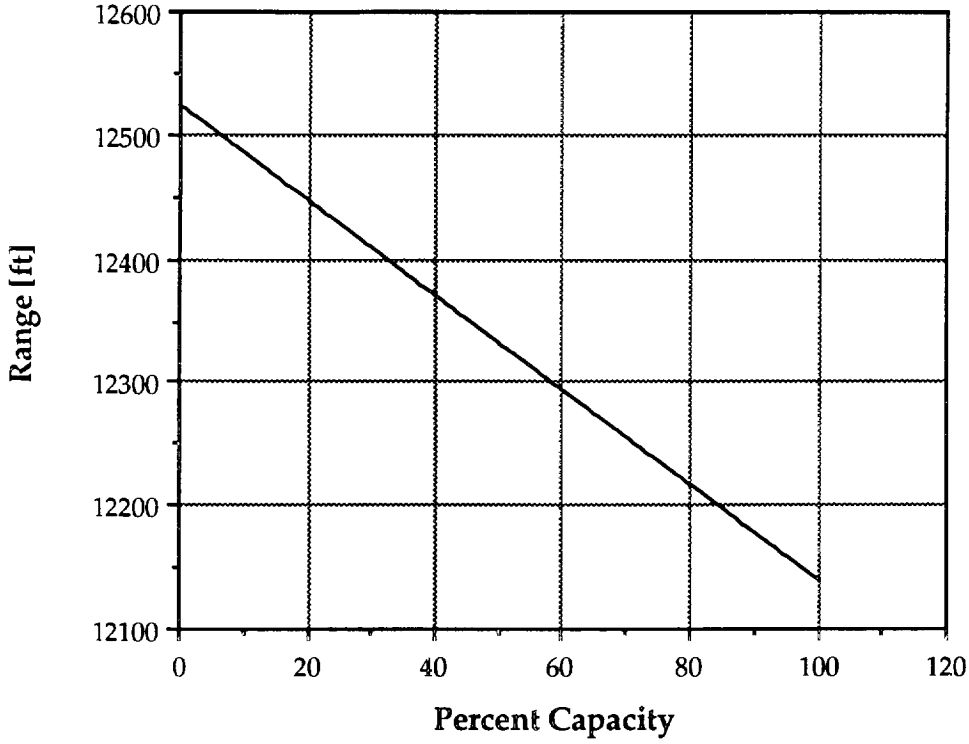

6.6 LANDING PERFORMANCE

Landing distance estimates were based on a relation found in Reference 6-4:

$$X_{land} = \frac{1.69\ W^2}{g\ \rho\ S\ C_{lmax}\ [D + \mu\ (W - L)]}$$

The resulting landing distance for the aircraft is 52.4 feet.

In conclusion, this performance analysis of the*Airplane* indicates that the design of the *Airplane* will meet or most likely exceed all of the performance requirements given in the Design Requirements and Objectives. In particular, the range objective is surpassed by over 2000 feet, and this will allow the *Airplane* to serve more of the market.

REFERENCES

6-1. Batill, S., "Takeoff Performance" Fortran computer program, University of Notre Dame, 1991.

6-2. Nelson, R.C. "Class notes", AE 348 Flight Mechanics class, University of Notre Dame, 1992.

6-3. Dunn, P., "RPV Performance" Excel computer program (modified), AE 454 Propulsion class, University of Notre Dame, 1992.

6-4. Anderson, J.D., Introduction to Flight, 2nd edition, McGraw Hill Book Company, New York, 1985.

7.0 ECONOMICS

7.1 ECONOMIC GOALS

One of the driving forces for design of the *Airplane* was to minimize its cost. Specifically, the goals were to decrease the costs in such a fashion so that:

* the *Airplane* operates at a lower cost at its design range (10000 feet) and full capacity (70 passengers) than the competitor HB-40 does at its design range (17000 feet) and full capacity (40 passengers). This translates to a cost per seat per 1000 feet (CPSPK) that is less than 0.9 cents at 10000 feet for the *Airplane.*

* the *Airplane* operates at a lower cost at its design range carrying 40 passengers than the HB-40 does at the same range at full capacity.

The achievement of the goals stated above will make the *Airplane* the most attractive aircraft in the AeroWorld market for ranges less than 10000 feet because of the potential savings involved for the prospective buyer.

7.2 COST ESTIMATES

The total cost of the *Airplane* represents the sum of the costs of fixed subsystems, raw materials, and manufacturing. Information on these costs were presented in Reference 7-1. The total fixed subsystems cost for the aircraft is $404. A complete breakdown of this cost, as well as others, is presented in Table 7-1. Raw materials costs were estimated at $175.00. This value was arrived upon based on the cost of raw materials for the HB-40 and the addition of another $25 because of the larger size of the *Airplane.* Manufacturing cost estimates are made

up of labor hours, tooling costs, and disposal costs (Reference 7-2). An estimated 100 labor hours at $10/hour will be needed to complete the manufacturing of the *Airplane*. The hazardous waste disposal cost is estimated at a conservative value of $300 due to the lack of experience of The Airplane Guys in the RPV manufacturing arena. The estimates combine to yield a total cost of $2094, some 11% less than the cost of the HB-40.

TABLE 7-1
Cost Breakdown of the *Airplane*

ITEM	COST
Fixed Subsystems:	
Radio Transmitter	$75.00
Radio Receiver	$35.00
Avionics Battery Pack	$10.00
Switch Harness	$ 5.00
Minature Servos (2)	$70.00
Electric Motor Speed Controller	$50.00
Astro-15 Motor	$107.00
P-90 SCR Batteries (12)	$36.00
Motor Power Wiring (2 feet)	$ 4.00
Landing Gear	$10.00
Zinger 12-8 Propeller	$ 2.00
SUBTOTAL	**$404.00**
Raw Materials:	
SUBTOTAL	**$175.00**
Manufacturing:	
Labor Costs (100 hours @ $10/hr)	$1000.00
Tooling	$215.00
Disposal of Hazardous Waste	$300.00
SUBTOTAL	**$1515.00**
TOTAL COST OF AIRCRAFT	**$2094.00**

The direct operating cost of the aircraft is the sum of depreciation, operation, and fuel costs (Reference 7-1). The depreciation cost was based upon a

design flight time of 0.0926 hours (at cruise). This translates into approximately 540 flights in the lifetime of the *Airplane* and a depreciation cost of $3.88 per flight. The operations costs, made up of flight crew and maintenance costs for coach seating, totalled $ 0.23 per flight. Fuel costs in AeroWorld range from $1.50 - $3.00 per amphour of battery usage, resulting in fuel costs ranging from $0.78 and $1.57 per flight (at maximum weight condition). The results lead to a direct operating cost ranging from $4.90 - $5.68 per flight. Thus, the maximum DOC of the *Airplane* is 7.2% lower than the maximum DOC of the HB-40. A summary of DOC calculations is presented in Table 7-2.

TABLE 7-2
DOC Summary

Total Cost of Aircraft	**$2094.00**
# Flights in Lifetime	540
Depreciation Expense (per flight)	**$3.88**
Operations Cost: (per flight)	
Flight Crew Costs	$0.20
Maintenance Costs (Coach only)	$0.03
SUBTOTAL	**$0.23**
Fuel Costs: (per flight at Max.Weight)	
Fuel Cost / Amphour	$1.50 - $3.00
Maximum Fuel Cost	**$1.57**
Minimum Fuel Cost	**$0.78**
DIRECT OPERATING COST	
Maximum DOC (per flight)	**$5.68**
Minimum DOC (per flight)	**$4.90**

7.3 CPSPK ANALYSIS

The CPSPK was calculated in order to allow comparison of flight costs at different passenger volumes and flight ranges. Figure 7-1 shows the flight costs for the *Airplane* at maximum capacity and at both maximum and minimum DOC.

The graph shows that CPSPK decreases with increasing range for a given payload. An increase in DOC does not have a substantial effect on CPSPK, yet any rise in cost can be significant in terms of overall profit. The difference in cost does become more pronounced at smaller ranges (less than 5000 feet).

FIGURE 7-1
CPSPK at Maximum and Minimum DOC (Full Capacity)

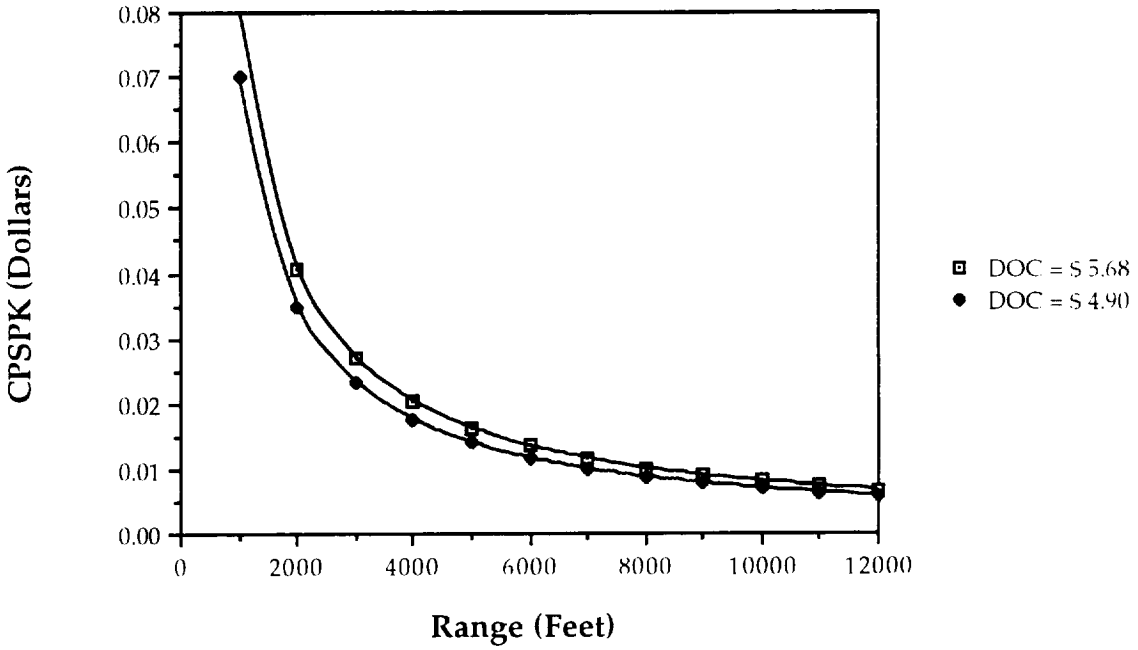

The CPSPK of the *Airplane* is $0.0081 at maximum DOC, while at minimum DOC, the CPSPK decreases to $0.007.

As mentioned previously, one of the economic goals was to have a cost lower than $0.009 at the *Airplane's* design flight range of 10000 feet. Figures 7-1 and 7-2 indicate that this goal will be successfully reached ($0.0081). The *Airplane* , therefore, is more economical at its design condition than the HB-40. Figure 7-2 compares the economic performance of the HB-40 and the *Airplane* when each aircraft carries forty passengers. Note that although this is an off-design condition for the *Airplane*, it still outperforms the HB-40 at all ranges less than

12000 feet in terms of CPSPK. Figure 7-2 shows that at 10000 feet, the cost of the *Airplane* at 40 passengers is 7.2% lower than that of the HB-40 carrying the same amount of passengers. This is significant because the second economic goal listed in section 7.1 has been achieved. Figure 7-2 also depicts the full capacity situation for the *Airplane* and the difference in economic performance between the two aircraft each at maximum payload capacity.

FIGURE 7-2
Comparison of CPSPK Costs with HB-40

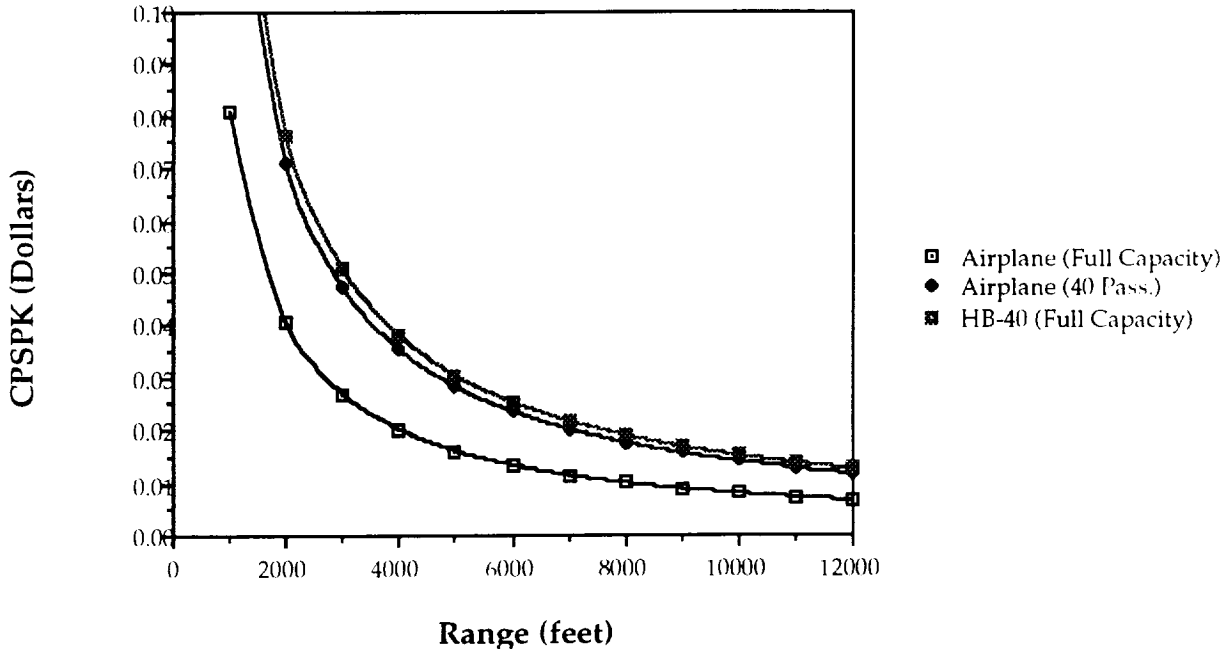

Figure 7-3 depicts the effect of changes in range and number of passengers on the CPSPK of the *Airplane*. Clearly, it is advantageous to fly with nearly all seats filled because this decreases the CPSPK. Similarly, higher ranges reduce the CPSPK. These flight configurations, however, are not always possible nor controllable. The aircraft must therefore be used efficiently in order to minimize costs. Based on the CPSPK analysis, one recommended use of the *Airplane* is to

fly at or near full capacity on routes of less than 6000 feet and to fly with no less than forty passengers on routes greater than 6000 feet.

FIGURE 7-3
Variation in CPSPK with Payload and Range at Max.DOC

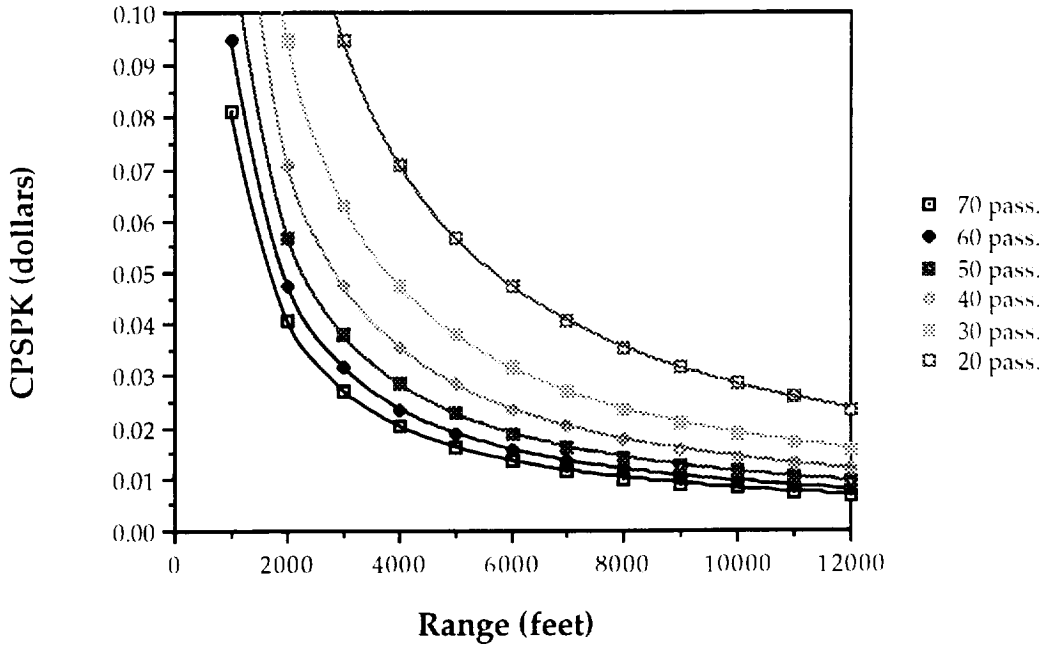

A summary of CPSPK data for ranges of 10000 and 6000 feet, maximum and minimum DOC, and different numbers of passengers is depicted in Table 7-3.

TABLE 7-3
Summary of CPSPK Data

Number of Passengers	CPSPK (6000 ft Range)	CPSPK (10000 ft Range)
70	1.16-1.35 cents	0.70-0.80 cents
60	1.63-1.89 cents	0.81-0.95 cents
40	2.04-2.37 cents	1.22-1.42 cents
20	4.08-4.73 cents	2.45-2.84 cents

REFERENCES

7-1. "Cost Data and Economic Analysis", AE 441: Aerospace Design class handout, University of Notre Dame, Spring 1993.

7-2. "Manufacturing Plan and Costing", AE 441: Aerospace Design class handout, University of Notre Dame, Spring 1993.

APPENDIX A
LINAIR 1.49 INPUTS AND RESULTS

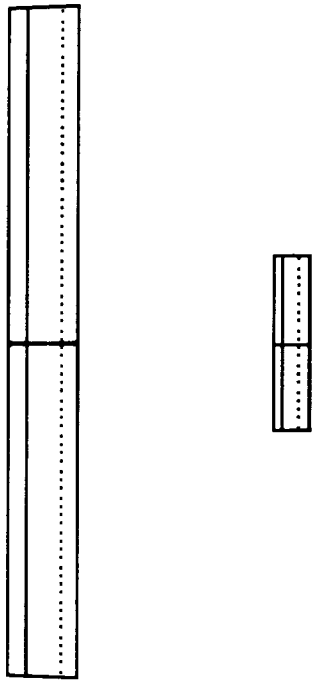

INPUT FILE:

Reference Values

Sref	bref	Xref	Yref	Zref	Nelem
9.5000	9.5000	.0000	.0000	.0000	2

alpha	Mach
12.00000	.02670

Element Geometry

Element # 2

Semi-Area	Semi-Span	Taper	Sweep	Dihedral
.62500	1.25000	1.00000	.00000	.00000

Xroot(c/4)	Yroot(c/4)	Zroot(c/4)	Root Inc.	Tip Inc.
3.62500	.00000	-.25000	.00000	.00000

# Panels	CD0	CD1	CD2
10	.01161	-.00012	.01658

Element Geometry

Element # 1

Semi-Area	Semi-Span	Taper	Sweep	Dihedral
4.75000	4.75000	1.00000	.00000	8.00000

Xroot(c/4)	Yroot(c/4)	Zroot(c/4)	Root Inc.	Tip Inc.
.00000	.00000	.00000	5.00000	5.00000

# Panels	CD0	CD1	CD2
38	.02342	-.03476	.02676

RESULTS ($\alpha = 10°$):

Element Forces and Moments

Element #	CL	CD	Cm
1	1.22314	.07677	-.03944
2	.05467	.00489	-.19708

Configuration Forces and Moments

Case #	alpha	CL	CD	Cm
1	.00000	.40319	.02111	.05204
2	2.00000	.58155	.02587	-.00194
3	4.00000	.75864	.03443	-.05804
4	6.00000	.93399	.04667	-.11600
5	8.00000	1.10719	.06248	-.17558
6	10.00000	1.27781	.08166	-.23652

Element Lift Distributions

Element# 1

X	Y	Z	$\frac{Cl*c*q}{cavg*q0}$	Cl
.00000	.06189	.00870	1.42982	1.42982
.00000	.18568	.02609	1.42866	1.42866
.00000	.30946	.04349	1.42710	1.42710
.00000	.43324	.06089	1.42529	1.42529
.00000	.55703	.07828	1.42324	1.42324
.00000	.68081	.09568	1.42094	1.42094
.00000	.80459	.11308	1.41835	1.41835
.00000	.92838	.13047	1.41545	1.41545
.00000	1.05216	.14787	1.41221	1.41221
.00000	1.17594	.16527	1.40860	1.40860
.00000	1.29973	.18266	1.40458	1.40458
.00000	1.42351	.20006	1.40011	1.40011
.00000	1.54729	.21746	1.39515	1.39515
.00000	1.67108	.23485	1.38967	1.38967
.00000	1.79486	.25225	1.38360	1.38360
.00000	1.91864	.26965	1.37688	1.37688
.00000	2.04243	.28704	1.36946	1.36946
.00000	2.16621	.30444	1.36124	1.36124
.00000	2.28999	.32184	1.35215	1.35215
.00000	2.41378	.33923	1.34206	1.34206
.00000	2.53756	.35663	1.33086	1.33086
.00000	2.66135	.37403	1.31840	1.31840
.00000	2.78513	.39142	1.30451	1.30451
.00000	2.90891	.40882	1.28898	1.28898
.00000	3.03270	.42622	1.27155	1.27155
.00000	3.15648	.44361	1.25192	1.25192
.00000	3.28026	.46101	1.22973	1.22973
.00000	3.40405	.47841	1.20450	1.20450
.00000	3.52783	.49580	1.17567	1.17567
.00000	3.65161	.51320	1.14248	1.14248
.00000	3.77540	.53060	1.10398	1.10398
.00000	3.89918	.54799	1.05888	1.05888
.00000	4.02296	.56539	1.00543	1.00543
.00000	4.14675	.58279	.94110	.94110
.00000	4.27053	.60018	.86211	.86211
.00000	4.39431	.61758	.76216	.76216
.00000	4.51810	.63498	.62926	.62926
.00000	4.64188	.65237	.43309	.43309

Element# 2

X	Y	Z	$\frac{Cl*c*q}{cavg*q0}$	Cl
3.62500	.06250	-.25000	.24552	.49104
3.62500	.18750	-.25000	.24431	.48861
3.62500	.31250	-.25000	.24170	.48340
3.62500	.43750	-.25000	.23740	.47481
3.62500	.56250	-.25000	.23098	.46195
3.62500	.68750	-.25000	.22177	.44353
3.62500	.81250	-.25000	.20871	.41742
3.62500	.93750	-.25000	.18996	.37992
3.62500	1.06250	-.25000	.16185	.32370
3.62500	1.18750	-.25000	.11519	.23039

ASTRO MOTOR PERFORMANCE

	amphr	step	frame	winding	rpm/volt	motor R	Io amps	volts	bat R	cells	ratio	gear eff	lg gear	pinion	
DATA	1.200	1.50	FAI 05	6T #19	2278	0.040	2.50	8.93	0.05	7.00	1.82	0.95	31.00	17.00	

load	motor	motor	power	power	motor	battery	motor	battery	motor	armature	gear	gear	gear	battery	gear
torque	AMPS	RPM	input	output	eff	volts	heat	heat	ohms	drop V	torque	RPM	eff	duration	POWER
0.0	2.50	19844	22.0	0.0	0.0%	8.81	22.0	0.3	0.04	0.10	0.00	10882	0.0%	28.8	0.0
4	9.00	18570	76.6	53.5	69.8%	8.52	23.2	3.7	0.04	0.36	6.70	10184	66.3%	8.0	50.8
5	10.50	18267	88.7	64.8	73.0%	8.45	23.9	5.0	0.04	0.43	8.24	10017	69.4%	6.9	61.5
6	12.00	17961	100.5	75.6	75.2%	8.38	24.9	6.6	0.04	0.49	9.79	9849	71.4%	6.0	71.8
7	13.50	17652	112.2	86.0	76.7%	8.31	26.2	8.3	0.04	0.56	11.33	9680	72.9%	5.3	81.7
7	15.00	17340	123.6	96.1	77.7%	8.24	27.6	10.2	0.04	0.63	12.88	9509	73.8%	4.8	91.2
8	16.50	17025	134.9	105.6	78.3%	8.17	29.3	12.4	0.04	0.70	14.43	9336	74.4%	4.4	100.3
9	18.00	16707	145.9	114.8	78.6%	8.11	31.2	14.7	0.04	0.77	15.97	9162	74.7%	4.0	109.0
10	19.50	16386	156.7	123.4	78.8%	8.04	33.3	17.3	0.04	0.84	17.52	8986	74.8%	3.7	117.3
11	21.00	16062	167.4	131.7	78.7%	7.97	35.7	20.1	0.04	0.92	19.06	8808	74.7%	3.4	125.1
12	22.50	15734	177.8	139.5	78.4%	7.90	38.3	23.0	0.04	0.99	20.61	8629	74.5%	3.2	132.5
13	24.00	15404	188.0	146.8	78.1%	7.83	41.2	26.2	0.04	1.07	22.15	8447	74.2%	3.0	139.4
14	25.50	15070	198.0	153.6	77.6%	7.76	44.4	29.6	0.05	1.15	23.70	8264	73.7%	2.8	145.9
15	27.00	14733	207.8	160.0	77.0%	7.70	47.9	33.2	0.05	1.23	25.25	8079	73.1%	2.7	152.0
15	28.50	14392	217.4	165.8	76.3%	7.63	51.6	37.0	0.05	1.31	26.79	7892	72.5%	2.5	157.5
16	30.00	14048	226.8	171.2	75.5%	7.56	55.6	41.0	0.05	1.39	28.34	7704	71.7%	2.4	162.6
17	31.50	13701	236.0	176.1	74.6%	7.49	59.9	45.1	0.05	1.48	29.88	7513	70.9%	2.3	167.3
18	33.00	13350	245.0	180.4	73.7%	7.42	64.5	49.5	0.05	1.56	31.43	7321	70.0%	2.2	171.4
19	34.50	12995	253.8	184.3	72.6%	7.36	69.5	54.2	0.05	1.65	32.97	7126	69.0%	2.1	175.1
20	36.00	12637	262.3	187.6	71.5%	7.29	74.7	59.0	0.05	1.74	34.52	6930	67.9%	2.0	178.2
21	37.50	12275	270.7	190.4	70.3%	7.22	80.3	64.0	0.05	1.83	36.07	6731	66.8%	1.9	180.9
22	39.00	11909	278.9	192.6	69.1%	7.15	86.2	69.2	0.05	1.92	37.61	6531	65.6%	1.8	183.0
in oz	amps	rpm	watts	watts	eff	volts	watts	watts	ohms	volts	in oz	rpm	eff	minutes	watts

|\012

ASTRO MOTOR PERFORMANCE

	amphr	step	frame	winding	rpm/volt	motor R	lo amps	volts	bat R	cells	ratio	gear eff	lg gear	pinion
DATA	1.200	1.00	COBALT 15	11T#21.5	1241	0.120	1.21	15.30	0.08	12.00	1.82	0.95	31.00	17.00

load torque	motor AMPS	motor RPM	power input	power output	motor eff	battery volts	motor heat	battery heat	motor ohms	armature drop V	gear torque	gear RPM	gear eff	battery duration	gear POWER
0.0	1.21	18690	18.4	0.0	0.0%	15.21	18.4	0.1	0.12	0.15	0.00	10249	0.0%	59.5	0.0
5	6.00	17504	89.0	68.2	76.6%	14.83	20.8	2.8	0.12	0.73	9.06	9599	72.8%	12.0	64.8
6	7.00	17246	103.3	81.2	78.6%	14.75	22.1	3.8	0.12	0.86	10.95	9458	74.7%	10.3	77.2
7	8.00	16985	117.4	93.8	79.9%	14.68	23.6	5.0	0.12	0.99	12.84	9315	75.9%	9.0	89.1
9	9.00	16721	131.4	106.0	80.6%	14.60	25.4	6.3	0.12	1.12	14.73	9170	76.6%	8.0	100.7
10	10.00	16454	145.2	117.6	81.0%	14.52	27.6	7.8	0.13	1.26	16.63	9023	77.0%	7.2	111.8
11	11.00	16184	158.9	128.9	81.1%	14.44	30.0	9.4	0.13	1.40	18.52	8875	77.1%	6.5	122.4
12	12.00	15910	172.4	139.6	81.0%	14.36	32.7	11.2	0.13	1.54	20.41	8725	77.0%	6.0	132.7
13	13.00	15633	185.7	149.9	80.7%	14.29	35.8	13.2	0.13	1.69	22.30	8573	76.7%	5.5	142.4
14	14.00	15352	198.9	159.7	80.3%	14.21	39.2	15.3	0.13	1.84	24.19	8419	76.3%	5.1	151.7
15	15.00	15068	212.0	169.0	79.7%	14.13	42.9	17.6	0.13	1.99	26.08	8263	75.8%	4.8	160.6
16	16.00	14780	224.8	177.8	79.1%	14.05	47.0	20.0	0.13	2.14	27.98	8105	75.1%	4.5	168.9
17	17.00	14489	237.6	186.1	78.3%	13.97	51.5	22.5	0.14	2.30	29.87	7946	74.4%	4.2	176.8
18	18.00	14194	250.1	193.9	77.5%	13.90	56.3	25.3	0.14	2.46	31.76	7784	73.6%	4.0	184.2
19	19.00	13896	262.5	201.1	76.6%	13.82	61.5	28.2	0.14	2.62	33.65	7620	72.8%	3.8	191.0
21	20.00	13594	274.8	207.8	75.6%	13.74	67.0	31.2	0.14	2.79	35.54	7455	71.8%	3.6	197.4
22	21.00	13288	286.9	213.9	74.6%	13.66	73.0	34.4	0.14	2.95	37.43	7287	70.8%	3.4	203.2
23	22.00	12978	298.8	219.5	73.4%	13.58	79.4	37.8	0.14	3.13	39.32	7117	69.8%	3.3	208.5
24	23.00	12664	310.6	224.5	72.3%	13.51	86.2	41.3	0.14	3.30	41.22	6945	68.6%	3.1	213.2
25	24.00	12346	322.3	228.9	71.0%	13.43	93.4	44.9	0.14	3.48	43.11	6771	67.5%	3.0	217.4
26	25.00	12025	333.8	232.7	69.7%	13.35	101.1	48.8	0.15	3.66	45.00	6594	66.2%	2.9	221.1
27	26.00	11699	345.1	235.9	68.4%	13.27	109.2	52.7	0.15	3.85	46.89	6415	64.9%	2.8	224.1
in oz	amps	rpm	watts	watts	eff	volts	watts	watts	ohms	volts	in oz	rpm	eff	minutes	watts

|\012

$K_V = 7.96 \times 10^{-4}$

ASTRO MOTOR PERFORMANCE

	amphr	step	frame	winding	rpm/volt	motor R	Io amps	volts	bat R	cells	ratio	gear eff	lg gear	pinion
DATA	1.200	1.00	COBALT 25	8T#20.5	878	0.138	1.53	17.85	0.09	14.00	1.82	0.95	31.00	17.00

load torque	motor AMPS	motor RPM	power input	power output	motor eff	battery volts	motor heat	battery heat	motor ohms	armature drop V	gear torque	gear RPM	gear eff	battery duration	gear POWER
0.0	1.53	15365	27.1	0.0	0.0%	17.71	27.1	0.2	0.14	0.21	0.00	8426	0.0%	47.1	0.0
7	6.00	14459	103.8	74.3	71.6%	17.30	29.5	3.3	0.14	0.84	11.95	7929	68.0%	12.0	70.6
8	7.00	14248	120.5	89.6	74.4%	17.21	30.9	4.5	0.14	0.99	14.62	7813	70.6%	10.3	85.1
10	8.00	14034	137.0	104.4	76.2%	17.12	32.6	5.8	0.14	1.14	17.30	7696	72.4%	9.0	99.2
12	9.00	13818	153.3	118.7	77.4%	17.03	34.6	7.4	0.14	1.29	19.97	7578	73.6%	8.0	112.7
13	10.00	13600	169.4	132.4	78.2%	16.94	37.0	9.1	0.15	1.45	22.64	7458	74.3%	7.2	125.8
15	11.00	13379	185.3	145.7	78.6%	16.85	39.7	11.0	0.15	1.61	25.32	7337	74.7%	6.5	138.4
16	12.00	13155	201.1	158.4	78.7%	16.76	42.7	13.1	0.15	1.78	27.99	7214	74.8%	6.0	150.4
18	13.00	12928	216.7	170.5	78.7%	16.67	46.2	15.4	0.15	1.94	30.67	7090	74.8%	5.5	162.0
19	14.00	12699	232.1	182.1	78.5%	16.58	50.0	17.8	0.15	2.11	33.34	6964	74.5%	5.1	173.0
21	15.00	12466	247.3	193.1	78.1%	16.49	54.2	20.5	0.15	2.29	36.01	6836	74.2%	4.8	183.4
22	16.00	12231	262.3	203.5	77.6%	16.39	58.8	23.3	0.15	2.46	38.69	6707	73.7%	4.5	193.3
24	17.00	11993	277.2	213.3	77.0%	16.30	63.8	26.3	0.16	2.64	41.36	6577	73.1%	4.2	202.6
25	18.00	11752	291.8	222.5	76.3%	16.21	69.3	29.5	0.16	2.83	44.03	6445	72.4%	4.0	211.4
27	19.00	11508	306.3	231.2	75.5%	16.12	75.1	32.9	0.16	3.01	46.71	6311	71.7%	3.8	219.6
29	20.00	11261	320.6	239.1	74.6%	16.03	81.5	36.4	0.16	3.20	49.38	6175	70.9%	3.6	227.2
30	21.00	11011	334.7	246.5	73.6%	15.94	88.2	40.1	0.16	3.40	52.05	6038	70.0%	3.4	234.2
32	22.00	10758	348.7	253.2	72.6%	15.85	95.5	44.0	0.16	3.60	54.73	5899	69.0%	3.3	240.5
33	23.00	10501	362.4	259.2	71.5%	15.76	103.2	48.1	0.17	3.80	57.40	5759	68.0%	3.1	246.3
35	24.00	10242	376.0	264.6	70.4%	15.67	111.4	52.4	0.17	4.00	60.07	5616	66.9%	3.0	251.4
36	25.00	9979	389.4	269.3	69.2%	15.57	120.1	56.9	0.17	4.21	62.75	5472	65.7%	2.9	255.8
38	26.00	9713	402.6	273.3	67.9%	15.48	129.3	61.5	0.17	4.42	65.42	5326	64.5%	2.8	259.6
in oz	amps	rpm	watts	watts	eff	volts	watts	watts	ohms	volts	in oz	rpm	eff	minutes	watts

|\012

APPENDIX B-2

PROPELLER DATA SHEET

A) Propeller Designation: ZingerJ 10-4

B) Number of Blades: 2 Diameter: 10 (Inches)

C) Select one of the following airfoil sections:
1) INVISCID FLAT PLATE
2) THIN FLAT PLATE
3) SYMMETRICAL
4) CLARK Y
5) RAF-6
--> 6) NACA44XXLOWRE

D) Blade thickness may be entered as either:
1) Fraction of chord
--> 2) Inches

E) Blade data may be entered at radial locations specified as:
1) Fractional Radius
--> 2) Inches

F) Radius* at which blade setting is measured: 3

G) Blade setting (i.e. ref angle for whole blade): 11.98

H) Enter the number of radial data positions: (3-9): 8

I)

Data Point	Radius*	Chord	Thickness*	Angle
1:	1	.622	.221	32.48
2:	1.5	.71	.163	23
3:	2	.801	.157	17.66
4:	2.5	.863	.153	14.29
5:	3	.881	.142	11.98
6:	3.5	.831	.126	10.31
7:	4	.745	.102	9.04
8:	4.5	.599	.075	8.05
9:	.....	.....	.....	.....

J) Select desired refinment of analysis:
--> 1) Analysis by simple blade element theory.
2) Analysis including induced velocity.
3) Analysis including induced velocity and tip losses.

K) These Cl/Cd coefficient adjustments may be selected
--> 1) No Cl/Cd adjustments
2) Mach number adjustment
3) Reynolds number adjustment
4) Mach and reynolds number adjustments

L) Select altitude in thousands of feet: 0

M) Specify one of the following:
--> 1) Airspeed FIXED at: 17 MPH
2) Propeller RPM FIXED at:

N) Range of Advance Ratio to be used in calculations:
J min: .1 J max: .8

NOTES: First data point must be less than 30% radius; others must progress outward.
Designation must start with a letter and may not contain a comma.
For square tip blades (only) use tip as last data point.
Angles must be specified in degrees, lengths in inches.
* Units must be as specified in lines D and E.

Zinger 10-4 @ ~~22~~ 17 mph

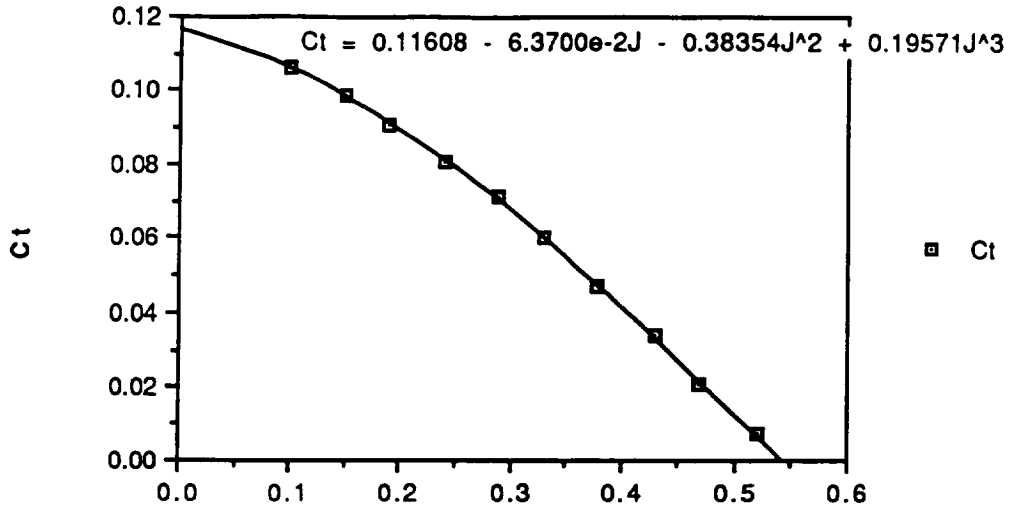

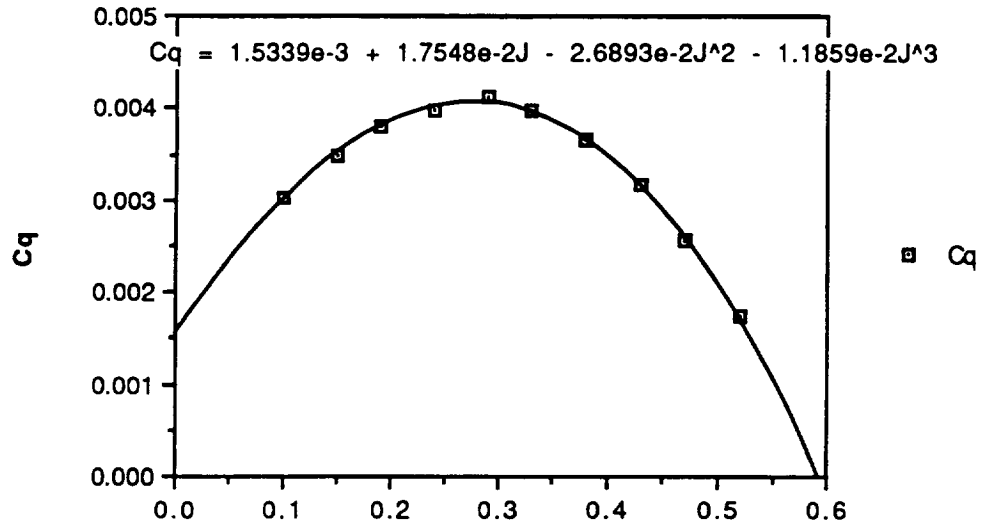

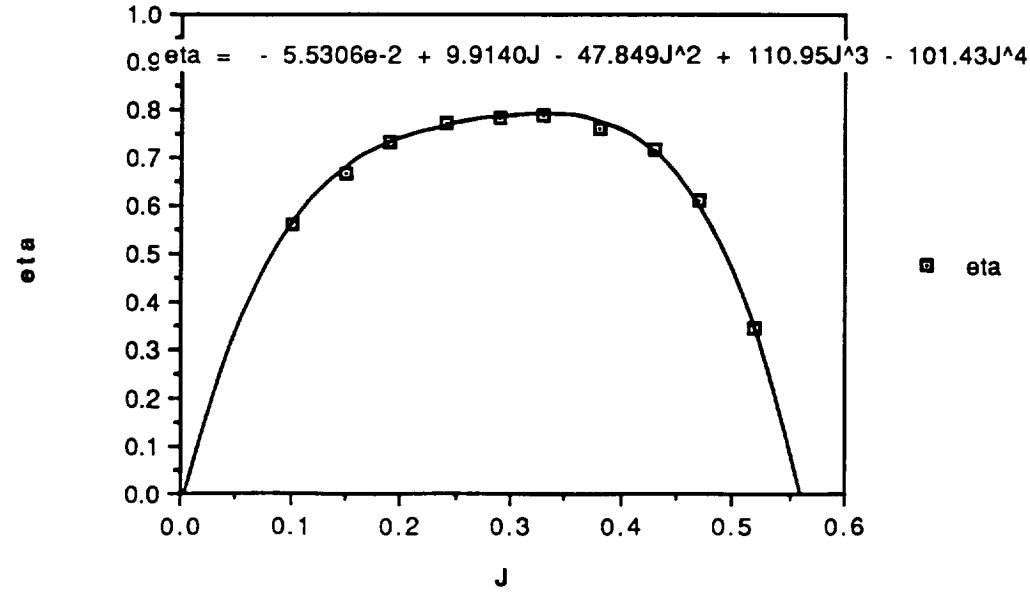

1

PROPELLER DATA SHEET

A) Propeller Designation: ZING 10-6 QUIRK

B) Number of Blades: 2 Diameter: 11 (Inches)

C) Select one of the following airfoil sections:
1) INVISCID FLAT PLATE
2) THIN FLAT PLATE
3) SYMMETRICAL
4) CLARK Y
5) RAF-6
--> 6) NACA44XXLOWRE

D) Blade thickness may be entered as either:
1) Fraction of chord
--> 2) Inches

E) Blade data may be entered at radial locations specified as:
1) Fractional Radius
--> 2) Inches

F) Radius* at which blade setting is measured: 3

G) Blade setting (i.e. ref angle for whole blade): 17.66

H) Enter the number of radial data positions: (3-9): 9

I)

Data Point	Radius*	Chord	Thickness*	Angle
1:1		.625	.248	43.68
2:1.5		.7188	.2	32.48
3:2		.8125	.2	25.52
4:2.5		.875	.192	20.91
5:3		.875	.176	17.66
6:3.5		.8313	.154	15.26
7:4		.7188	.133	13.43
8:4.5		.5938	.107	11.98
9:5		.4375	.079	10.81

J) Select desired refinment of analysis:
--> 1) Analysis by simple blade element theory.
2) Analysis including induced velocity.
3) Analysis including induced velocity and tip losses.

K) These Cl/Cd coefficient adjustments may be selected
--> 1) No Cl/Cd adjustments
2) Mach number adjustment
3) Reynolds number adjustment
4) Mach and reynolds number adjustments

L) Select altitude in thousands of feet: 0

M) Specify one of the following:
--> 1) Airspeed FIXED at: 17 MPH
2) Propeller RPM FIXED at:

N) Range of Advance Ratio to be used in calculations:
J min: .1 J max: .8

NOTES: First data point must be less than 30% radius; others must progress outward.
Designation must start with a letter and may not contain a comma.
For square tip blades (only) use tip as last data point.
Angles must be specified in degrees, lengths in inches.
* Units must be as specified in lines D and E.

Zinger 10-6 @ 17 mph

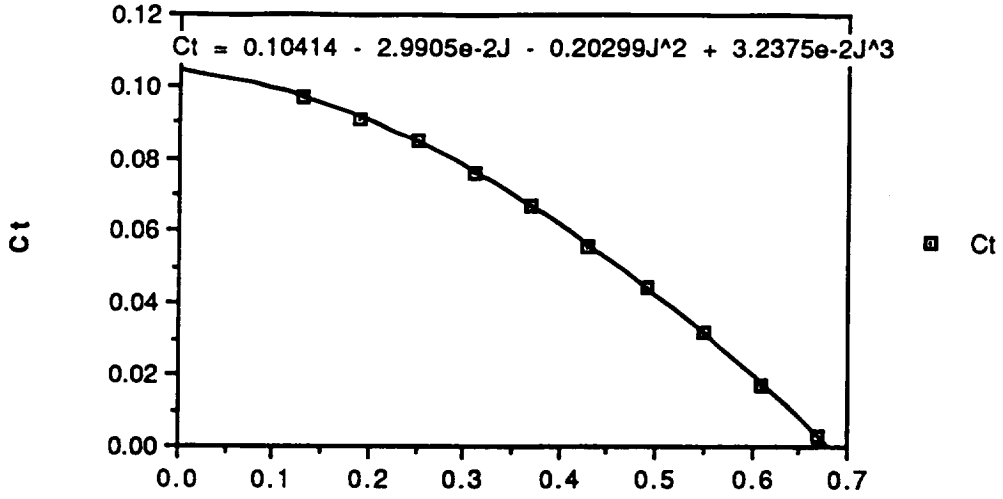

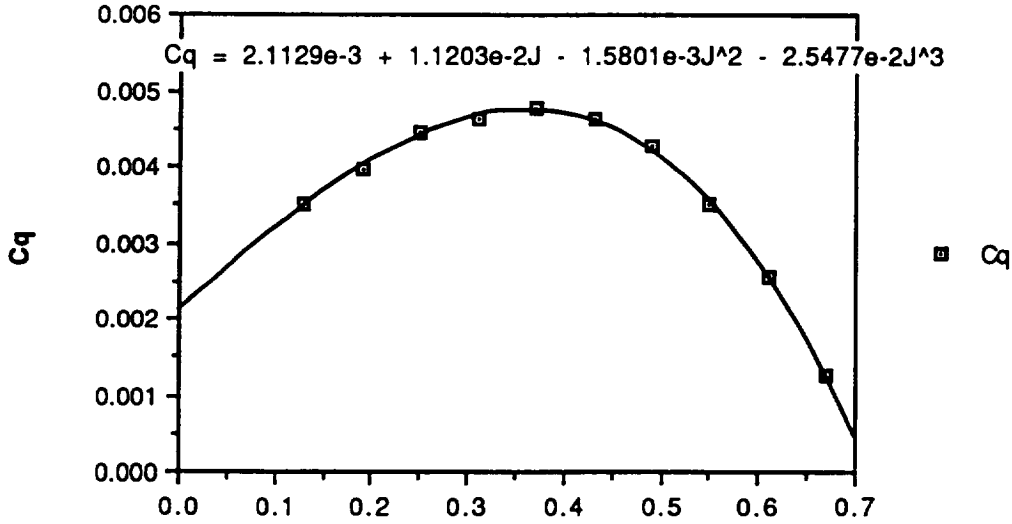

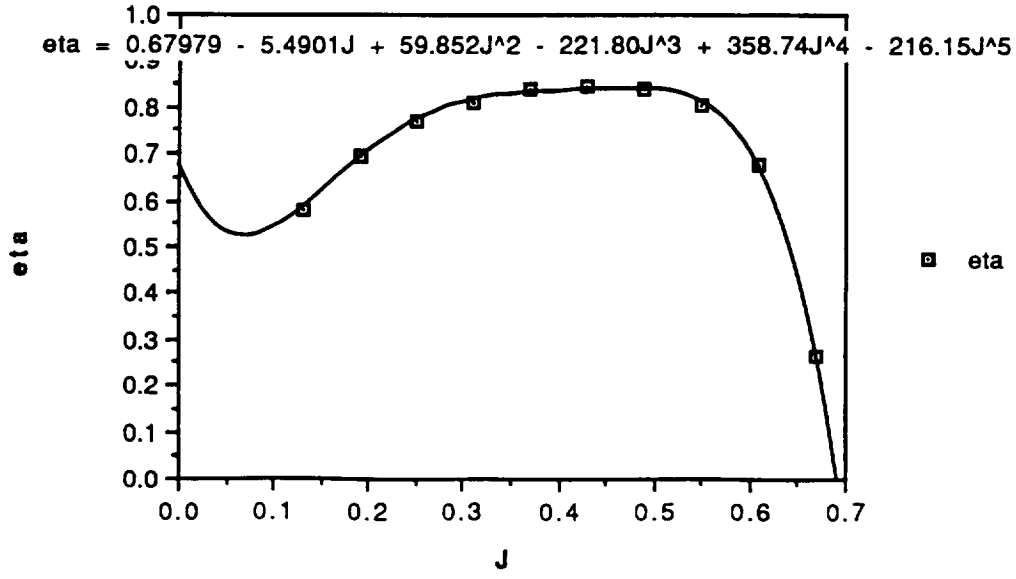

1

PROPELLER DATA SHEET

A) Propeller Designation: ZING 11-5 QUIRK

B) Number of Blades: 2 Diameter: 11 (Inches)

C) Select one of the following airfoil sections:
1) INVISCID FLAT PLATE
2) THIN FLAT PLATE
3) SYMMETRICAL
4) CLARK Y
5) RAF-6
--> 6) NACA44XXLOWRE

D) Blade thickness may be entered as either:
1) Fraction of chord
--> 2) Inches

E) Blade data may be entered at radial locations specified as:
1) Fractional Radius
--> 2) Inches

F) Radius* at which blade setting is measured: 3

G) Blade setting (i.e. ref angle for whole blade): 14.86

H) Enter the number of radial data positions: (3-9): 8

I)

Data Point	Radius*	Chord	Thickness*	Angle
1:	1.5	.784	.198	27.95
2:	2	.862	.193	21.7
3:	2.5	.918	.182	17.66
4:	3	.931	.172	14.86
5:	3.5	.904	.157	12.81
6:	4	.839	.139	11.25
7:	4.5	.759	.118	10.03
8:	5	.634	.098	9.04
9:	.....	.....	.....	.....

J) Select desired refinment of analysis:
--> 1) Analysis by simple blade element theory.
2) Analysis including induced velocity.
3) Analysis including induced velocity and tip losses.

K) These Cl/Cd coefficient adjustments may be selected
--> 1) No Cl/Cd adjustments
2) Mach number adjustment
3) Reynolds number adjustment
4) Mach and reynolds number adjustments

L) Select altitude in thousands of feet: 0

M) Specify one of the following:
--> 1) Airspeed FIXED at: 17 MPH
2) Propeller RPM FIXED at:

N) Range of Advance Ratio to be used in calculations:
J min: .1 J max: .8

NOTES: First data point must be less than 30% radius; others must progress outward.
Designation must start with a letter and may not contain a comma.
For square tip blades (only) use tip as last data point.
Angles must be specified in degrees, lengths in inches.
* Units must be as specified in lines D and E.

Zinger 11-5 @ 17 mph

(Including induced velocity and tip losses)

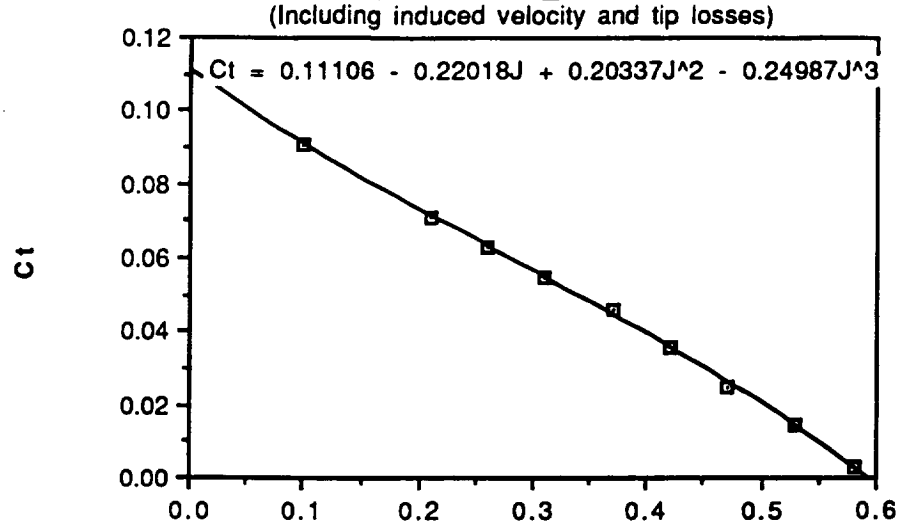

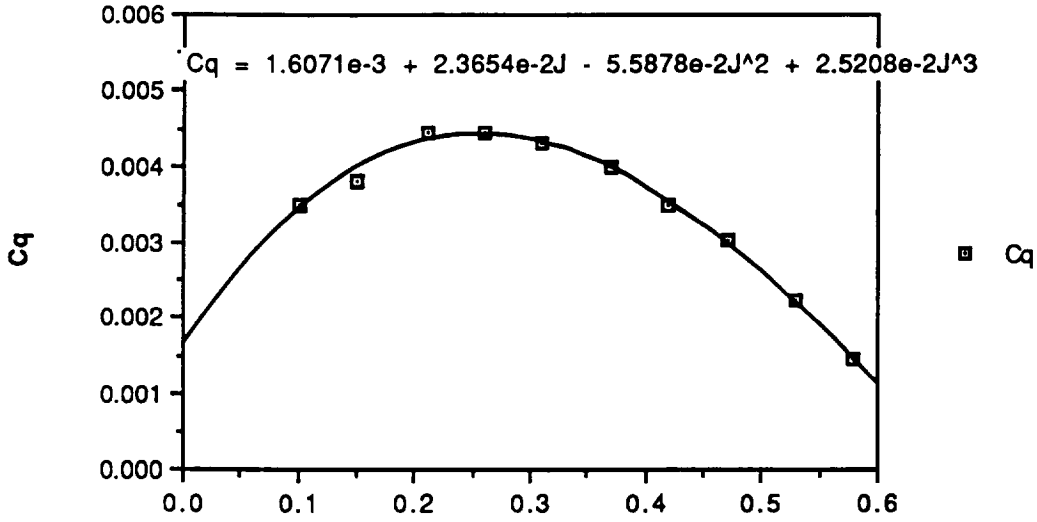

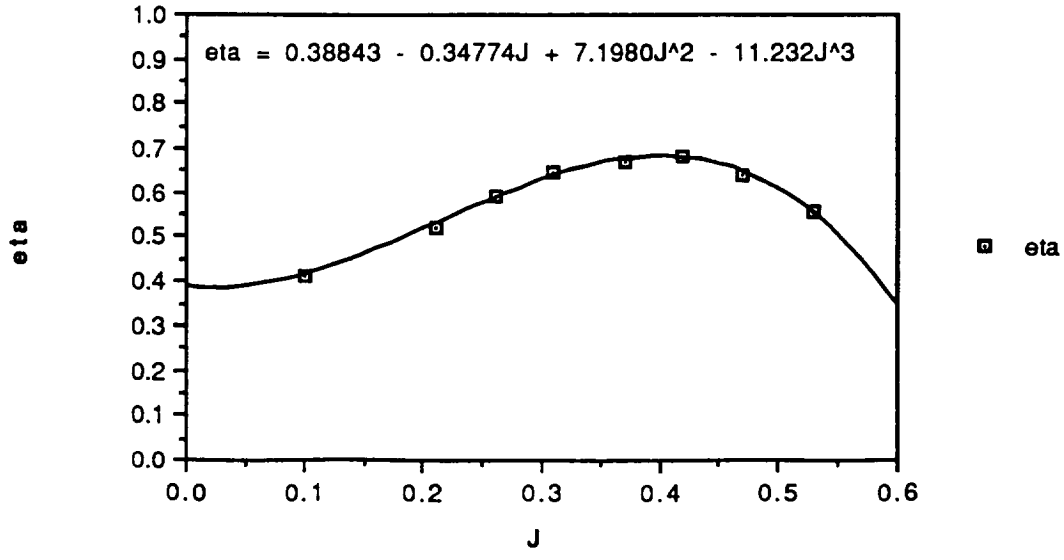

PROPELLER DATA SHEET

A) Propeller Designation: ZING 11-7 QUIRK

B) Number of Blades: 2 Diameter: 11 (Inches)

C) Select one of the following airfoil sections:
1) INVISCID FLAT PLATE
2) THIN FLAT PLATE
3) SYMMETRICAL
4) CLARK Y
5) RAF-6
--> 6) NACA44XXLOWRE

D) Blade thickness may be entered as either:
1) Fraction of chord
--> 2) Inches

E) Blade data may be entered at radial locations specified as:
1) Fractional Radius
--> 2) Inches

F) Radius* at which blade setting is measured: 3

G) Blade setting (i.e. ref angle for whole blade): 20.37

H) Enter the number of radial data positions: (3-9): 9

I)

Data Point	Radius*	Chord	Thickness*	Angle
1:	1.5	.77	.233	36.6
2:	2	.875	.212	29.12
3:	2.5	.9375	.196	24.02
4:	3	.9375	.18	20.37
5:	3.5	.875	.169	17.66
6:	4	.8125	.153	15.56
7:	4.5	.75	.122	13.91
8:	5	.625	.077	12.56
9:	5.5	.4375	.069	11.45
9:	.....	.....	.....	.....

J) Select desired refinment of analysis:
--> 1) Analysis by simple blade element theory.
2) Analysis including induced velocity.
3) Analysis including induced velocity and tip losses.

K) These Cl/Cd coefficient adjustments may be selected
--> 1) No Cl/Cd adjustments
2) Mach number adjustment
3) Reynolds number adjustment
4) Mach and reynolds number adjustments

L) Select altitude in thousands of feet: 0

M) Specify one of the following:
--> 1) Airspeed FIXED at: 17 MPH
2) Propeller RPM FIXED at:

N) Range of Advance Ratio to be used in calculations:
J min: .1 J max: .8

NOTES: First data point must be less than 30% radius; others must progress outward.
Designation must start with a letter and may not contain a comma.
For square tip blades (only) use tip as last data point.
Angles must be specified in degrees, lengths in inches.
* Units must be as specified in lines D and E.

Zinger 11-7 @ 17 mph

(Including induced velocity and tip losses)

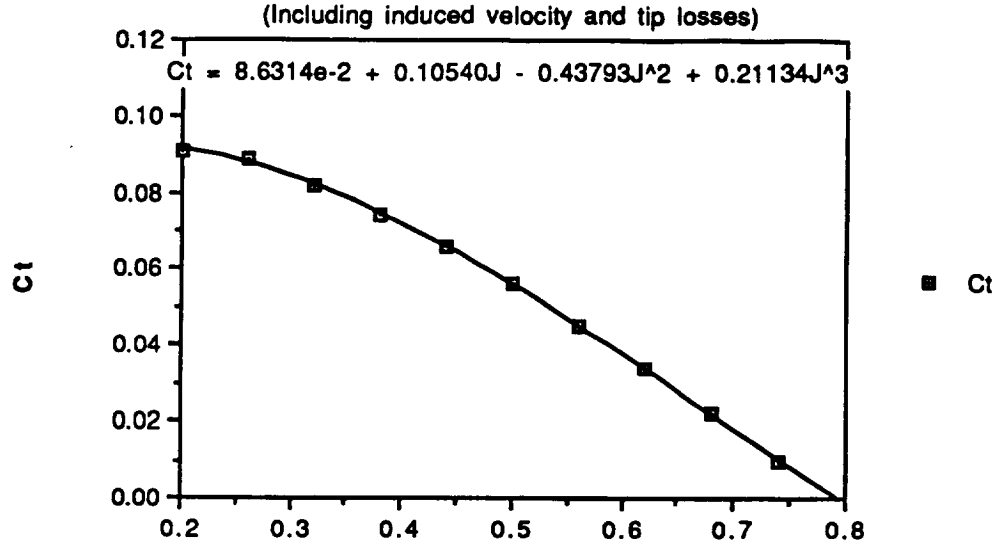

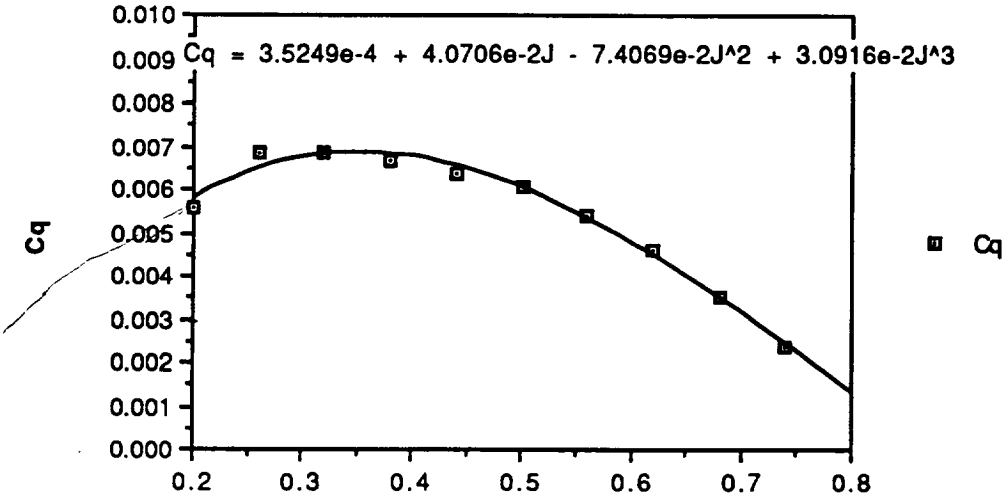

$C_Q = \frac{C_q}{2\pi}$

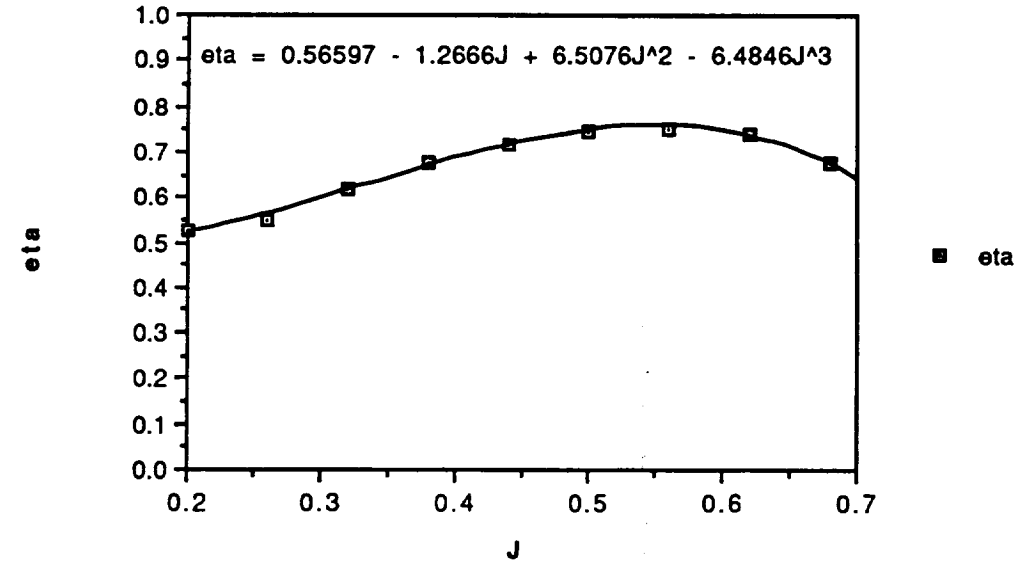

PROPELLER DATA SHEET

A) Propeller Designation: ZING 11-8 QUIRK

B) Number of Blades: 2 Diameter: 11 (Inches)

C) Select one of the following airfoil sections:
1) INVISCID FLAT PLATE
2) THIN FLAT PLATE
3) SYMMETRICAL
4) CLARK Y
5) RAF-6
--> 6) NACA44XXLOWRE

D) Blade thickness may be entered as either:
1) Fraction of chord
--> 2) Inches

E) Blade data may be entered at radial locations specified as:
1) Fractional Radius
--> 2) Inches

F) Radius* at which blade setting is measured: 3

G) Blade setting (i.e. ref angle for whole blade): 23

H) Enter the number of radial data positions: (3-9): 8

I)

Data Point	Radius*	Chord	Thickness*	Angle
1:	1.5	.831	.212	40.33
2:	2	.914	.204	32.48
3:	2.5	.97	.193	26.99
4:	3	.984	.175	23
5:	3.5	.952	.162	20
6:	4	.887	.141	17.66
7:	4.5	.785	.123	15.8
8:	5	.659	.1	14.29
9:	.....	.....	.....	.....

J) Select desired refinment of analysis:
1) Analysis by simple blade element theory.
2) Analysis including induced velocity.
--> 3) Analysis including induced velocity and tip losses.

K) These Cl/Cd coefficient adjustments may be selected
--> 1) No Cl/Cd adjustments
2) Mach number adjustment
3) Reynolds number adjustment
4) Mach and reynolds number adjustments

L) Select altitude in thousands of feet: 0

M) Specify one of the following:
--> 1) Airspeed FIXED at: 17 MPH
2) Propeller RPM FIXED at:

N) Range of Advance Ratio to be used in calculations:
J min: .1 J max: .8

NOTES: First data point must be less than 30% radius; others must progress outward.
Designation must start with a letter and may not contain a comma.
For square tip blades (only) use tip as last data point.
Angles must be specified in degrees, lengths in inches.
* Units must be as specified in lines D and E.

Zinger 11-8 @ 17 mph

(Including induced velocities and tip losses)

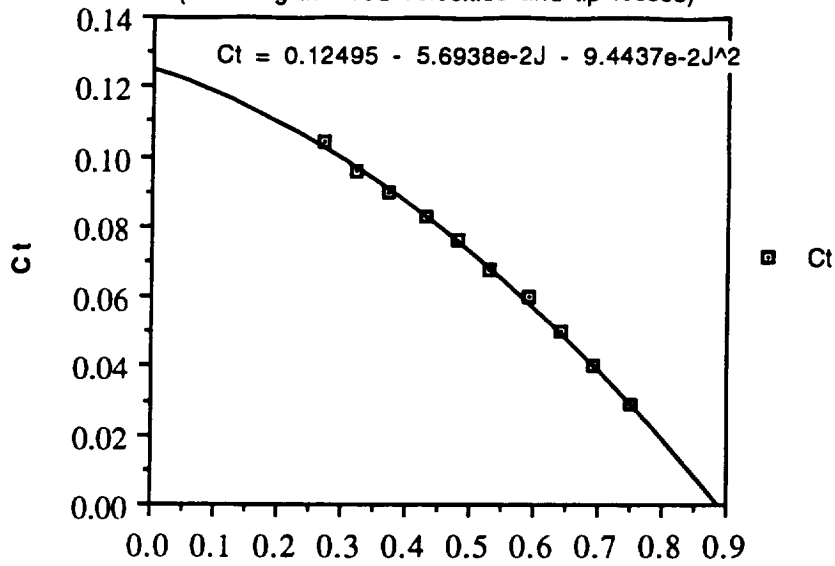

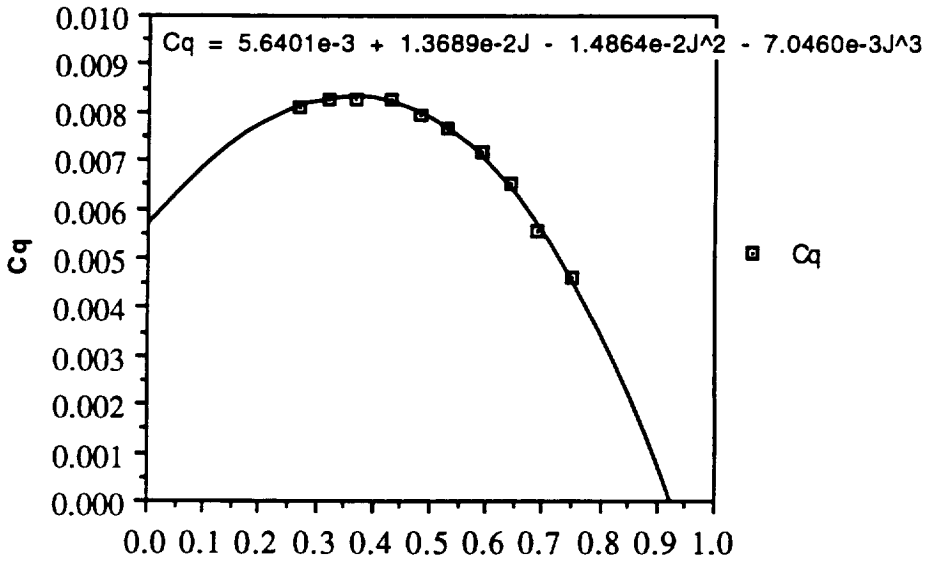

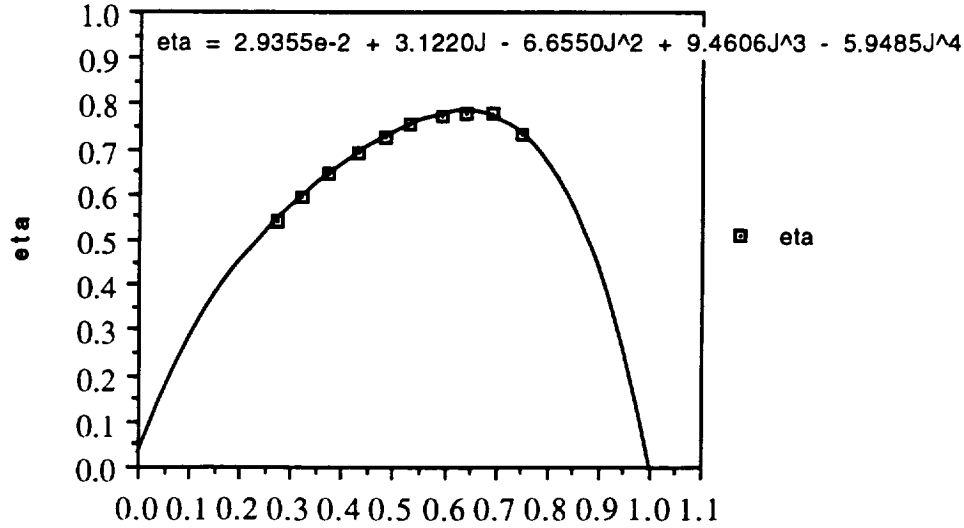

PROPELLER DATA SHEET

A) Propeller Designation: ZING 12-4 QUIRK

B) Number of Blades: 2 Diameter: 12 (Inches)

C) Select one of the following airfoil sections:
1) INVISCID FLAT PLATE
2) THIN FLAT PLATE
3) SYMMETRICAL
4) CLARK Y
5) RAF-6
--> 6) NACA44XXLOWRE

D) Blade thickness may be entered as either:
1) Fraction of chord
--> 2) Inches

E) Blade data may be entered at radial locations specified as:
1) Fractional Radius
--> 2) Inches

F) Radius* at which blade setting is measured: 3

G) Blade setting (i.e. ref angle for whole blade): 11.98

H) Enter the number of radial data positions: (3-9): 9

I)

Data Point	Radius*	Chord	Thickness*	Angle
1:1.5		.786	.205	23
2:2		.875	.2	17.66
3:2.5		.949	.192	14.29
4:3		.989	.184	11.98
5:3.5		1	.169	10.31
6:4		.971	.155	9.04
7:4.5		.906	.138	8.05
8:5		.898	.118	7.26
9:5.5		.8	.097	6.6

J) Select desired refinment of analysis:
--> 1) Analysis by simple blade element theory.
2) Analysis including induced velocity.
3) Analysis including induced velocity and tip losses.

K) These Cl/Cd coefficient adjustments may be selected
--> 1) No Cl/Cd adjustments
2) Mach number adjustment
3) Reynolds number adjustment
4) Mach and reynolds number adjustments

L) Select altitude in thousands of feet: 0

M) Specify one of the following:
--> 1) Airspeed FIXED at: 17 MPH
2) Propeller RPM FIXED at:

N) Range of Advance Ratio to be used in calculations:
J min: .1 J max: .8

NOTES: First data point must be less than 30% radius; others must progress outward.
Designation must start with a letter and may not contain a comma.
For square tip blades (only) use tip as last data point.
Angles must be specified in degrees, lengths in inches.
* Units must be as specified in lines D and E.

Zinger 12-4 @ 17 mph

(Including induced velocity and tip losses)

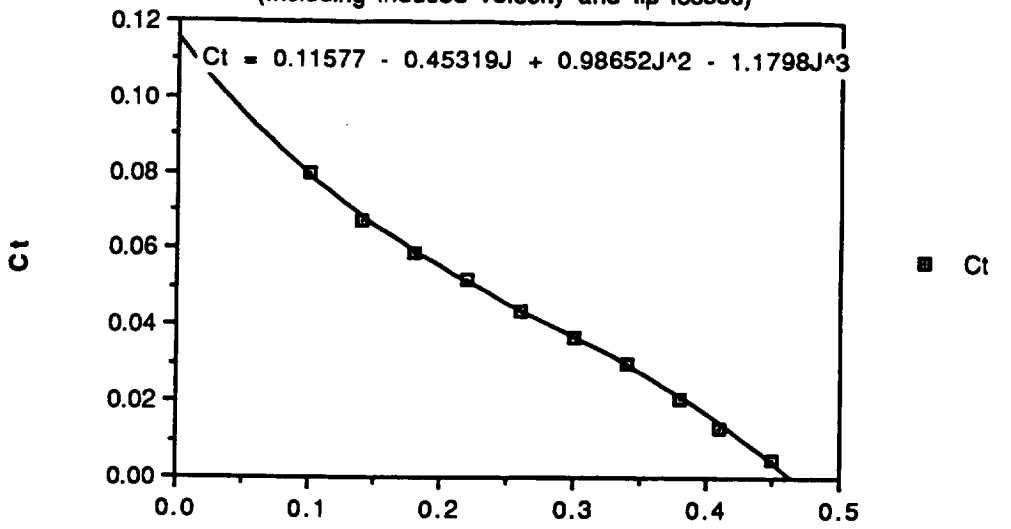

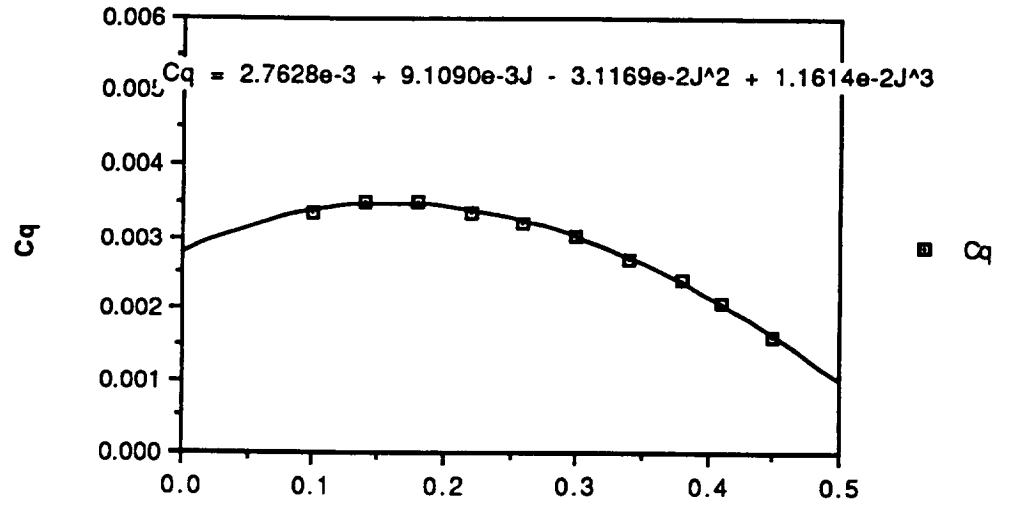

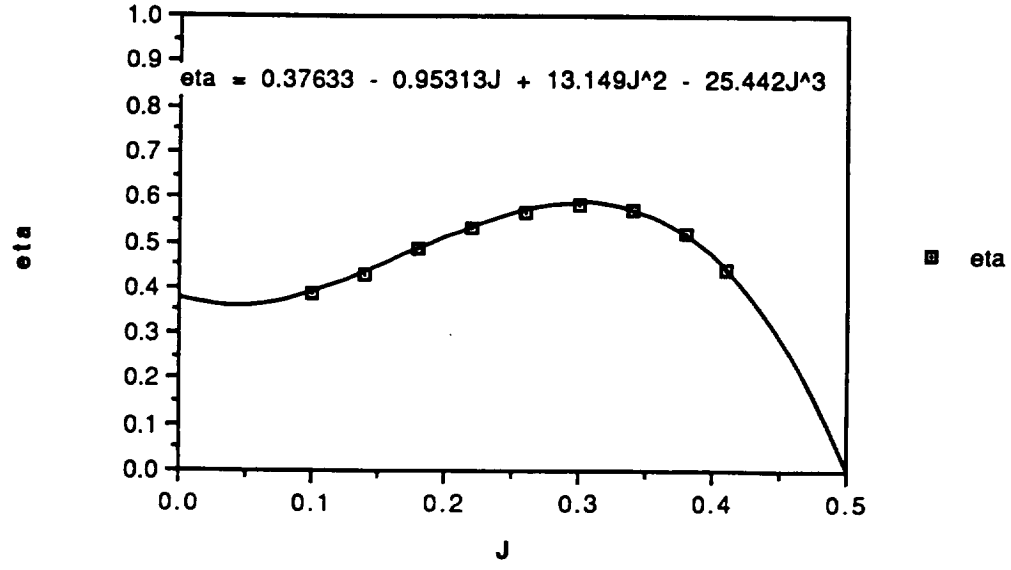

PROPELLER DATA SHEET

A) Propeller Designation: ZING 12-6 QUIRK

B) Number of Blades: 2 Diameter: 12 (Inches)

C) Select one of the following airfoil sections:
1) INVISCID FLAT PLATE
2) THIN FLAT PLATE
3) SYMMETRICAL
4) CLARK Y
5) RAF-6
--> 6) NACA44XXLOWRE

D) Blade thickness may be entered as either:
1) Fraction of chord
--> 2) Inches

E) Blade data may be entered at radial locations specified as:
1) Fractional Radius
--> 2) Inches

F) Radius* at which blade setting is measured: 3

G) Blade setting (i.e. ref angle for whole blade): 17.66

H) Enter the number of radial data positions: (3-9): 9

I)

Data Point	Radius*	Chord	Thickness*	Angle
1:1.5		.689	.216	32.48
2:2		.75	.21	25.5
3:2.5		.869	.203	20.91
4:3		1	.197	17.66
5:3.5		1	.185	15.26
6:4		.969	.17	13.43
7:4.5		.875	.159	11.98
8:5		.813	.131	10.81
9:5.5		.625	.106	9.85

J) Select desired refinment of analysis:
--> 1) Analysis by simple blade element theory.
2) Analysis including induced velocity.
3) Analysis including induced velocity and tip losses.

K) These Cl/Cd coefficient adjustments may be selected
--> 1) No Cl/Cd adjustments
2) Mach number adjustment
3) Reynolds number adjustment
4) Mach and reynolds number adjustments

L) Select altitude in thousands of feet: 0

M) Specify one of the following:
--> 1) Airspeed FIXED at: 17 MPH
2) Propeller RPM FIXED at:

N) Range of Advance Ratio to be used in calculations:
J min: .1 J max: .8

NOTES: First data point must be less than 30% radius; others must progress outward.
Designation must start with a letter and may not contain a comma.
For square tip blades (only) use tip as last data point.
Angles must be specified in degrees, lengths in inches.
* Units must be as specified in lines D and E.

Zinger 12-6 @ 17 mph

(Including induced velocity and tip losses)

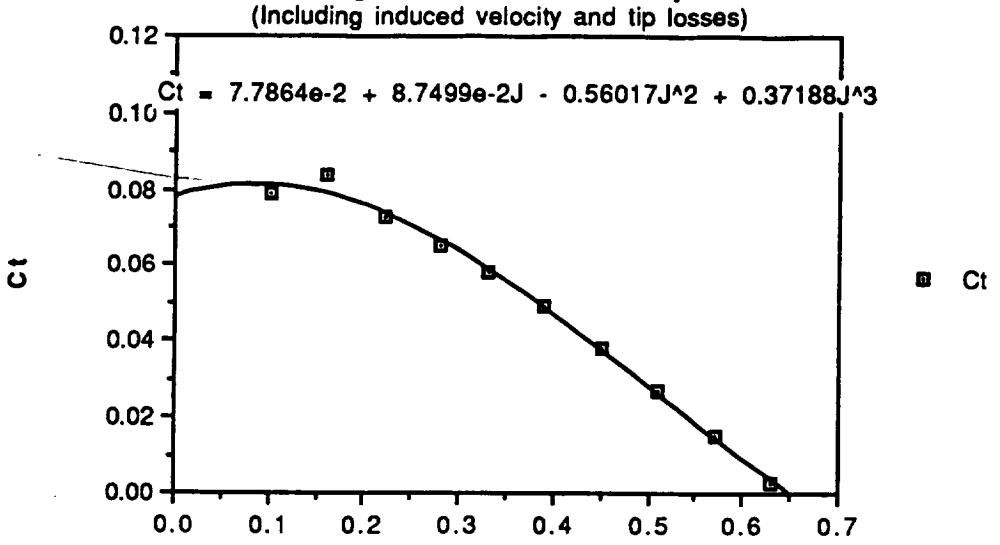

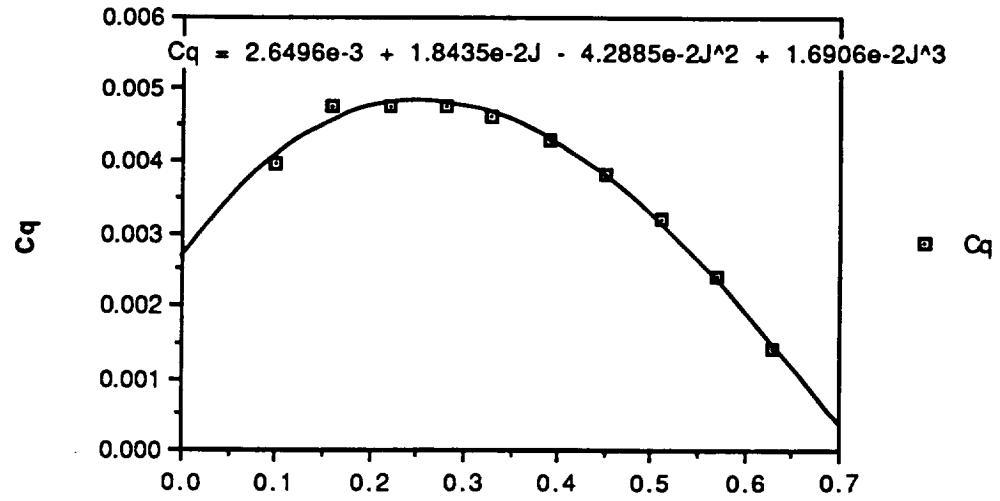

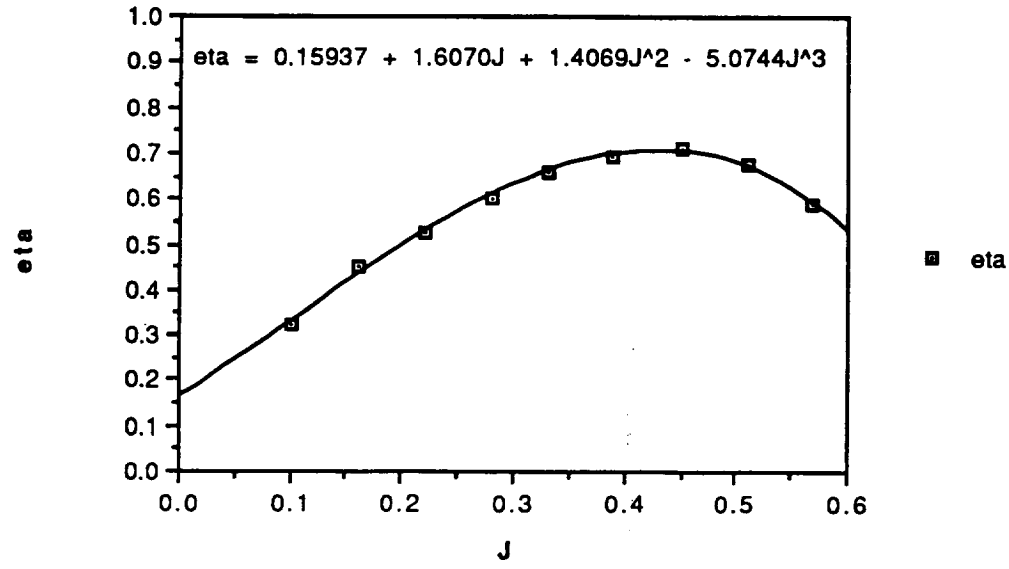

PROPELLER DATA SHEET

A) Propeller Designation: ZING 12-8 APPROX QUI

B) Number of Blades: 2 Diameter: 12 (Inches)

C) Select one of the following airfoil sections:
1) INVISCID FLAT PLATE
2) THIN FLAT PLATE
3) SYMMETRICAL
4) CLARK Y
5) RAF-6
--> 6) NACA44XXLOWRE

D) Blade thickness may be entered as either:
1) Fraction of chord
--> 2) Inches

E) Blade data may be entered at radial locations specified as:
1) Fractional Radius
--> 2) Inches

F) Radius* at which blade setting is measured: 3

G) Blade setting (i.e. ref angle for whole blade): 23

H) Enter the number of radial data positions: (3-9): 9

I)

Data Point	Radius*	Chord	Thickness*	Angle
1:1.5		.689	.216	40.33
2:2		.75	.21	32.48
3:2.5		.869	.203	26.99
4:3		1	.197	23
5:3.5		1	.185	19.99
6:4		.969	.17	17.66
7:4.5		.875	.159	15.8
8:5		.813	.131	14.29
9:5.5		.625	.106	13.03

J) Select desired refinment of analysis:
1) Analysis by simple blade element theory.
2) Analysis including induced velocity.
--> 3) Analysis including induced velocity and tip losses.

K) These Cl/Cd coefficient adjustments may be selected
--> 1) No Cl/Cd adjustments
2) Mach number adjustment
3) Reynolds number adjustment
4) Mach and reynolds number adjustments

L) Select altitude in thousands of feet: 0

M) Specify one of the following:
--> 1) Airspeed FIXED at: 17 MPH
2) Propeller RPM FIXED at:

N) Range of Advance Ratio to be used in calculations:
J min: .1 J max: .8

NOTES: First data point must be less than 30% radius; others must progress outward.
Designation must start with a letter and may not contain a comma.
For square tip blades (only) use tip as last data point.
Angles must be specified in degrees, lengths in inches.
* Units must be as specified in lines D and E.

Zinger 12-8 @ 17 mph

(Including induced velocity and tip losses)

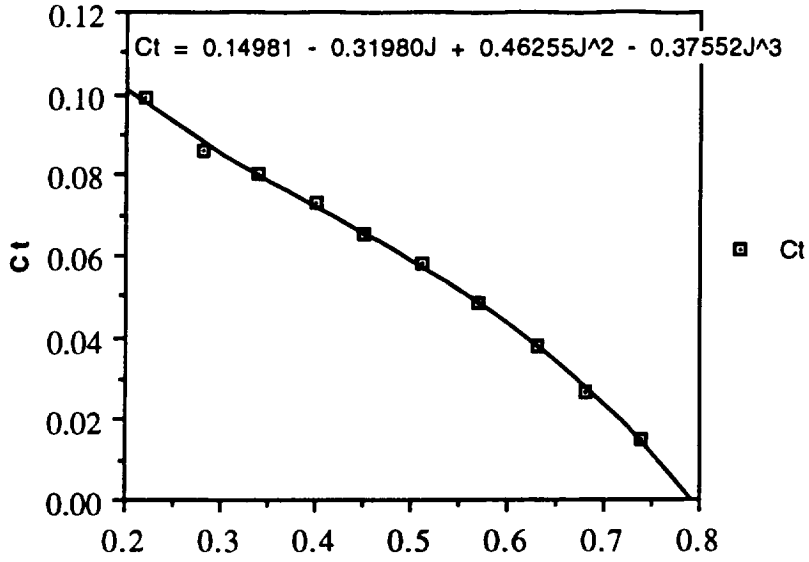

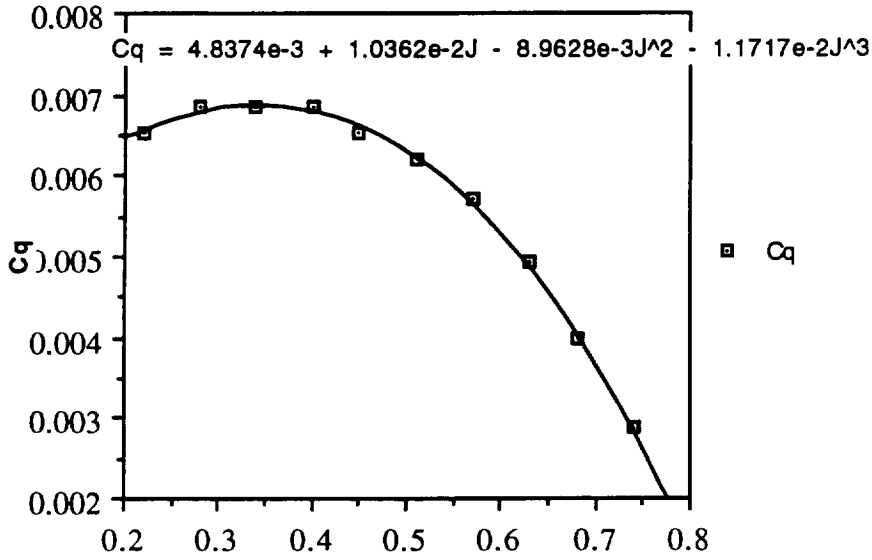

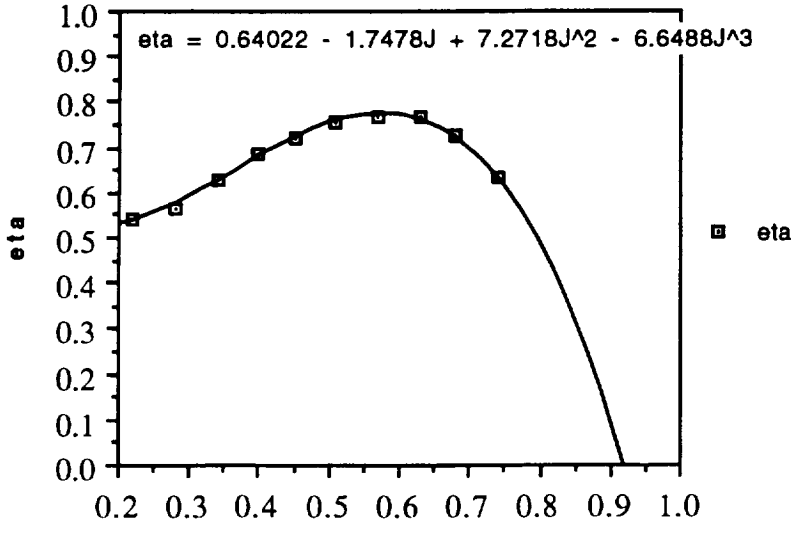

APPENDIX B-3

Calculation of Power Available for an Electric Motor

1. Set number of revolutions of motor:

$$N_m = \#$$

2. Advance ratio

$$J = \frac{V_\infty \times 60 \times GR}{N_m \times d_p}$$

3. Propeller: Efficiency, Torque Coefficient, Power Coefficient from propeller anaylsis:

eta = funct (J) Cq = funct (J) C_p = funct (J) = 2 * Pi * Cq

4. Revolutions of propeller:

$$N_{prop} = N_m / GR$$

5. Power of the motor:

$$P_{motor\ out} = \frac{1.356 \times C_p \times \rho \times \frac{N_{prop}{}^3}{60} \times d_{prop}{}^5}{\eta_{gear}}$$

6. Current draw:

$$i_a = \frac{P_{motor\ out}}{.0007397 \times N_m \times k_t} + \frac{T_{loss}}{k_t}$$

7. Power of the motor using the current draw:

$$P_{motor\ out} = .00073797 \times N_m \times (k_t \times i_a - T_{loss})$$

8. Power available:

$$P_{avail} = P_{motor\ out} \times \eta_g \times \eta$$

9. Recalculate the number of motor revolutions using the current:

$$N_m = \frac{V_{actual} - i_a \times (R_a + R_{bat})}{k_v}$$

10. Iterate number of motor revolutions until (9) = (1)

Power Available Spreadsheet
Astro 15 motor and Zinger 12-8 Propeller

eta-J fit						
a1=	0.64022					
a2=	-1.7478		**Nm (rpm)=**	**8645**		
a3=	7.2718		**volts=**	**8.1**		
a4=	-6.6488		**velocity=**	**30**		
Cq-J fit			**OUTPUTS**			
b1=	0.0048374		CL=	0.485	=	B25*B26*2*B22/(B21*B28^2*B23^2)
b2=	0.010362		CD=	0.052	=	B24+(E8^2/(PI()*B27*B22))
b3=	-0.0089628		Preq(W)=	**21.585**	=	1.356*B21*B28^3*B23^2*E9/(2*B22)
b4=	-0.011717		J=	0.496	=	B28*60*B30/(E3*B29)
			eta=	0.751	=	B2+B3*E11+B4*E11^2+B5*E11^3
INPUTS			Cp=	0.040	=	2*PI()*(B8+B9*E11+B10*E11^2+B11*E11^3)
Ra(ohm)=	0.120		Nprop(rpm)=	3632.353	=	E3/B30
Rbat(ohm)=	0.100		Pmotorout[b](W)=	30.026	=	0.0007397*E3*(B18*E18-B20)
Vactual(V)=	**8.100**		Pmotorout[c](W)=	30.026	=	1.356*E13*B21*(E14/60)^3*B29^5/B19
kv(V/rpm)=	7.96E-04		Pavail(W)=	**21.414**	=	E15*B19*E12
kt(in.-oz/a)=	1.134		ia[b](a)=	5.536	=	E16/(0.0007397*E3*B18)+(B20/B18)
etag=	0.950		ROC(ft/s)=	-0.025	=	0.7376*(E17-E10)/B26
Tloss(in.-oz)=	1.585		Nm[a](rpm)=	**8645.721**	=	(B16-E18*(B14+B15))/B17
rho(slugs/ft3)=	2.38E-03		Nm choice(rpm)=	**8645.000**	=	E3
AR=	9.500		flttime (hr) =	0.116	=	B32/E18
span(ft)=	9.500		range (ft) =	12523.680	=	B28*E22*3600
CD0=	0.041					
load factor=	1.000					
weight(lb)=	4.930					
efficiency=	0.704					
vel(ft/s)=	**30.000**					
dprop(ft)=	1.000					
gear ratio=	2.380					
bat cap + Loiter	0.800	(amp-hr)				
bat cap - Loiter	0.642	(amp-hr)				
ia @ loiter (a)=	4.740					

APPENDIX C

TK SOLVER PLUS: WING SPAR STRESS ANALYSIS

The Rules:

```
zbar=t/2-h/2
I=2*(zbar^2*A+b*h^3/12)+tweb*t^3/12
Mroot=(span/4)*(L/2)
zmax=t/2
t=c*tc
stress=Mroot*zmax/I
Q=b*h*(t/2-h/2)+tweb*t^2/4
Vroot=L/2
taumax=Vroot*Q/(I*tweb)
A=h*b
L=n*Wtot
numrib=round(span/ribspace)+1
Srib=t*c/2
Wspar=2*A*span*rhospar*16
Wrib=Srib*trib*rhobalsa*numrib*16
Wweb=tweb*t*span*rhobalsa*16
Wle=Ale*span*rhobalsa*16
Wte=Ate*span*rhobalsa*16
Wsur=2*span*c*rhomonokote*16
```

Input and Output (n=1.3, with web)

Input	Name	Output	Units	Comment
	zbar	.530125	in	
	t	1.404	in	airfoil thickness
.34375	h	in		height of spar cap
	I	.11440435	in^4	I for spar
	A	.171875	in^2	Area of one spar cap
.5	b	in		width of spar cap
.0625	tweb	in		web thickness
	Mroot	97.25625	lb-in	moment at root
114	span	in		span length
	L	6.825	lb	total wing lift
	zmax	.702	in	point of max stress
12	c		in	chord
.117	tc			thickness/chord ratio
	stress	596.77701	psi	stress at root
	Q	.12191548		
	Vroot	3.4125	lb	shear at wing root
	taumax	58.184722	psi	
1.3	n			load factor
5.25	Wtot		lb	estimated total weight plane
	numrib	30		number of ribs
4	ribspac		in	spacing between ribs
	Srib	8.424	in^2	

Input	Name	Output	Units	Comment
	Wspar	10.032	oz	spar wt
.016	rhospar		lb/in^3	spruce density
	Wrib	1.465776	oz	rib wt.
.0625	trib		in	thickness of rib
.0058	rhobals		lb/in^3	balsa density
	Wweb	.9283248	oz	web wt.
	Wle	.6612	oz	weight of LE spar
.0625	Ale		in^2	area of leading edge spar
	Wte	.9918	oz	weight of TE spar
.09375	Ate		in^2	area of te spar
	Wsur	4.9248	oz	
.0001125	rhomono		lb/in^2	density of MonoKote
	Wtotal	19.0039	oz	total wing weight

APPENDIX D
CRITICAL FIGURES AND TABLES

1. Range-Payload Diagram
2. Airfoil lift curve
3. Aircraft lift curve
4. Aircraft drag polar

   -tabular component drag breakdown
5. L/D curve for complete aircraft
6. Pitching moment coefficient vs. alpha
7. Power required/available vs. flight speed
8. Propeller efficiency vs. advance ratio
9. Weight/Balance diagram
10. Weight estimate for each component
11. V-n diagram
12. External 3-view drawing
13. Internal 2-view drawing

FIGURE 6-8
Range vs. Payload
(not including the two minute loiter range)

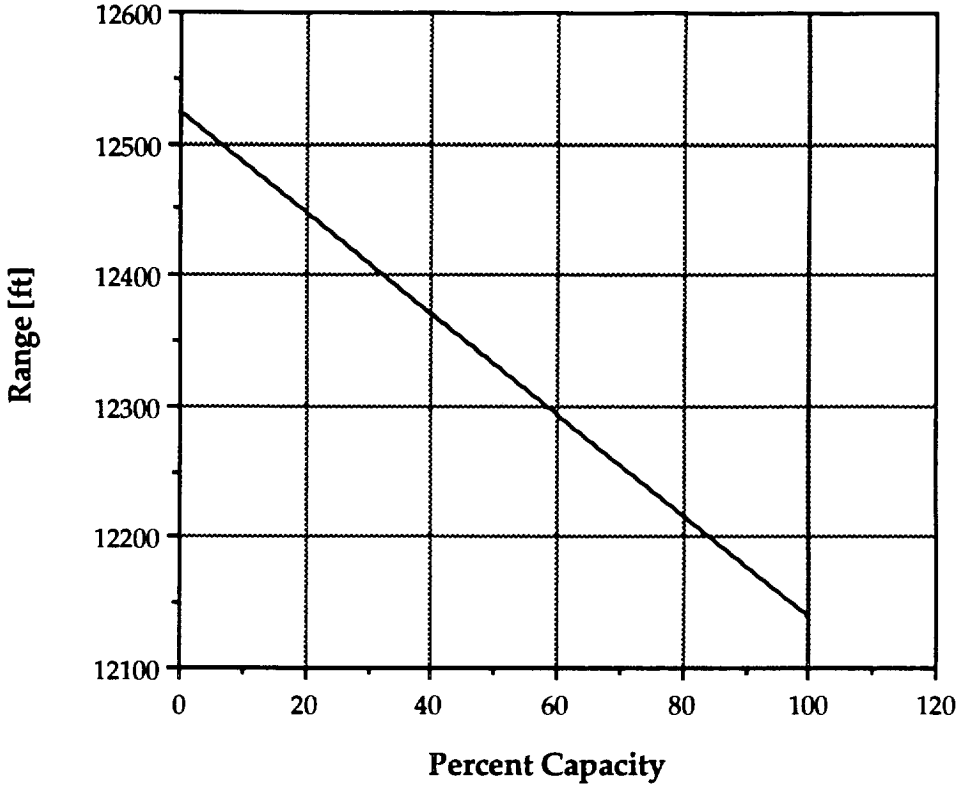

FIGURE 2-1
Section Lift Coefficient vs. Alpha
Spica PT/Re = 202300

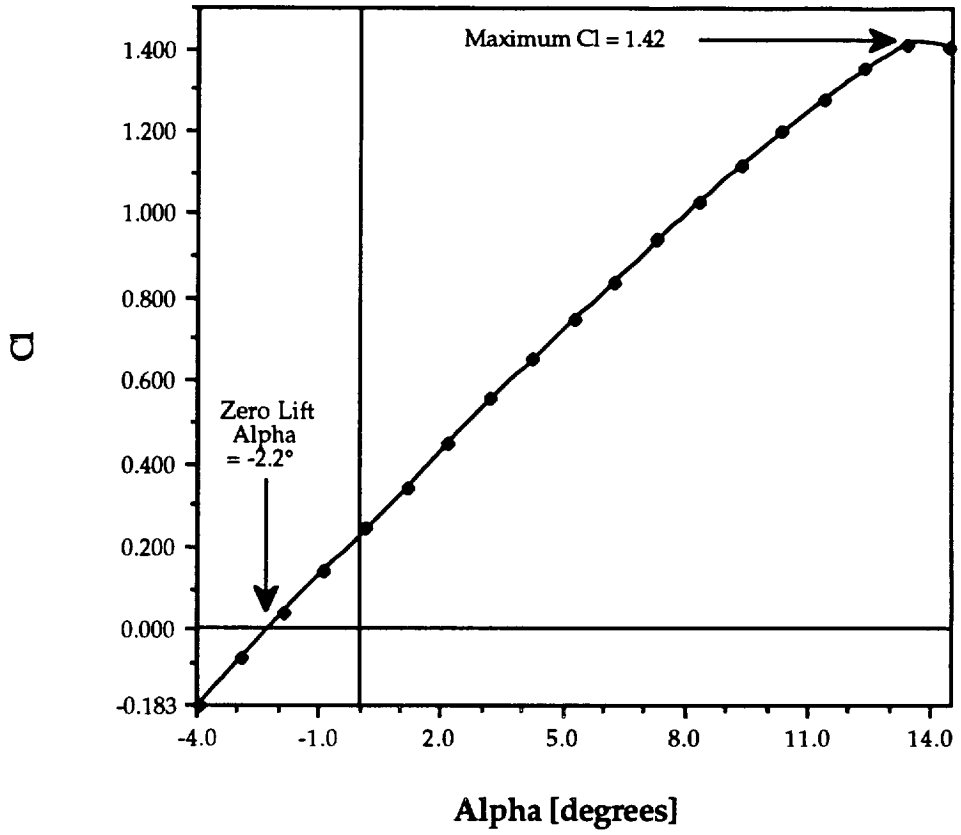

FIGURE 2-2
Complete Aircraft CL/Alpha Curve

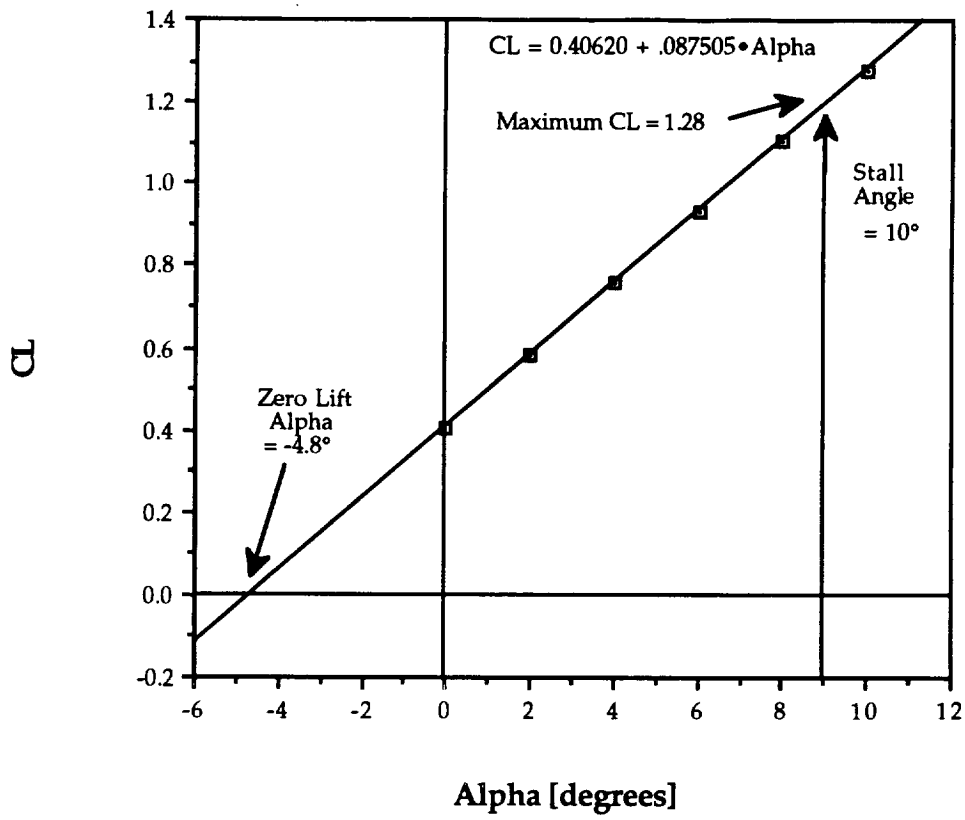

FIGURE 2-3
Drag Polar

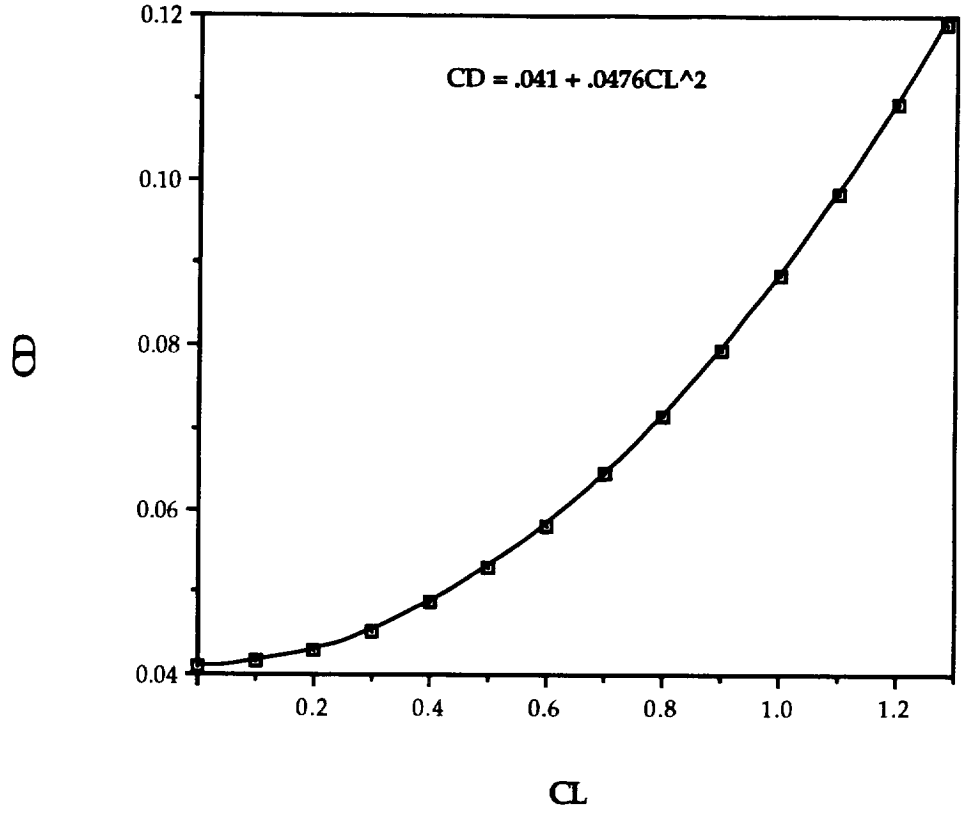

TABLE 2-2
Component Drag Buildup

Component	$C_{D\pi}$	A_{π} [ft ^{2}]	$\frac{C_{D\pi}A_{\pi}}{S_{ref}}$	% of C_{Do}	Reference
Wing	.007	9.5	.007	19.6	2-4.
Fuselage	.9	.208	.0197	55.1	2-5.
Vert. Tail	.008	1.25	.0011	3.1	2-4.
Horiz. Tail	.008	.833	.0007	1.9	2-4.
Front Gear	1.0	.0668	.007	19.6	2-5.
Rear Gear	0.2	.0122	.00026	.7	2-5.
Total	N/A	N/A	.0357	100	N/A

FIGURE 2-4
Entire Aircraft CL/CD VS. CL

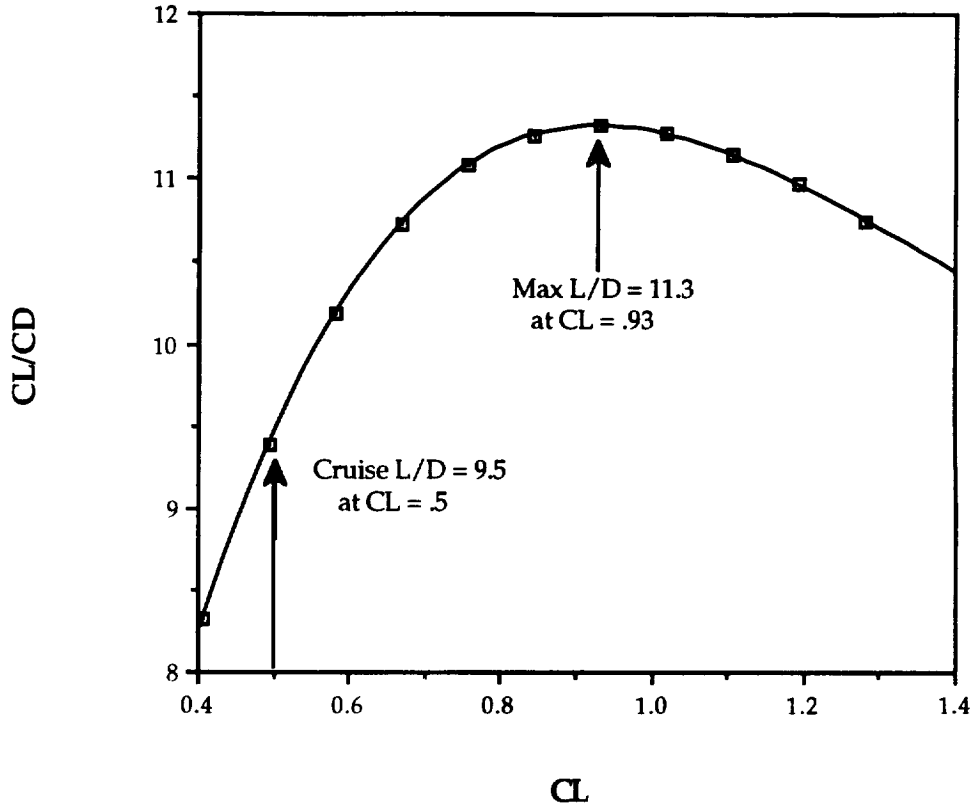

FIGURE 5-2
Cm vs. Alpha for extreme c.g. locations

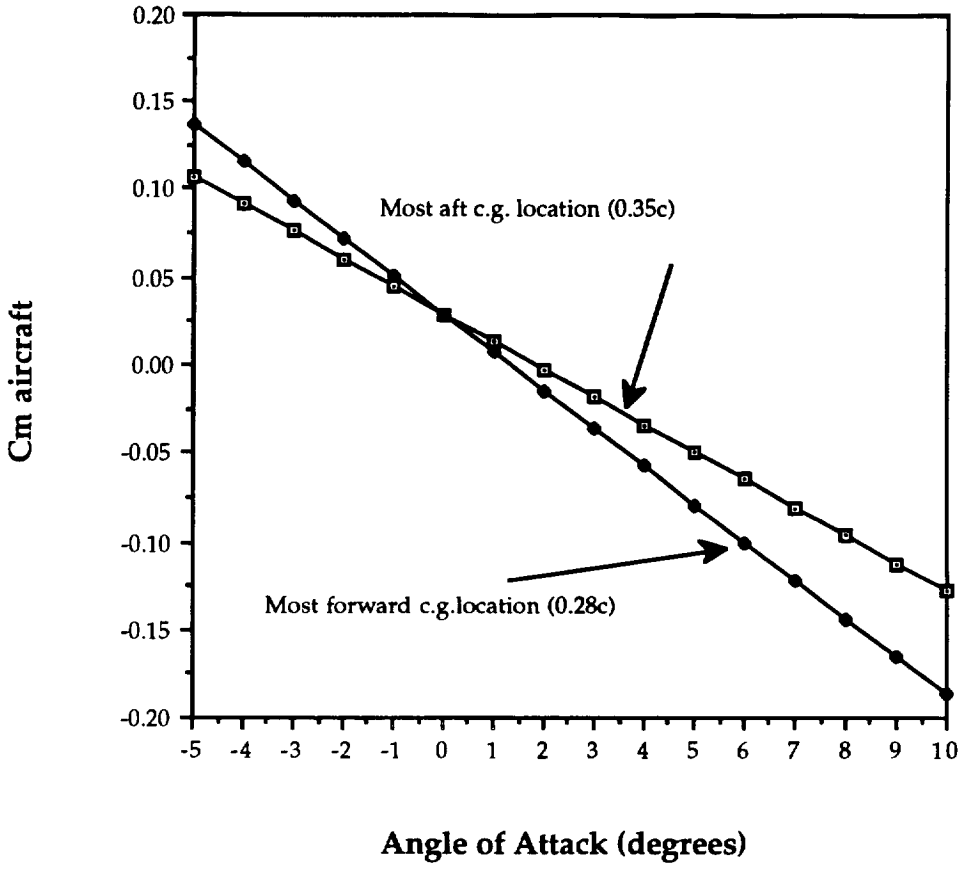

FIGURE 6-1
Power Required and Power Available for Flight Regime

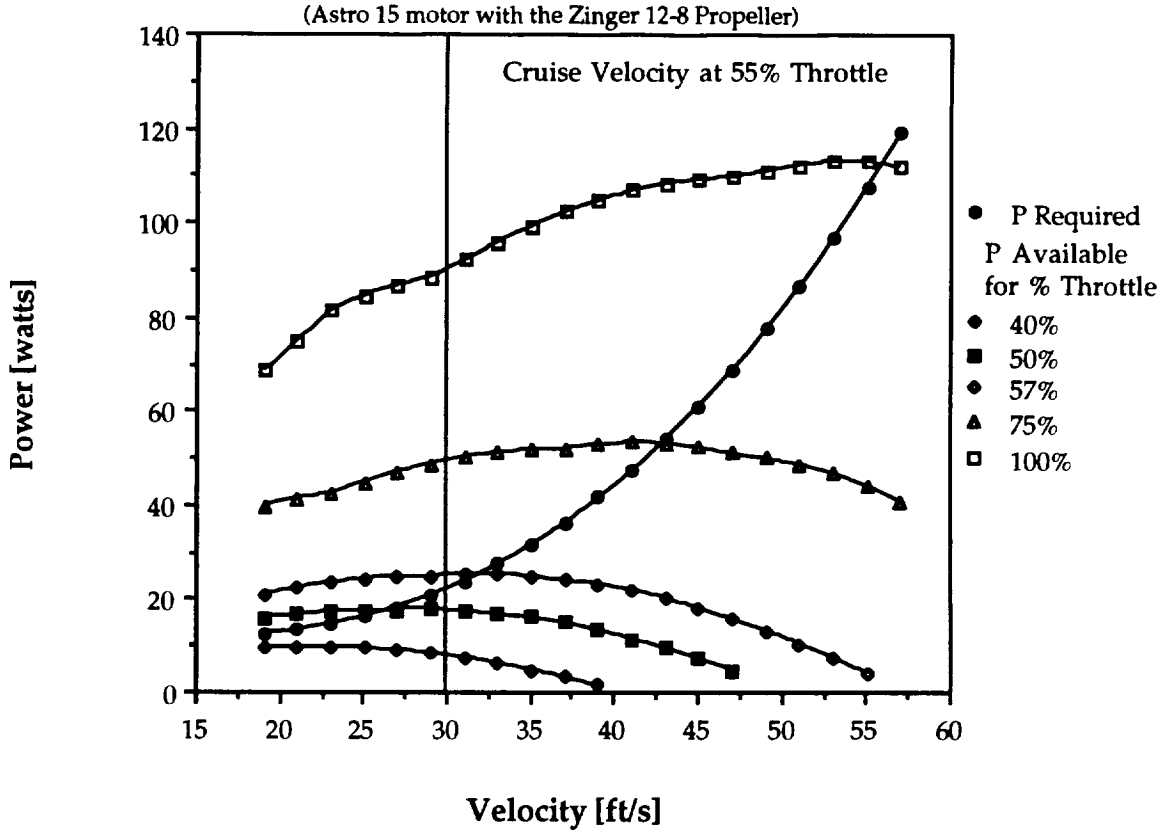

FIGURE 3-4

Zinger 12 - 8 Propeller Efficiency

(including induced velocity and tip losses)

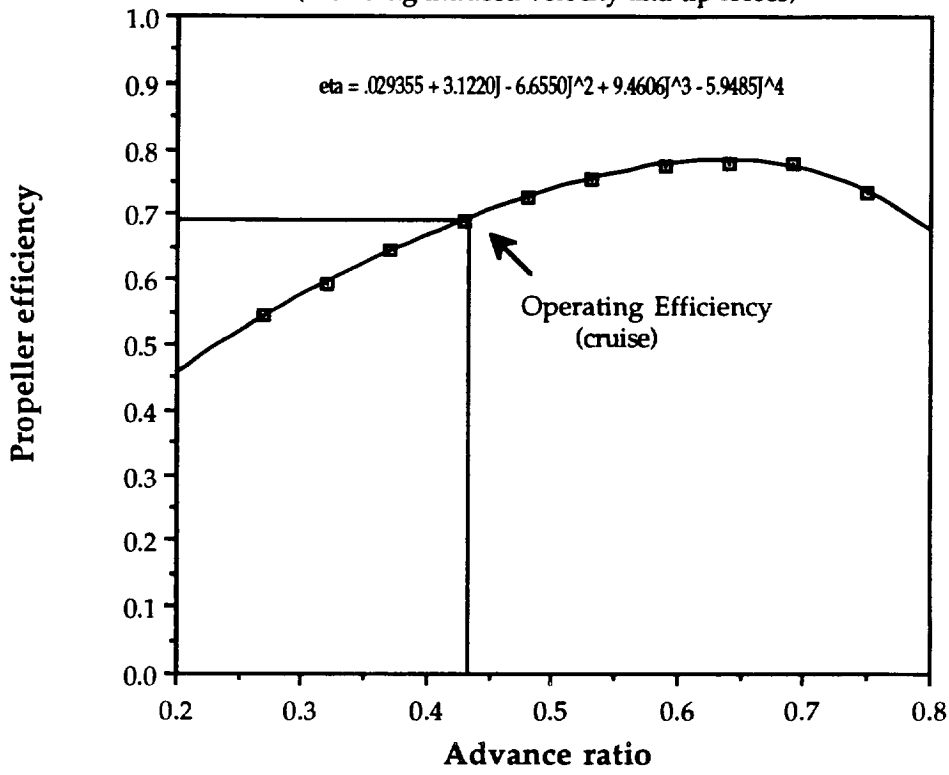

FIGURE 4-13
Weight-Balance Diagram for Front to Back Seating

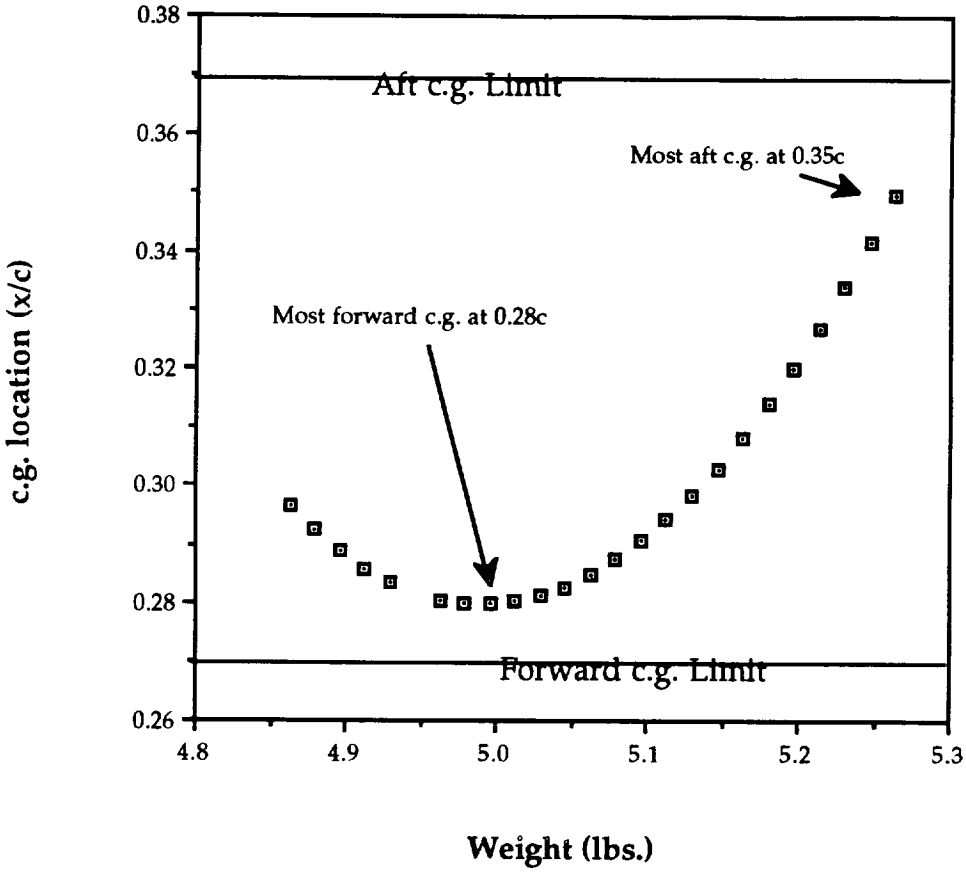

TABLE 4-3
Component Weight Breakdown for the *Airplane*

Component	Weight (oz)	X (in)	Weight Percentage
Propeller	1	0	1.2
Motor	10.3	2	12.2
Main Gear	3.5	19	4.2
Batteries	14.76	8.91	17.5
Receiver	0.95	8.91	1.1
System Battery	2	8.91	2.4
Servos (2)	1.2	8.91	1.4
Speed Controller	1.8	8.91	2.1
Wing	16	22	19.0
Fuselage	17	28	20.2
Passengers	6.4	28	7.6
Floorboard	4	28	4.8
Tailwheel	1.5	52	1.8
Empennage	3.8	60	4.5
Horizontal Tail	2.0	60	2.4
Vertical Tails	1.8	60	2.1

FIGURE 4-10
Graphical Representation of Weight Components

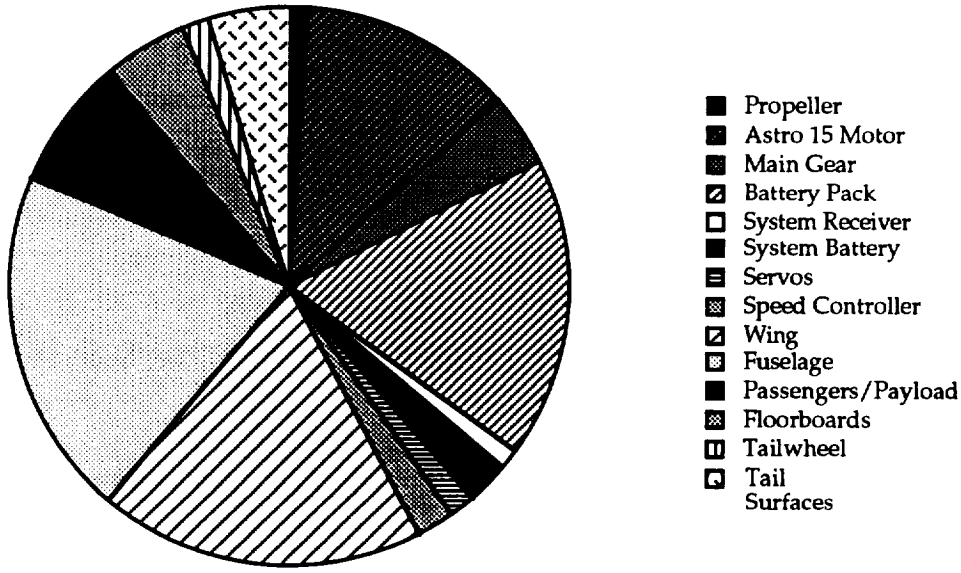

FIGURE 4-1
V-n Diagram
For Empty and Maximum Weight

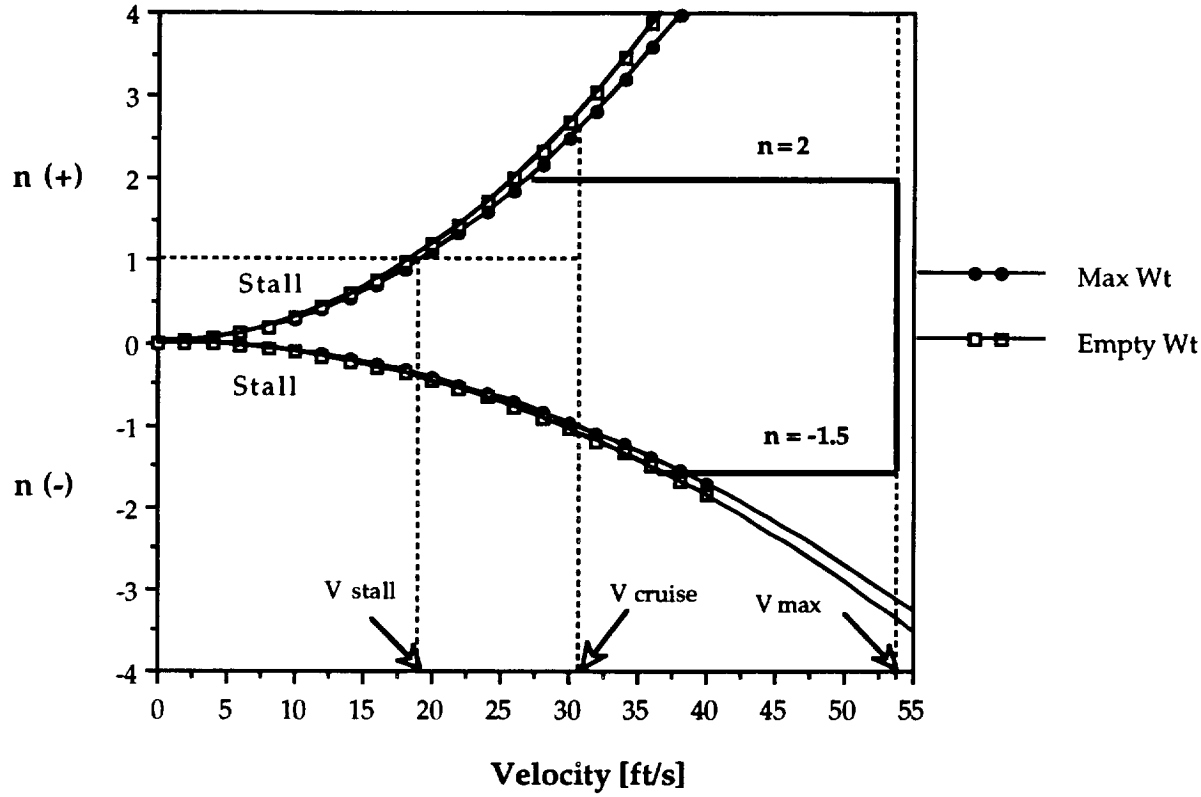

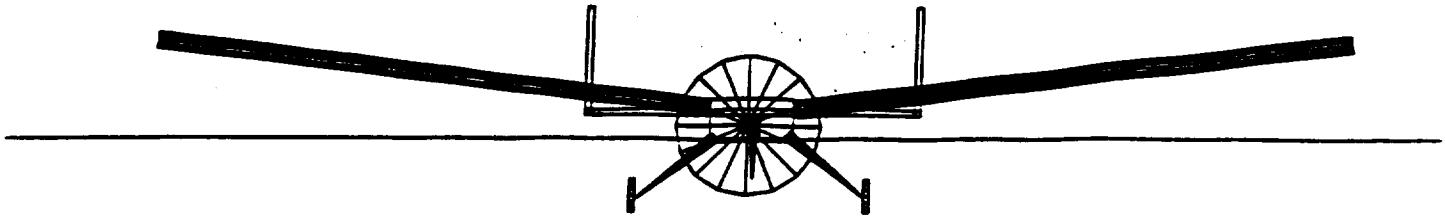

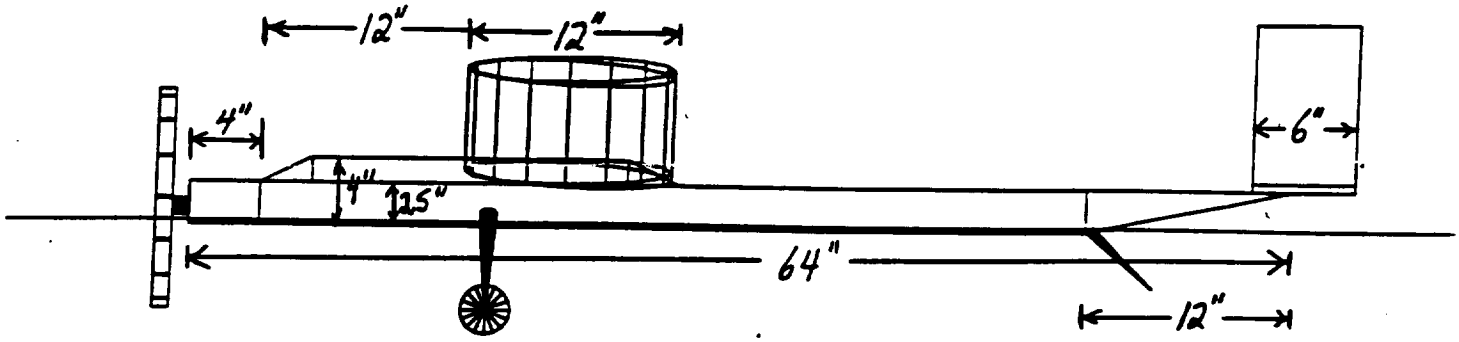
12"
12"
4"
4"
2.5"
6"
64"
12"

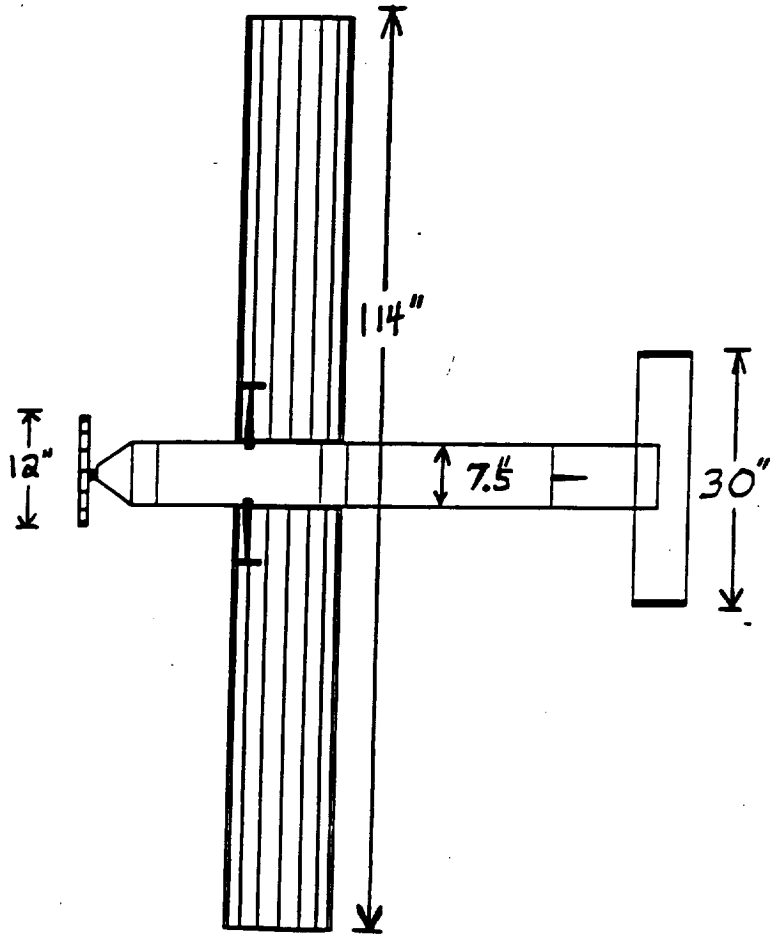
114"
12"
7.5"
30"

FIGURE 1-7
Internal Configuration

○ - passenger
✱ - flight attendant
● - pilot

1 inch = 8 inches

Level 1

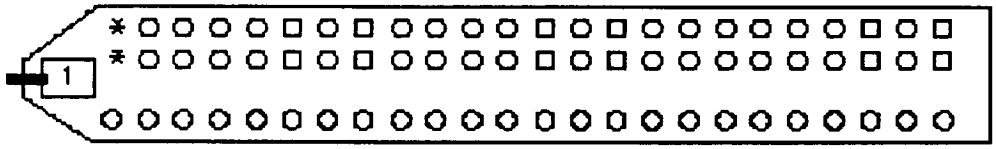

Level 2

Room to move batteries forward/aft for proper c.g. position

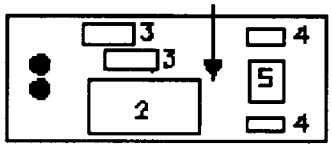

2 - batteries
3 - receiver battery pack/speed controller
4 - servos
5 - receiver

Side

THE AIRPLANE GUYS
APPENDIX E
MANUFACTURING PLAN

This appendix details the plans for the assimilation of the technology demonstrator. This was completed before the actual construction; therefore, certain technologies and additions are expected and will not be included in this section. Rather, they will be described in the actual technology demonstrator section.

The ideas for manufacturing were primarily compiled from analysis of previous designs because no members of the *Airplane Guys* have previous experience in the fabrication of such a model. Again, variations are expected.

This appendix will include specifics of design for the primary structural components, including diagrams, an assembly plan, a fabrication schedule, and a manhour estimate. Raw materials cost estimates were presented in the economic analysis and final costs will be presented in the technology demonstrator appendix.

E.1 Primary Structural Components

The wing is a fairly simple, lightweight design. It will be built in two sections, each with a span of 4'5.25". The fuselage section width of 7.5" will act as the rest of the 9.5 foot total wing span. The fabrication of two sections will allow for easy transportation of the vehicle because the sections are removable/replaceable in less than two minutes with a small Phillips screwdriver.

Two views of the wing are shown below:

Rib/Spars - Side View

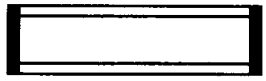

Rib/Spars - Front View

It can be seen that the primary load carriers of the wing are the main spars (spruce) located at approximately the quarter chord. The leading edge will be a normal balsa beam rounded at the front edge by sanding. The trailing edge is a triangular shaped piece of balsa. The spars are connected to the 14 ribs (per section) by carving their shapes into the ribs themselves and gluing the beams into place. The ribs will all be made of balsa sheets except for the rib at the root, which will be made of plywood. Rectangular pieces of balsa sheet will also be glued on either side of the main spars between the ribs to strengthen the structure and help maintain the spacing of the ribs. At the trailing edge root, a plywood tab will be attached to the wing and will be screwed into another piece of plywood attached to a spruce beam on the fuselage. The spar attachment device is shown below:

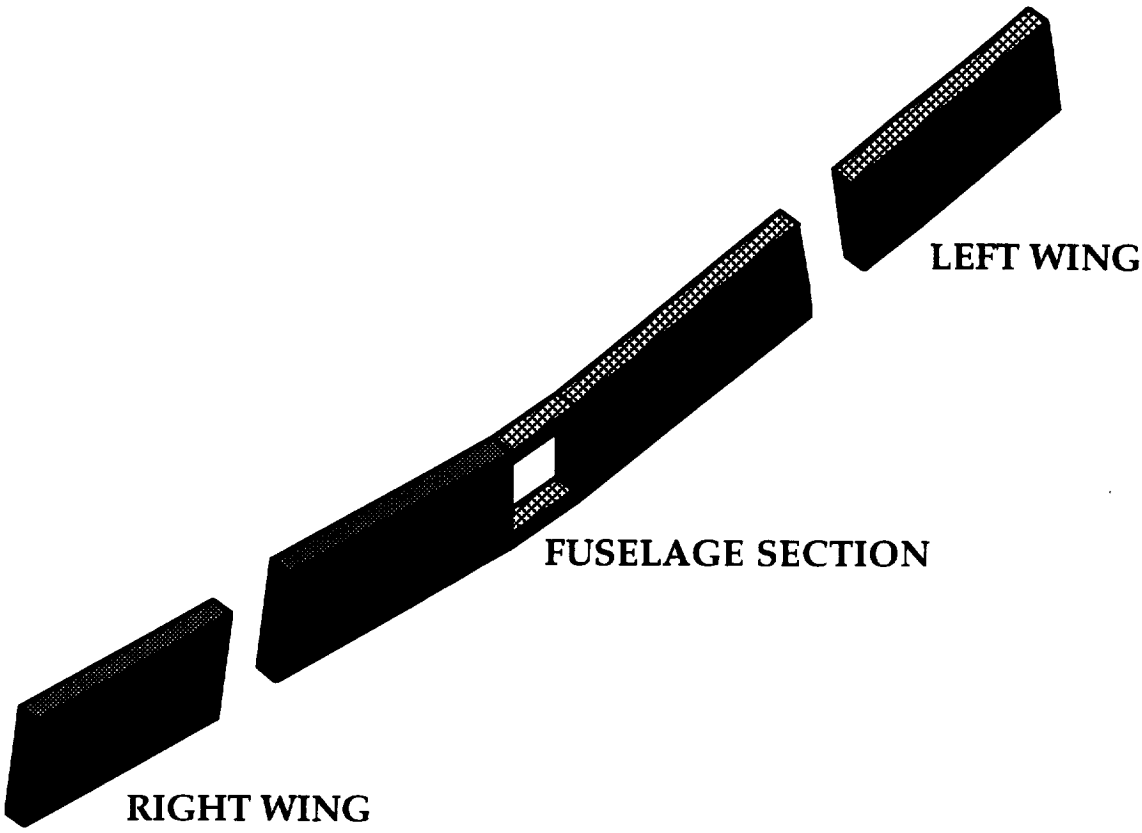

The fuselage portion will be made out of spruce beams on top and bottom (same cross-sectional area as the wing main spars) and plywood side supports. It is in this device that the 8° of dihedral will be given. The box attachment sections for each wing will be attached at the center with spruce beams and attached with glue to the fuselage and avionics compartment spruce longerons.

The fuselage configuration will be very similar to designs of previous years, with spruce longerons and balsa supports. A side view of the fuselage is shown below:

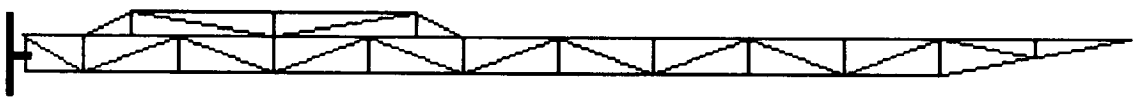

At certain crucial locations, i.e., the wing and tail attachment areas, spruce supports will be used. The bases of the engine and avionics compartments will be spruce supports with plywood planks on top. All avionics components will be screwed into the plywood except for the battery pack, which will be attached with velcro so that it may be easily relocated. There will be a "door" made of MonoKote and thin balsa beams which will open at one end (attached with tape for easy access to the compartment) and attached to a main fuselage support at the other.

The empennage is a more complex design because of the twin rudder design. Only the elevator is a conventional design with a standard servo connection. The rudders will be built as shown below:

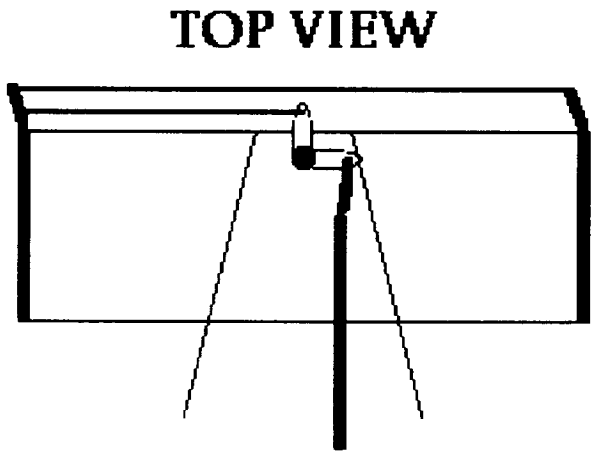

As seen, the servo will be connected to an L-shaped plastic horn which pivots on a long screw attached to a piece of spruce at the end of the empennage. The

opposite end of the horn will be connected to one rudder with a piece of music wire of sufficient thickness to prevent buckling. The second rudder will be coordinated with the first by another piece of stiff music wire connected between the two.

The two vertical stabilizers will be attached as shown above with added support beams on the inside of the stabilizers glued to the main spar of the horizontal stabilizer.

The landing gear configuration is described as a tail dragger. The main gear are to be attached with the foam rubber wheels 15° ahead of the center of gravity. These gear will be attached with plastic restraints and screws as shown below:

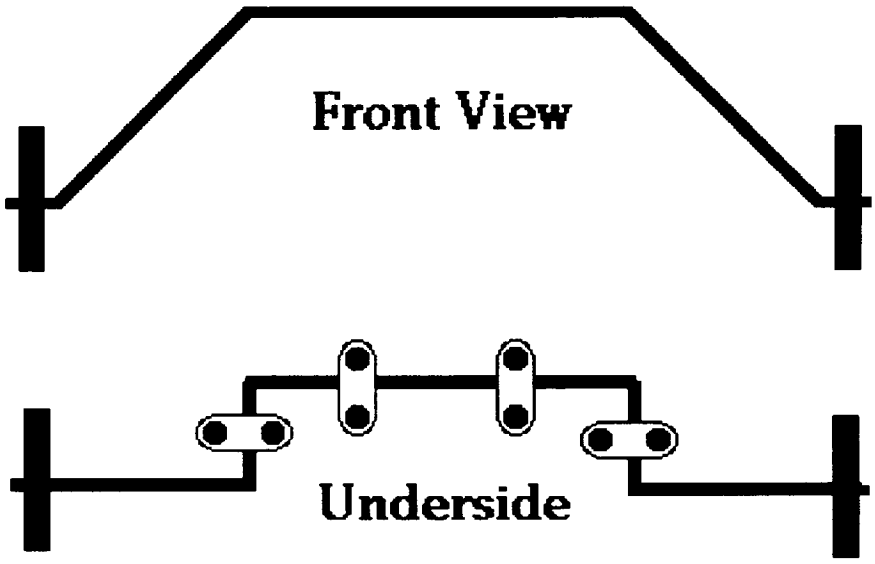

The thick music wire which holds the wheels will be bent as shown to avoid movement of the gear in any direction. The ends of the music wire just before the wheels will be attached to one another with a flexible wire to restrict the give in the structure.

At the tail, there is no wheel, but rather, a piece of bent music wire which will be turned in coordination with the rudder servo. The tail is designed to lift off before the aircraft to reduce friction drag during takeoff roll.

E.2 Assembly Sequence and Schedule

The sequence and schedule are outlined below:

- STEP 1: THURS. 4/15 - THURS. 4/22

  -Group divided into halves A and B
  -Group A - Wing Construction
    -Trace/Cut ribs
    -Cut/Splice spars
    -Round leading edge
    -Assemble
    -MonoKote
  -Group B - Fuselage Construction
    -Draw to scale
    -Measure/Cut main beams
    -Measure/Cut supports
    -Assemble
    -Add bases to compartments/landing gear mount
    -Add wing attachment device

- STEP 2: THURS. 4/22 - SAT. 4/24

  -Empennage construction
    -Horizontal stabilizer - measure/cut
    -Vertical stabilizers - measure/cut
    -Assemble
    -Elevator/Rudders - measure/cut
    -Attach control surfaces to stab.'s (MonoKote)
    -Attach to fuselage
    -Attach servos/coordinator

- STEP 3: SAT. 4/24 - MON. 4/26

  -Attach landing gear
  -Place motor/avionics/prop

- STEP 4: MON. 4/26 - FLYOFF

  -Minor adjustments
  -C.G. PLACEMENT

E.3 Time Estimate

The group plans to construct the technology demonstrator in under 100 hours. The exact time/money spent will be included in the fabrication appendix.

APPENDIX F

Technology Demonstrator Characteristics

Cost Comparison

The overall construction of the Airplane took 135 hours as compared with a prediction of 100 hours. The following table itemizes the costs associated with all aspects of the construction of the technology demonstrator. The costs are shown in comparison to the estimates made prior to construction.

Costs	Actual Tech Demo	Estimated
Raw Materials	$ 112.05	$ 175.00
Change Orders	$ 505.90	$0
Fixed Subsystems	$ 404.00	$ 404.00
Tooling	$ 45.15	$ 215.00
Labor	$1350.00	$1000.00
Disposal	$ 203.22	$ 300.00
Hazardous Waste	$0	$0
Total Airplane Cost	**$2620.32**	**$2094.00**
DOC (max and min fuel)	$ 5.86 - $ 6.65	$ 4.90 - $ 5.68
CPSPK	$ .0081 - $ .0095	$ .007 - $ .0081

As the table shows, the actual *Airplane* cost exceeds the estimate by $526.32. This is due to the large penalty incurred when change orders were needed to add to the raw materials used. This penalty was $505.90 and almost completely accounts for the aircraft cost difference. The change orders were a direct result of the inexperience of the design team in manufacturing. Because no member had experience in building, gluing, integrating, etc., the amount of materials, especially the amount of glue used, was greatly underestimated. Also, as progress was made in construction, plans changed causing the need to purchase new, unforeseen items. Namely, the group changed the design of the landing gear and decided to purchase a $15.00 landing gear device which was charged as $150.00 AeroWorld dollars.

Labor Hours Breakdown

The chart below depicts how the 135 labor hours were spent. As shown, the integration of the various substructures into the final aircraft took the most time (56.35%). Integration included, among other things, the attachment of the servos and control surfaces, the reinforcement of the wing attachment to the fuselage, the attachment of the landing gear, tails and motor/fuel assembly.

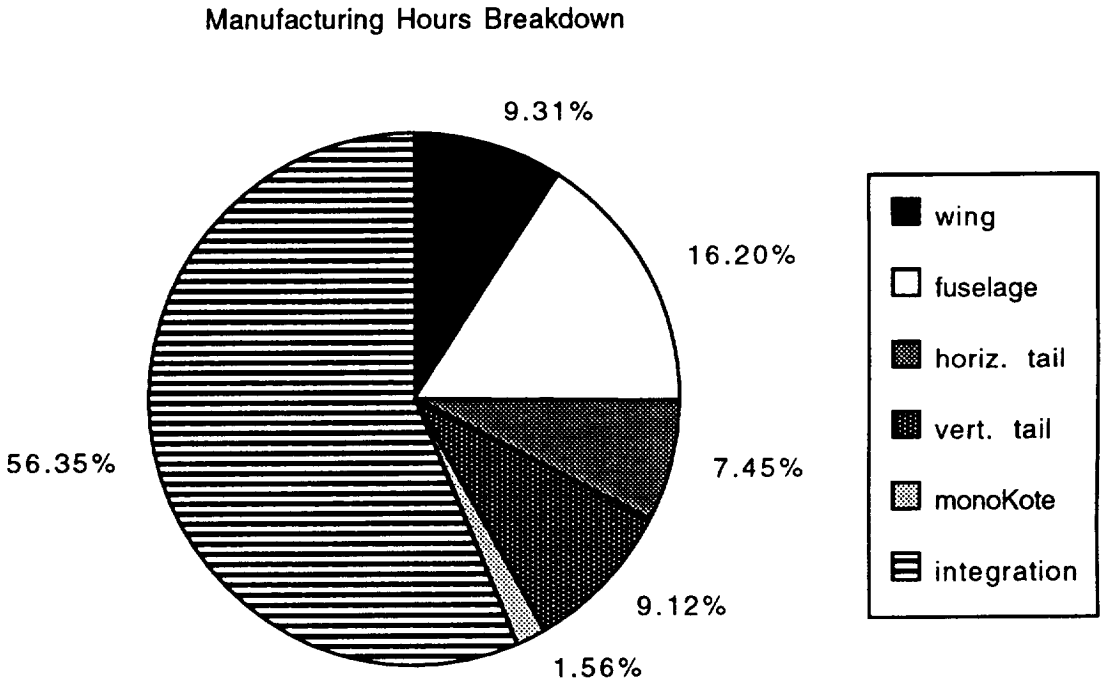

Weight Comparison

The weight of the technology demonstrator was 5.8 lbs. as compared to a predicted weight of 5.25 lbs. This reflects the bulking up of both the horizontal tail surface and the landing gear to provide structural integrity of the aircraft. Also, since 900 milliamp hour batteries were unavailable, heavier 1000 milliamp hour batteries were used to power the

Airplane. Because the horizontal tail was increased in weight by a factor of two, the center of gravity of the aircraft without batteries was slightly aft of the design point of 35 % of the mean aerodynamic chord. This was compensated for by the addition of extra space so that the batteries could be moved forward and the center of gravity relocated as desired.

It was necessary to stiffen the horizontal tail with spruce spars and a boxlike frame since it was shown to be lacking in rigidity after its initial construction. The landing gear, both the main gear and tailwheel, failed during a hard landing during the taxi test and were bulked up in both their supports and individual structures so that problems could be alleviated in the future.

General Observations

- It is very important to lay out the aircraft in as detailed a manner as possible so that the amount of material for fabrication can be accurately determined.

- A visit to Hobbyland early on is crucial to determining availability of certain lengths and strengths of materials. A complete inventory of products is generally available at this one location.

- Developing a checklist of specific tasks in the order of completion would allow individuals to come in at random intervals and know which tasks need to be worked on.

- Using the human resources available, i.e., Joe Mergen and Dr. Batill, aids in learning practical knowledge in such areas as attachment devices, servo control, etc.

- Buying more than enough glue at the beginning will save money because of its high cost and the penalty multiplier.

- If you are not part of the solution, you are most likely part of the problem.

- Having a person keep track of time and materials helped to keep a closer eye on the developing costs of these aspects of the fabrication.

- Taking time to assure that joints are flush will decrease the amount of required sanding and simplify the Monokoting process.

- Working in shifts of two to three people more efficiently utilizes the costly man hours.

- Using spruce or bass for the essential structural (i.e. load bearing) components is crucial to provide adequate strength and avoid failure.

- Because of lack of experience, having a little extra material at the start to allow some room for error is a good idea.